

Simon Pressler, BSc

Tayloring the Complexation of Phenyl Aza Crown Ethers

MASTER'S THESIS

to achieve the university degree of

Diplom-Ingenieur

Master's degree programme: Technical Chemistry

submitted to

Graz University of Technology

Supervisor

Univ.-Prof. Dipl.-Chem. Dr.rer.nat. Ingo Klimant

Institute of Analytical Chemistry and Food Chemistry

Graz, July 2019

Affidavit


I declare that I have authored this thesis independently, that I have not used other than the declared sources/resources, and that I have explicitly indicated all material which has been quoted either literally or by content from the sources used. The text document uploaded to TUGRAZonline is identical to the present master's thesis.

Eidesstattliche Erklärung

Ich erkläre an Eides statt, dass ich die vorliegende Arbeit selbstständig verfasst, andere als die angegebenen Quellen/Hilfsmittel nicht benutzt, und die den benutzten Quellen wörtlich und inhaltlich entnommenen Stellen als solche kenntlich gemacht habe. Das in TUGRAZonline hochgeladene Textdokument ist mit der vorliegenden Masterarbeit identisch.

July 20, 2019

Date

A handwritten signature in black ink, consisting of stylized letters, likely 'S' and 'P', written over a horizontal line.

Signature

Danksagung

Auf diesem Wege möchte ich mich bei allen Personen bedanken, die mich während meiner Studienzeit begleitet haben. Danke Ingo, dass du mir die Möglichkeit gegeben hast meine Masterarbeit auf der acfc zu schreiben. Lieber Luki, danke dass du mir als Zweitbetreuer mit Rat und Hilfe beiseite gestanden bist und dir immer selbstverständlich Zeit für mich genommen hast. Ich war immer sehr von deiner großartigen Arbeitsmoral begeistert und möchte diese auch für meine zukünftigen Aufgaben mitnehmen. Danke an alle meine Labor- und Institutskollegen, die das Arbeiten auf der acfc sehr angenehm und kollegial gemacht haben. Sabrina, danke für die lustige Zeit im Schreibraum und die spaßigen Kaffee- und Essenspausen. Ich hoffe wir werden uns auch in Zukunft noch oft sehen.

Vor allem möchte ich mich bei meinen Freunden bedanken, ohne die meine Studienzeit nur halb so lustig gewesen wäre. Max, ich bin froh mich zu deinen Freunden zählen zu dürfen und freue mich schon auf unser nächstes Treffen, sei es zum Sport oder Biertrinken. Danke Roman, dass du nicht nur studientechnisch mir oft weitergeholfen hast, sondern auch immer für eine abendliche Online-Gaming Session zu haben warst. Ich hoffe wir werden noch viele Nächte hinein diverse Onlinewelten zusammen unsicher machen. Lieber Lorenz, danke für die vielen gemeinsamen Abende und deine Unterstützung gegen Ende dieser Masterarbeit hin. Fabio, danke für deinen Rat und deine Freundschaft! Ich möchte mich auch bei allen nicht namentlich genannten Freunden bedanken und ich hoffe, dass ich euch alle auch noch weiterhin oft sehen werde, egal wohin es in der Zukunft für mich geht.

Zum Schluss möchte ich mich bei meiner Familie bedanken. Danke Mama, Martin und Papa, dass ihr mir mein Leben lang vermittelt habt, dass Bildung wichtig ist und mich in allen meinen bildungs- und studientechnischen Entscheidungen unterstützt habt. Jakob, ich finde deine Lebenseinstellung und deine

nachhaltige Lebensweise bewundernswert und möchte davon auch etwas für die Zukunft mitnehmen. Judith, ich bin froh eine so musikalische, künstlerische und kreative kleine Schwester zu haben. Ich bin mir sicher, dass du deine Zukunftswünsche zur Wirklichkeit machen wirst. Danke David, für die vielen nächtlichen Gamingsessions und deine brüderliche Loyalität und Liebe. Ich hoffe, ich kann dir auch in Zukunft in manchen Bereichen ein Vorbild sein. Liebe Clara, du bist der lebenswürdigste und sozialste Mensch, den ich kenne. Seit ich mich erinnern kann, warst du immer an meiner Seite und meine Rauf- und Spielkumpanin. Du bist schon seit langem mein persönliches Vorbild und ich möchte dir deswegen diese Arbeit widmen.

Schön, dass es euch alle gibt!

A handwritten signature in black ink, appearing to be 'S.P.' with a stylized flourish underneath.

July 20, 2019

Abstract

In this thesis an attempt was made to develop an improved receptor for potassium ions based on phenyl aza crown ethers. Additionally, we wanted to gain a better understanding about the factors that influence the host guest stability of these receptors. The main question to answer was whether the positional or electronic factors of adding substituents to the receptors played a bigger role for the complex stability. For this purpose various phenyl aza crown ethers were synthesized and their stability constants towards potassium ions determined via UV-Vis spectrometry. The measurements confirmed that the positional factor of adding additional complexating groups plays a much bigger role than only adding electron donating groups to the receptor. Furthermore, a cross sensitivity survey was conducted. This confirmed the cross sensitivity of these specific crown ethers towards NH_4^+ . This can mainly be attributed to the very similar ion diameters of NH_4^+ and K^+ .

Contents

Abstract	v
I. Introduction	1
1. Theoretical Background	3
1.1. Luminescence	3
1.1.1. Absorption of UV-Visible Light	4
1.1.2. Forbidden Transitions	7
1.1.3. The Franck-Codon Principle	7
1.1.4. Radiative and Non-Radiative Transitions between Electronic States	8
1.1.5. Intermolecular De-Excitation Processes	12
1.2. Host Guest Chemistry	15
1.2.1. History of Crown Ethers and Crown-type Ligands	17
1.2.2. Properties of Crown Ethers	20
1.2.3. Crown Ethers as Cation Receptors	21
1.3. Concepts of Sensors	26
1.3.1. Fluorescent PET Cation Sensors	26
1.3.2. Fluorescent PCT Cation Sensors	27
1.3.3. Fluorescent RET Sensors	28
1.4. Determination of Stability Constants	31
1.4.1. NMR Titrations	34
1.4.2. UV-Vis Titrations	35
1.4.3. Fluorescence Titrations	35
1.4.4. Other Titration Techniques	36

II. Experimental	37
2. Materials and Methods	39
2.1. Chemicals	39
2.2. Nuclear Magnetic Resonance Spectrometry	39
2.3. Mass Spectrometry	39
2.4. Absorption Spectra	40
2.5. Emission and Excitation Spectra	40
2.6. Thin Layer Chromatography (TLC)	40
2.7. Flash Column Chromatography	40
3. Synthesis	43
3.1. Crown Ether 1	44
3.2. Crown Ether 3	45
3.2.1. Synthesis of Precursor 3a	45
3.2.2. Synthesis of Crown Ether 3	46
3.3. Crown Ether 4	47
3.3.1. Synthesis of Precursor 4a	47
3.3.2. Synthesis of Crown Ether 4	48
3.4. Crown Ether 5	49
3.4.1. Synthesis of Precursor 5a	49
3.4.2. Synthesis of Crown Ether 5	50
3.5. Crown Ether 6	51
3.5.1. Synthesis of Precursor 6a	51
3.5.2. Synthesis of Crown Ether 6	52
3.6. Crown Ether 7	53
3.6.1. Synthesis of Precursor 7a	53
3.6.2. Synthesis of Crown Ether 7	54
3.7. Synthesis of Crown Forming Agent	55
3.8. Synthesis of Crown Ether 2	56
3.8.1. Synthesis of Precursor 2a	56
3.8.2. Synthesis of Precursor 2b	57
3.8.3. Synthesis of Precursor 2c	58
3.8.4. Synthesis of Crown Ether 2	59

III. Results and Discussion	61
4. Synthetic Considerations	63
5. Stability Constants	67
5.1. Calibration Method	67
5.2. Crown Ether 1	72
5.3. Crown Ether 3	73
5.4. Crown Ether 4	74
5.5. Crown Ether 5	75
5.6. Crown Ether 6	76
5.7. Crown Ether 7	77
5.8. Methoxyethoxy Crown Ether	78
5.9. Triazacryptand	79
5.10. Cross Sensitivity	80
5.11. Fluorescence Spectrometry	82
6. Conclusion	85
Bibliography	89
Appendix	97
A. NMR Spectra	99
B. UV-Vis Spectra	115
C. Fluorescence Spectra	123

List of Figures

1.1. Processes of light-matter interactions	4
1.2. All possible electronic transitions	5
1.3. Singlet state vs. triplet state	6
1.4. Franck-Codon principle	8
1.5. Perrin-Jablonski diagram	9
1.6. Static vs. dynamic quenching	12
1.7. Stern-Volmer plots	14
1.8. Photoinduced electron transfer	14
1.9. Examples for host molecules	15
1.10. Pedersen nomenclature	17
1.11. Various types of crown ethers	17
1.12. The structure of a [2.2.2]-cryptand	18
1.13. Kryptofix-5 - A common podand	19
1.14. Structures of podandocoronands	19
1.15. Oxocrown and spherand	20
1.16. Impact of heteroatoms on complexation	23
1.17. 18-crown-6 complexation of a potassium ion	23
1.18. Lariat ether vs. cryptand complexation	24
1.19. NH_4^+ complexation: crown ether vs. lariat ether	25
1.20. PET sensor mechanism	26
1.21. Various PET based sensors	27
1.22. PCT sensors: spectral shifts	28
1.23. PCT sensor examples	29
1.24. Resonance Energy Transfer	30
1.25. Calixarene based RET sensor	30
3.1. Compound Overview	43
3.2. Synthesis of Crown Ether 1	44
3.3. Synthesis of Precursor 3a	45

List of Figures

3.4. Synthesis of Crown Ether 3	46
3.5. Synthesis of Precursor 4a	47
3.6. Synthesis of Crown Ether 4	48
3.7. Synthesis of Precursor 5a	49
3.8. Synthesis of Crown Ether 5	50
3.9. Synthesis of Precursor 6a	51
3.10. Synthesis of Crown Ether 6	52
3.11. Synthesis of Precursor 7a	53
3.12. Synthesis of Crown ether 7	54
3.13. Synthesis of Crown Forming Agent	55
3.14. Synthesis of Precursor 2a	56
3.15. Synthesis of Precursor 2b	57
3.16. Synthesis of Precursor 2c	58
3.17. Synthesis of Crown Ether 2	59
4.1. Crown Ether Synthesis: Step 1	64
4.2. Crown Ether Synthesis: Step 2	64
4.3. Crown Ether 2: Additional steps	65
5.1. Additional receptors for measurement	68
5.2. Nitrogen lone pair upon complexation - comparison	69
5.3. Absorption KCl titration spectra for Crown Ether 4	70
5.4. Double logarithmic Benesi-Hildebrand plot for Crown Ether 4	71
5.5. Absorption KCl Titration - Crown Ether 1	72
5.6. Absorption KCl Titration - Crown Ether 3	73
5.7. Absorption KCl Titration - Crown Ether 4	74
5.8. Absorption KCl Titration - Crown Ether 5	75
5.9. Absorption KCl Titration - Crown Ether 6	76
5.10. Absorption KCl Titration - Crown Ether 7	77
5.11. Absorption Absorption KCl titration spectra for Methoxyethoxy Crown Ether	78
5.12. Absorption Absorption KCl titration spectra for Triazacryptand	79
5.13. Cross Sensitivity - Crown Ether 4	81
5.14. Fluorescence spectrometry - Crown Ether 7	82
6.1. Outlook - Possible structures	86
A.1. ¹ H-NMR spectrum of compound 1	100

List of Figures

A.2.	¹ H-NMR spectrum of precursor 3a	101
A.3.	¹ H-NMR spectrum of crown ether 3	102
A.4.	¹ H-NMR spectrum of precursor 4a	103
A.5.	¹ H-NMR spectrum of crown ether 4	104
A.6.	¹ H-NMR spectrum of precursor 5a	105
A.7.	¹ H-NMR spectrum of crown ether 5	106
A.8.	¹ H-NMR spectrum of precursor 6a	107
A.9.	¹ H-NMR spectrum of crown ether 6	108
A.10.	¹ H-NMR spectrum of precursor 7a	109
A.11.	¹ H-NMR spectrum of crown ether 7	110
A.12.	¹ H-NMR spectrum of Crown Forming Agent	111
A.13.	¹ H-NMR spectrum of precursor 2a	112
A.14.	¹ H-NMR spectrum of precursor 2b	113
A.15.	¹ H-NMR spectrum of precursor 2c	114
B.1.	Crown Ether 1 - Zoomed response peak	115
B.2.	Crown Ether 3 - Zoomed response peak	116
B.3.	Crown Ether 4 - Zoomed response peak	116
B.4.	Crown Ether 5 - Zoomed response peak	117
B.5.	Crown Ether 6 - Zoomed response peak	117
B.6.	Crown Ether 7 - Zoomed response peak	118
B.7.	Methoxyethoxy Crown Ether - Zoomed response peak	118
B.8.	Triazacryptand - Zoomed response peak	119
B.9.	Crown Ether 1 - Cross Sensitivity	119
B.10.	Crown Ether 5 - Cross Sensitivity	120
B.11.	Crown Ether 6 - Cross Sensitivity	120
B.12.	Methoxyethoxy Crown Ether - Cross Sensitivity	121
B.13.	Triazacryptand - Cross Sensitivity	121
C.1.	Crown Ether 1 - Fluorescence	123
C.2.	Crown Ether 3 - Fluorescence	124
C.3.	Crown Ether 5 - Fluorescence	124
C.4.	Crown Ether 6 - Fluorescence	125
C.5.	Methoxyethoxy Crown Ether - Fluorescence	125
C.6.	Triazacryptand - Fluorescence	126

Part I.
Introduction

1. Theoretical Background

The following section about luminescence is based on references [1, 2] and only additional sources will be referenced separately.

1.1. Luminescence

Luminescence is a word used for the emission of infrared, visible or ultraviolet light from an electronically excited species. The word “luminescenz” was first used by Eilhardt Wiedemann in 1888 to be used for “all those phenomena of light which are not solely conditioned by the rise in temperature”. In this case the distinction between “cold light” caused by luminescence and “hot light” caused by incandescence is essential. Compounds that exhibit luminescence can be very different and are generally divided into three groups: organic compounds (hydrocarbons, fluoresceins, coumarins, amino acids etc.), inorganic compounds (lanthanide ions, doped glasses, crystals etc.) and organometallic compounds (ruthenium complexes, lanthanide ion complexes, complexes with chelating flourogenic agents etc.). Fluorescence and phosphorescence are two particular cases of photoluminescence. Photoluminescence describes the process of emitting photons as part of the de-excitation process. However there is a variety of other processes that can occur when light interacts with matter (see fig. 1.1). Once a molecule is excited by absorption of light it may return to its ground state through fluorescence emission. However many other de-excitation processes are also possible: internal conversion (direct return to the ground state without fluorescence emission), intersystem crossing (may be followed by phosphorescence emission), intermolecular charge transfer or conformation change. These de-excitation processes can compete with fluorescence emission granted they occur within a time-scale that is comparable to the time the molecule stays in an excited state.

1. Theoretical Background

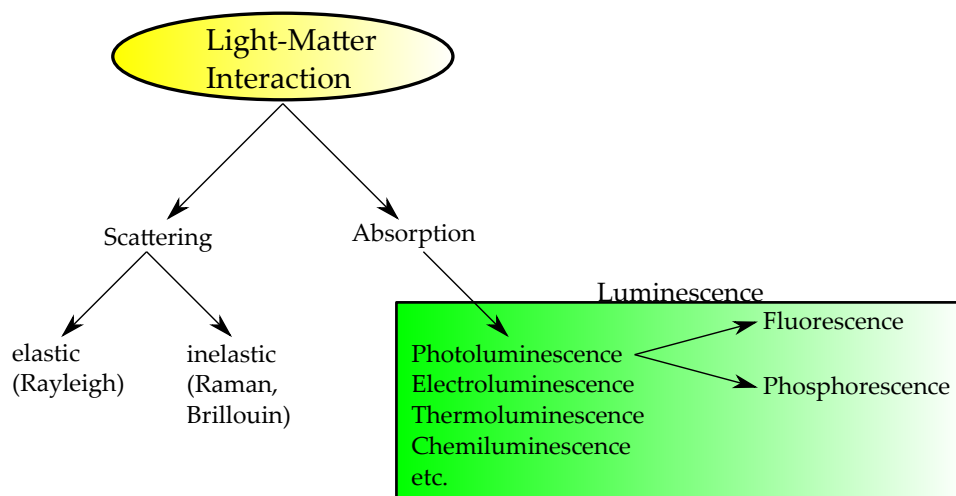


Figure 1.1.: Processes of light-matter interactions

1.1.1. Absorption of UV-Visible Light

An electronic transition occurs when an electron of a molecule in its ground state is promoted to an energetically higher unoccupied orbital. This process is induced by the absorption of light. There are different kinds of orbitals that can be distinguished by the nature of the bond it corresponds to. A σ orbital corresponds to a σ -bond (either one s- and one atomic p-orbital or two atomic p-orbitals overlapping) and a π orbital is formed by a π -bond (two atomic p-orbitals overlapping laterally). Furthermore molecules may also possess non-bonding electrons that are usually located on heteroatoms such as oxygen or nitrogen. The orbital of these non-bonding electrons is called n orbital. By absorption of a photon with the appropriate energy an electron in a π orbital can be promoted to an anti-bonding orbital π^* which is denoted with $\pi \rightarrow \pi^*$. The promotion of an electron in an n orbital to a π^* orbital is also possible and is denoted $n \rightarrow \pi^*$. Promoting a σ electron to an excited state is energetically much less favorable and is not considered here. The corresponding energy for these electronic transitions are in the following order:

$$n \rightarrow \pi^* < \pi \rightarrow \pi^* < \sigma \rightarrow \pi^* < \sigma \rightarrow \sigma^* \quad (1.1)$$

1.1. Luminescence

All possible possible energy state transitions are depicted in fig. 1.2.

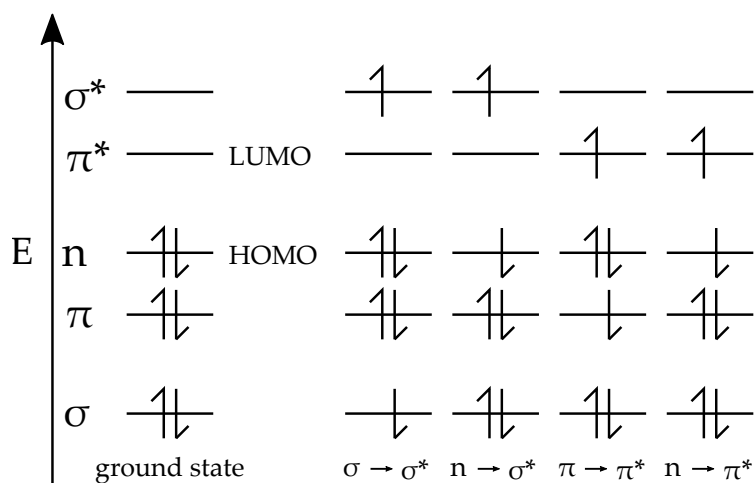


Figure 1.2.: All possible electronic transitions

The most important orbitals in fluorescence and absorption spectroscopy are called HOMO (Highest Occupied Molecular Orbital) and LUMO (Lowest Unoccupied Molecular Orbital). Both of these only refer to the ground state of the molecule. Usually an electronic transition is the promotion of an electron in the highest occupied molecular orbital to one of the unoccupied molecular orbitals. When one of the electrons (with opposite spins) in a ground state orbital is promoted to an unoccupied orbital of higher energy, its spin usually remains unchanged. This results in a total spin quantum number of zero ($S = \sum_i s_i$ with $s_i = +\frac{1}{2}$ or $-\frac{1}{2}$). The multiplicity $M = 2S + 1$ of both the ground state and the excited state equal one which is called *singlet state*. Aside from singlet-singlet transitions it is also possible for an excited molecule to undergo a conversion where the promoted electron changes its spin. Since in this state there are two electrons with parallel spin the molecule's spin quantum number S is one which in turn means that its multiplicity M is three. This state is a so-called *triplet-state* as it exhibits three different states of equal energy. *Hund's Rule* says that a triplet state is energetically lower than a singlet state. A visual representation of a singlet state and a triplet state on an energetic level can be seen in fig. 1.3.

The efficiency with which a molecule can absorb photons of a certain wavelength

1. Theoretical Background

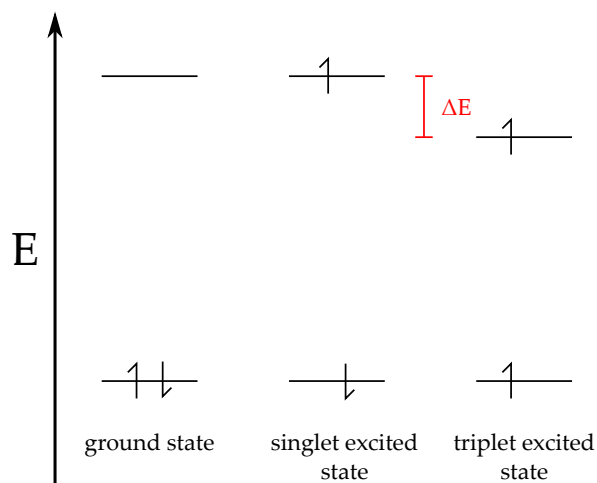


Figure 1.3.: Singlet state vs. triplet state

λ is characterized by the absorbance $A(\lambda)$ or the transmittance $T(\lambda)$. They are defined as

$$A(\lambda) = \log \frac{I_{\lambda}^0}{I_{\lambda}} = -\log T(\lambda) \quad (1.2)$$

where I_{λ}^0 is the intensity of a light beam entering the medium and I_{λ} the intensity of the beam exiting the light absorbing medium. In many cases the absorbance can be described with the *Beer-Lambert-Law*

$$A(\lambda) = \log \frac{I_{\lambda}^0}{I_{\lambda}} = \epsilon(\lambda)cd \quad (1.3)$$

where as $\epsilon(\lambda)$ stands for the molar decadic absorption coefficient (usually $\text{L mol}^{-1} \text{cm}^{-1}$), c is the absorbing species' concentration (mol L^{-1}) and d is the thickness of the absorbing medium (cm). According to IUPAC³ the decadic $\epsilon(\lambda)$ is the “linear decadic absorbance divided by the optical path length through the sample divided by the amount concentration”. Generally, a high $\epsilon(\lambda)$ means a high absorption / attenuation at a certain wavelength.

1.1. Luminescence

1.1.2. Forbidden Transitions

For absorption transitions there are two important selection rules that are called spin-forbidden transitions and symmetry forbidden transitions.

Spin-forbidden transitions: While transitions between alike states like singlet-singlet transitions or triplet-triplet transitions are allowed transitions between different multiplicities are forbidden. However, there is a weak interaction between different multiplicities' wave-functions due to spin-orbit coupling. That means that a singlet-state wave-function also contains a small part of a triplet state wave-function and vice-versa. This results in a small however non-negligible transition between singlet and triplet. Although the molar absorption coefficients of these transitions are very small they can still be observed. Due to this spin-orbit coupling intersystem crossing (see fig. 1.5) is possible. The efficiency of this coupling increases with the atomic number of the partaking atoms which results in heavy atoms being favorable for spin-forbidden transitions.

Symmetry-forbidden transitions: Symmetry can also be a factor for an electronic transition being forbidden. However it is still possible to observe symmetry-forbidden transitions due to molecular vibrations that depart the molecule from perfect symmetry. This effect is called vibronic coupling.

1.1.3. The Franck-Codon Principle

The motions of electrons are much faster and rapid than those of atoms in a molecule. This is according to the Born-Oppenheimer approximation.⁴ It takes around 10^{-15} s to promote an electron to an anti-bonding orbital. This process is very quick in comparison to the characteristic time for molecular vibrations which is in the range of 10^{-12} s to 10^{-10} s. The Franck-Codon principle is based upon this circumstance. It is assumed that the transition of an electron occurs without any positional changes of the atoms in a molecule. This is a so called vertical transition and results in a Franck-Codon state. In fig. 1.4 the potential energy curve is plotted as a function of nuclear configuration which can be described as a Morse function. The width of an absorption band depends on two factors: homogeneous and inhomogeneous broadening. Homogeneous broadening is caused addition vibrational sublevels withing each electron state.

1. Theoretical Background

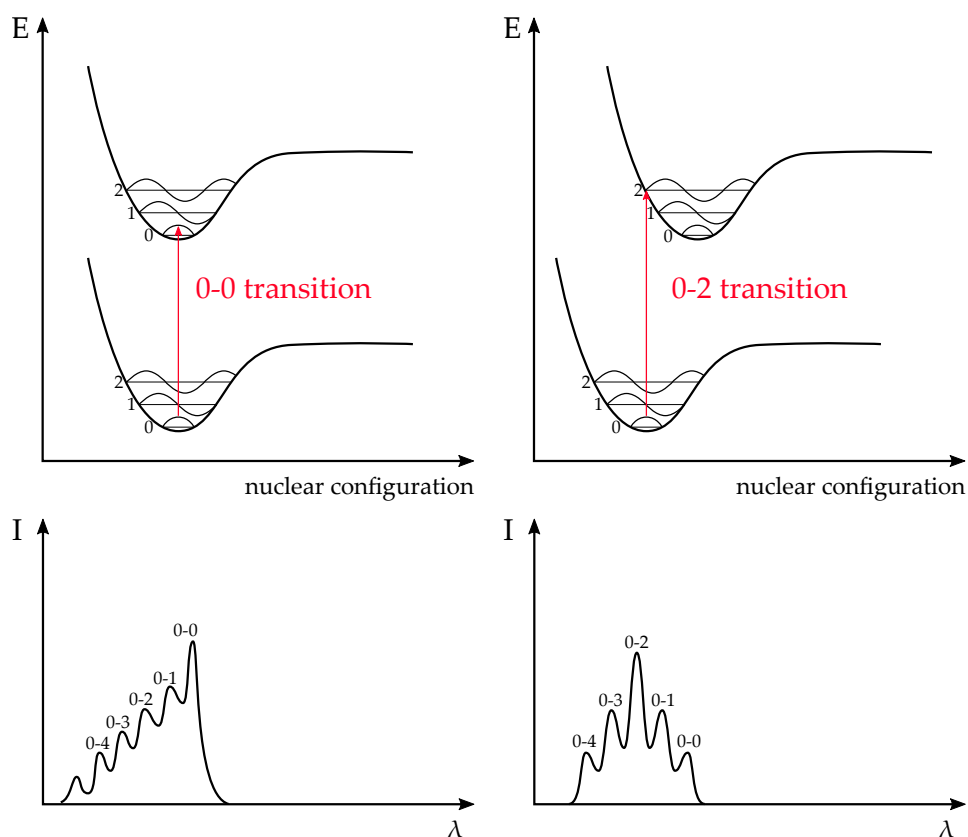


Figure 1.4.: Top: Potential energy diagrams with vertical transitions. Bottom: Shape of absorption diagrams

Inhomogeneous broadening is caused by changes and fluctuations in the solvent shell of the molecule. These broadening effects also exist for emission spectra.

1.1.4. Radiative and Non-Radiative Transitions between Electronic States

The Perrin-Jablonski diagram (fig. 1.5) is a great tool for visualizing the processes between an electron's initial excitation and return to ground state: photon absorption, internal conversion, fluorescence, intersystem crossing, phosphorescence, delayed fluorescence and triplet-triplet transitions. The singlet electron

1.1. Luminescence

states are denoted as S_0 , S_1 etc. and the triplet electronic states as T_1 and T_2 . All electronic states possess additional vibrational energy levels. The vertical arrows start at the lowest vibrational level of S_0 as the grand majority of electrons are in this state at room temperature.

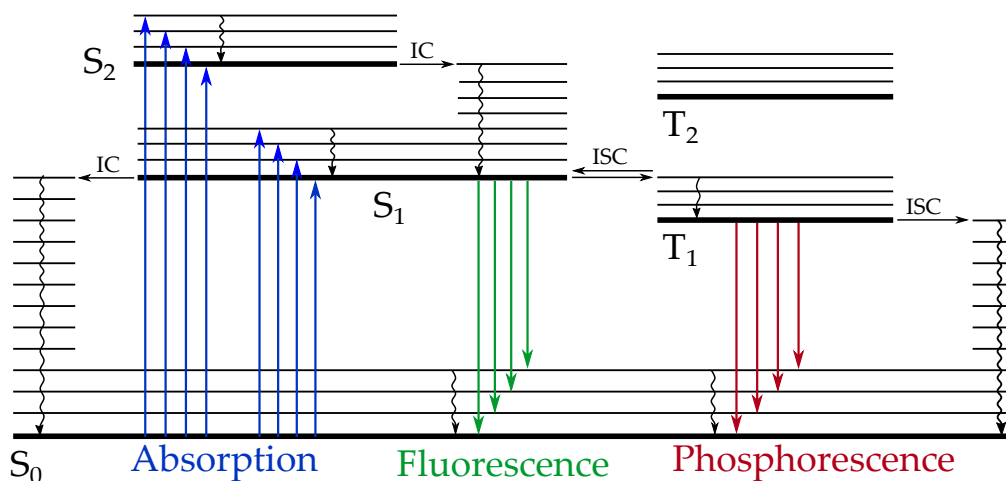


Figure 1.5.: Perrin-Jablonski diagram

Internal Conversion and Vibrational Relaxation

Internal conversion (IC) is a non-radiative process occurring between two electronic states with the same spin multiplicity M . If the molecule is in solution then the internal conversion is followed by vibrational relaxation to the lowest vibrational level of the final electronic state. During vibrational relaxation the excess energy can be transferred to surrounding solvent molecules. This vibrational relaxation takes place in a time-scale of 10^{-13} s to 10^{-11} s. Internal conversion between S_1 and S_0 is in theory possible however this process competes with photon emission (fluorescence) and intersystem crossing from which emission of photons (phosphorescence) may also occur. The smaller the energy gap between two electronic states the more efficient is the internal conversion process.

1. Theoretical Background

Fluorescence

A $S_1 \rightarrow S_0$ relaxation that is accompanied by the emission of photons is called fluorescence. Apart from a few exceptions fluorescence always occurs between S_1 and S_0 and is therefore independent of the excitation wavelength. Generally the fluorescence emission is always at higher wavelengths and lower energy than its excitation wavelength (Stokes rule). This is due to the loss of energy caused by vibrational relaxation (see fig. 1.5). Contrary to the Stokes rule it is often possible to observe a small overlap in absorption and emission bands. This is due to the fact that at room temperature a small number of electrons occupy vibrational levels higher than zero in the ground state and even in the excited state. With lower temperatures this overlap of absorption and excitation bands should minimize.

Intersystem Crossing

Intersystem crossing (ISC) is a non-radiative process between two vibrational levels of the same energy that belong to different multiplicities. An example for intersystem crossing is the transition $S_1 \rightarrow T_n$ from the lowest vibrational level in S_1 to the energetically equivalent vibrational level in T_n . Intersystem crossing takes place in 10^{-9} s to 10^{-7} s and competes with other de-excitation processes such as fluorescence and internal conversion $S_1 \rightarrow S_0$. Changing the state of multiplicity M is in principle forbidden however the spin-orbit coupling may be large so that intersystem crossing is still observed (see section 1.1.2).

Phosphorescence

There are two possible paths of de-excitation from the triplet state T_1 : radiative transition (phosphorescence) and non-radiative transition. Typically non-radiative transitions are favored however decreasing the temperature can increase the amount of radiative transition. Furthermore the time an electron stays in the T_1 state (lifetime) is considerably larger than the lifetimes in S_1 . This is due to the forbidden nature of the intersystem crossing process which makes electron in T_1 become effectively “trapped” in this electronic state. Thus phosphorescence can be observed in significantly large time frames than fluorescence.

1.1. Luminescence

Also phosphorescence exhibits higher wavelengths than fluorescence due to T_1 being energetically lower than S_1 .

Delayed Fluorescence

There are two ways how reverse intersystem crossing $T_1 \rightarrow S_1$ can occur: Via thermal activation or via triplet-triplet annihilation. When the energy difference between T_1 and S_1 is low enough it is possible for the electron to undergo reverse intersystem crossing via thermal activation. Since this electron has resided in T_1 state for a significant amount of time the resulting fluorescence is delayed. The efficiency of this thermally activated reverse intersystem crossing increases with temperature. When the solution is of high enough chromophore concentration a collision between two molecules in T_1 state can provide enough energy to cause one of the excited electrons to undergo reverse intersystem crossing and return to the S_1 state. This process is called triplet-triplet annihilation. The resulting fluorescence is also delayed due to the electron's prior residence in T_1 state.

Triplet-Triplet Transitions

An electron in T_1 state can absorb photons of a different wavelength and transition into a higher T_n state. This is due to the fact that triplet-triplet transitions are spin-allowed.

Table 1.1.: Luminescence: characteristic times

process	characteristic time
absorption	10^{-15} s
vibrational relaxation	10^{-12} s to 10^{-10} s
lifetime of the excited state S_1	10^{-10} s to 10^{-7} s
intersystem crossing	10^{-10} s to 10^{-8} s
internal conversion	10^{-11} s to 10^{-9} s
lifetime of the excited state T_1	10^{-6} s to 1 s

1. Theoretical Background

1.1.5. Intermolecular De-Excitation Processes

Aside from intrinsic de-excitation processes there are also intermolecular de-excitation processes. A process that leads to a decrease in fluorescence is generally referred to as *quenching*. There are several known intermolecular processes which can lead to quenching such as photoinduced electron transfer (PET), photoinduced proton transfer (PPT), formation of excimers / exciplexes or collision with heavy atoms. It is important to realize that these processes do not alter the chemical configuration of an excited molecule but rather quench its luminescence. All quenching mechanisms can be divided into two categories: static quenching and dynamic quenching. For describing the quenching mechanism the excited molecule is denoted as M^* and the quenching molecule as Q .

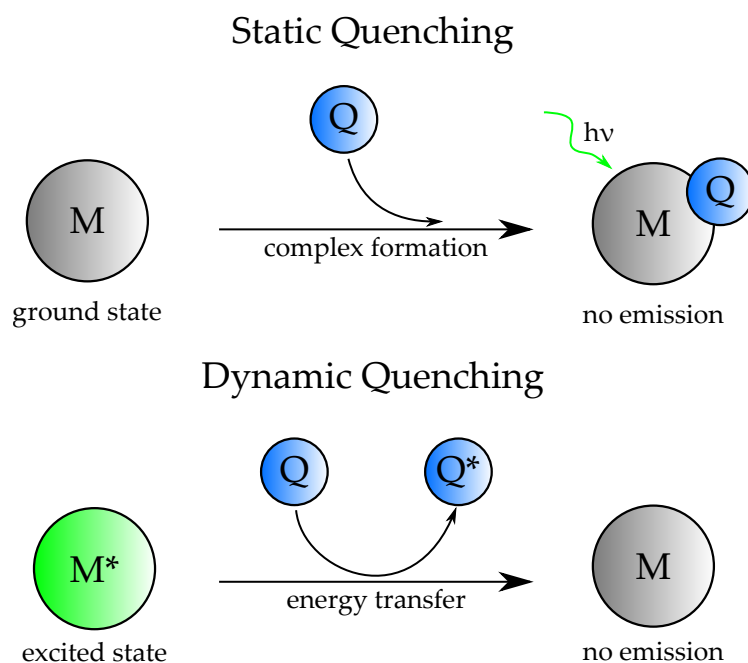


Figure 1.6.: Static vs. dynamic quenching

Static quenching takes place when the molecule M and the quenching molecule Q form a complex that shows no luminescence emission. This results in a reduction of the concentration of the fluorophore M which in turn

1.1. Luminescence

decreases the luminescence intensity. Static quenching can be mathematically described as

$$\frac{I_0}{I} = 1 + K_a[Q] \quad (1.4)$$

with K_a being the association constant of the MQ complex and $[Q]$ being the concentration of the quenching molecule Q . In static quenching the lifetime of the fluorophore stays unaffected.

Dynamic quenching describes the collision between the excited molecule M^* and the quenching molecule Q . It is therefore a diffusion rate controlled process. During dynamic quenching the excited molecule M^* transfers its energy to the quenching molecule Q which causes the molecule M to return to its ground state without photon emission. Since in dynamic quenching the rate constant is time dependent both the fluorescence intensity and the lifetime are affected. Dynamic quenching can be mathematically described as

$$\frac{I_0}{I} = \frac{\tau_0}{\tau} = 1 + K_{SV}[Q] = 1 + k_q\tau_0[Q] \quad (1.5)$$

with k_q being the bimolecular quenching constant, τ_0 the unquenched lifetime of the fluorophore and K_{SV} being the Stern-Volmer constant. A Stern-Volmer plot of both static and dynamic quenching as well as both combined can be seen in fig. 1.7.

Photoinduced Electron Transfer

The photoinduced electron transfer (PET) is one of the mechanisms responsible for fluorescence quenching. During this quenching mechanism the excited fluorophore either accepts or receives an electron from a quenching molecule. Which mechanism takes place is determined by the HOMO and LUMO orbitals respective to the same orbitals of the excited molecule. An electron rich quenching with a higher LUMO than the excited molecule's HOMO will donate an electron

1. Theoretical Background

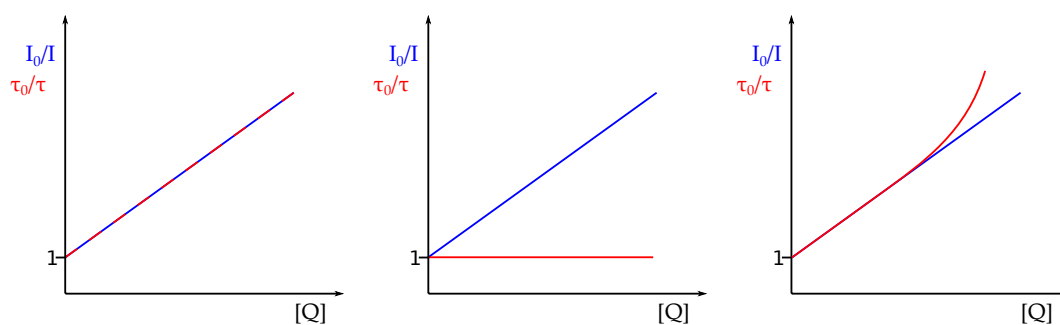


Figure 1.7.: Stern-Volmer plots - Left: dynamic quenching Middle: static quenching Right: dynamic and static quenching

to the partially occupied HOMO of the excited molecule thus quenching its fluorescence. Conversely, when the quenching molecule's HOMO and LUMO are both lower than their excited molecule's counterparts the excited molecule donates an electron to the lower lying LUMO of the quenching molecule. This also quenches the excited molecule's fluorescence.

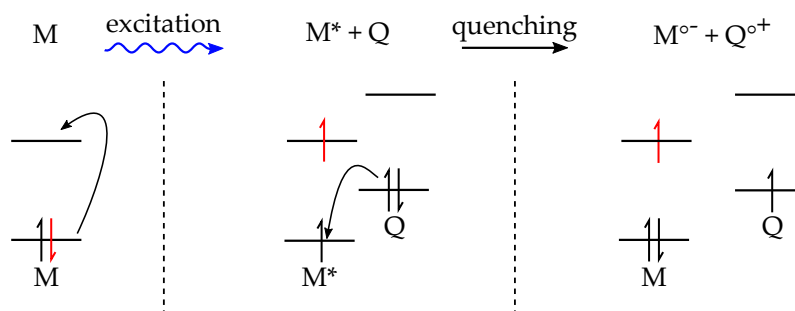


Figure 1.8.: Photoinduced electron transfer

1.2. Host Guest Chemistry

1.2. Host Guest Chemistry

In 1987 Lehn, Cram and Pedersen won the Nobel prize for their leading discoveries in supramolecular chemistry.⁵ This kick-started the rapid developing research field of supramolecular chemistry. The key component of optical ion sensors is the receptor which belongs to an area of research that is called *host guest chemistry*. Host guest chemistry describes the formation of a complex that is formed between two ions or molecules through non-covalent binding. These molecules / ions are held together because of their complementary structural relationship. In the last few decades this concept has been applied numerous times in a lot of different areas of research such as catalysis, sensors, electronic devices, nanomedicine, functional materials etc..⁶⁻¹⁰ Usually the host moiety is an organic molecule that provides a cavity and a binding site for the guest component. The guest moiety can be any molecule or ion that can fit into the cavity of the host and form a non-covalent binding relationship. Host moieties are usually highly specialized molecules that are specifically designed to accommodate only a specific type of guest compound. After the last few decades an enormous amount of research effort has gone into this area and a lot of different types of hosts have already been developed. Among those are cyclodextrines,¹¹ cyclophanes,¹² calixarenes¹³ and crown ethers¹⁴ to name a few.

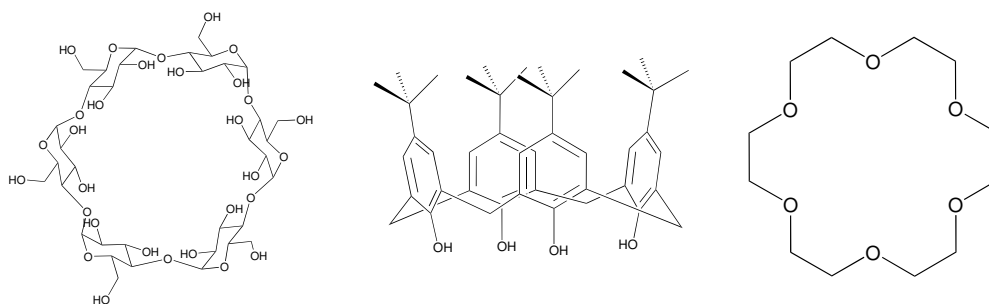


Figure 1.9.: Left: Cyclodextrine Middle: Calixarene Right: Crown ether

Since the interactions between host and guest are non-covalent there needs to be some form of binding interaction between those in order to form a complex. Usually this includes coulomb forces in case of charged compounds, Van-der-Waals forces for uncharged compounds or H-bonding for suitable molecules. Because

1. Theoretical Background

of this non-covalent linkage by relatively weak interactions supramolecular materials have a reversible character which allows the association and dissociation processes at low energy cost.¹⁵ Another important factor is the complexation enthalpy and entropy which contribute to the solvophobic force.¹⁶ Since guest molecules are commonly solvated they are surrounded by a solvation shell of solvent molecules. In order for the guest to form a complex with the host the former must lose its solvent shell which is accompanied by an increase in entropy ΔS_0 . This change in entropy also contributes to a change in the Gibbs free energy ΔG_0 . Usually the chance of a host-guest complex formation decreases with increasing solvent polarity. This is due to the increased solvation forces of the host molecule.¹⁷

The stability of a host-guest complex can be described with stability constant K_s . This constant is defined by a simple equilibrium equation between the host H , the guest G and the host-guest complex HG .



$$K_s = \frac{[HG]_{eq}}{[H]_{eq}[G]_{eq}} \quad (1.7)$$

Another very useful constant is the dissociation constant K_d which is the inverse of the association / stability constant K_s .

$$K_d = \frac{[H]_{eq}[G]_{eq}}{[HG]_{eq}} \quad (1.8)$$

The benefit of this transformation is the fact that similarly to the pKs it directly correlates to a guest concentration $[G]_{eq}$ when $\frac{[H]_{eq}}{[HG]_{eq}}$ equal one. Hence K_d is a great value to compare different complexation affinities of host-guest pairs. K_d can be determined via titration of the host with guest molecule followed by detection of the complexed and the uncomplexed compound. This can be done via a variety of measurement methods such as measurement of electrochemical potential,¹⁸ mass spectroscopy,¹⁹ NMR and UV-VIS spectroscopy.²⁰

1.2. Host Guest Chemistry

1.2.1. History of Crown Ethers and Crown-type Ligands

Crown ethers

The first synthetic ionophores were described by Pedersen²¹ which were simply denoted [18]-crown-6 and dibenzol[18]-crown-6 as in contrast to their cumbersome IUPAC names (see fig. 1.10). “dibenzo” stands for the benzene moieties annexed to the ring while “[18]” stands for the number of ring atoms. The class is specified as “crown” and is followed the number of heteroatoms in the the ring - in this case “6”. Nowadays the above mentioned Pedersen nomenclature²² is universally accepted and serves as a rough description of cyclic polyethers in which the oxygen atoms are typically separated by ethano bridges.

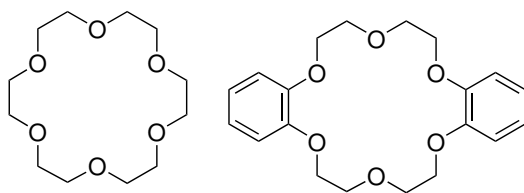


Figure 1.10.: Left: [18]-crown-6 Right: dibenzol[18]-crown-6

Since then there have been constant research activities around *crown ethers* (*coronands*). These research efforts resulted in a large variety of crown ethers that vary in size, distribution and type of heteroatoms.

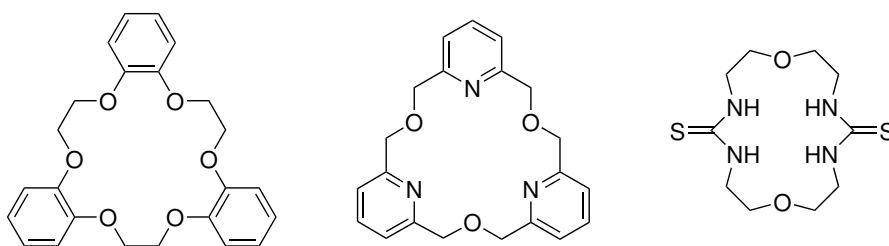


Figure 1.11.: Various types of crown ethers

1. Theoretical Background

Cryptands

The bridging of classical monocyclic crown ethers with an additional oligoether chain produced a new bicyclic type of ligand.²³ Their discoverer, Lehn, named them “*cryptands*” (greek word cryptos = cave) to describe their topological shape.²⁴ A conventional cryptand consists of two bridgehead nitrogen atoms which are connected to three oligoether chains that can vary in length and number of donor moieties. A simple notation is used to describe cryptands: it is derived from the number of bridges and oxygen donor atoms in each bridge. Thus the term “[2.2.2]cryptand” is used for the most common member of the cryptand family which is depicted in fig. 1.12. Various forms of cryptands have since been synthesized such as nitrogen-lacking cryptands,²⁵ sulfur analogous cryptands²⁶ or cryptands with heteroatomic rings as replacement for donor sites.²⁷

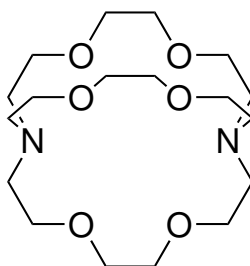


Figure 1.12.: The structure of a [2.2.2]-cryptand

Podands

“*Podand*” is a term used for open-chain crown type compounds and cryptands. The first open-chain crown compound with glyme-like structure (glyme = oligoethylene glycol dimethyl ethers) was the bis(quinoline)oligo-ether.²⁸ In comparison to its cyclic counterparts isolation of stoichiometric alkali and earth alkali metal complexes were easily obtained. This podand is commercially available as “Kryptofix-5”. It contains two quinoline residues at both ends of a glyme polyether moiety.

This construction principle is based on stiffening the polyether chain with rigid terminal end groups. A variety of end groups can be incorporated to modify

1.2. Host Guest Chemistry

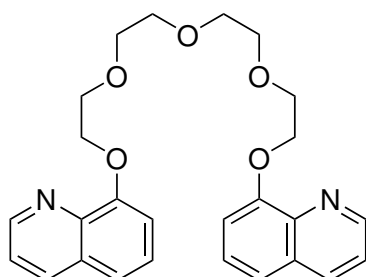


Figure 1.13.: Kryptofix-5 - A common podand

the “stiffness” of the polyether chain. Besides 8-quinoline, 2-methoxyphenol, 2-nitrophenol and salicylic ester have proven to be particularly good donor end groups. This donor end-group concept²⁹ was then combined with the cryptand idea which resulted in the synthesis of three- and four-armed open chain cryptands.³⁰ Overall, podands comprise all ligands that possess an open-chain oligoether moiety or consist of chains bearing heteroatoms in a particular arrangement.

Podandocoronands

The class of “*podandocoronands*” (also known as lariat ethers) is a structural borderline case of all three ligand classes described in this section. The idea behind podandocoronands was to combine some of the individual features of the other ligand types.³¹ The donor-active side arms dictate whether a spherical cryptand-type structure or a two-dimensional crown ether type structure is favored.

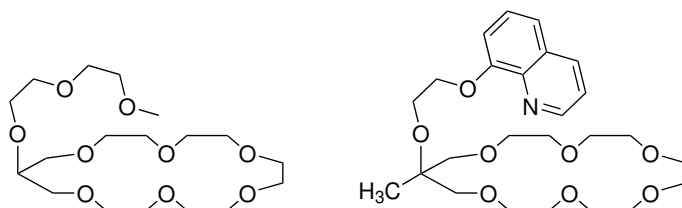


Figure 1.14.: Podandocoronands - The additional sidearms increase the complex stability with alkali- and earth alkali cations

1. Theoretical Background

Oxocrowns and Spherands

The principle of oxocrowns³² was based on incorporating functional groups as donors. Despite the absence of ether oxygen atoms oxocrowns retain their crown ether properties and thus their complexation properties. In spherands donor groups are attached to a rigid framework which results in a spherical complex arrangement.³³ They are counted among the most rigid arrangements of donor groups.

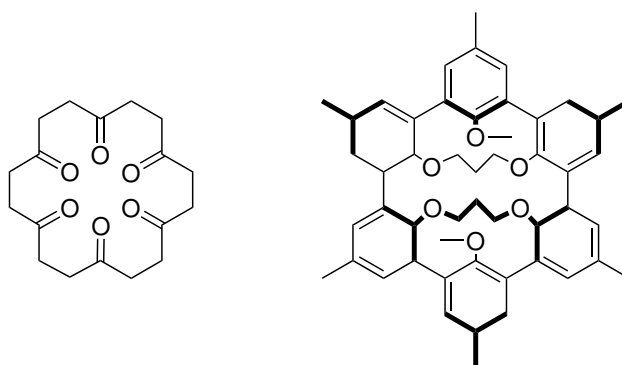


Figure 1.15.: Left: Oxocrown. Right: Spherand

1.2.2. Properties of Crown Ethers

Hydrophilicity / Lipophilicity

Crown ethers and all other crown-type ligands consist of a series of lipophilic (alkyl chains / methylene groups) as well as hydrophilic groups (ether oxygen, nitrogen atoms etc.). Thus their behavior in a hydrophilic medium is very similar to that of a (molecular) fat droplet in water. The hydrophobic moieties are centered inwards while the hydrophilic structures are arranged at the outer edge of the molecule. Conversely, this polarization is shifted in a lipophilic medium. The lipophobic moieties are then shifted toward the molecular center while the lipophilic groups are arranged at the outer edge of the molecule. The crown then behaves like a (molecular) water droplet in oil. While the lipophilic interior is too small for the complexation of a lipophilic guest the hydrophilic

1.2. Host Guest Chemistry

electronegative cavity is perfectly suited to accommodate alkali and earth alkali metal ions provided the sizes are compatible.²⁴

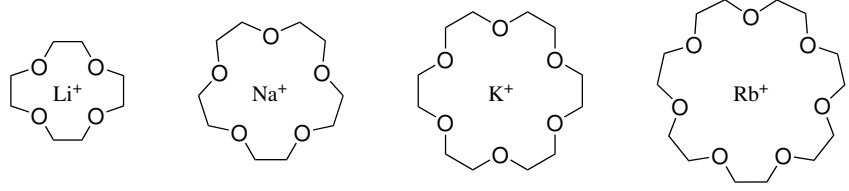
1.2.3. Crown Ethers as Cation Receptors

The high selectivity of crown ethers towards cations can be based on the spatial fit concept which describes the relationship between the diameter of the uncomplexed ion and the diameter of the (hydrophilic) crown ether cavity. In case of the ion being too big or too small for the crown ether cavity the noncovalent binding forces between the crown ether's heteroatoms and the ion are not optimal thus resulting in lower complexation rates and stabilities. Therefore it is important to match the crown ether cavity diameter and the ion diameter accordingly to achieve the optimal complexation interaction. Spatially less fitting cations may be tolerated within certain limits, for example by moving the cation out of the ring plane or small deformation of the ring itself. For drastic diameter discrepancies for example the cation diameter being a lot bigger than the cavity diameter or vice versa sandwich complexes (2:1 stoichiometry) and two-nuclei complexes (1:2) can be formed. Measured complexation constants confirm the excellent fit of K^+ for the 18-crown-6 ring.³⁴ However, as can be seen in table 1.2 the ammonium ion NH_4^+ possesses almost the same ion diameter as the K^+ ion. This possible cross-sensitivity will be briefly discussed in section 1.2.3.

To distinguish between different cations from each other a crown ether has to have differences in their respective complexation stabilities. This discrimination ability towards different cations is expressed in their respective stability constants K_s which is defined by the law of mass equilibrium of the complexation reaction and is always based on a specific solvent.³⁵ If a crown ether displays a high selectivity for several ions (similar of size and charge) but for another group of ions the selectivity is lower one speaks of "plateau selectivity".²⁴ In another case when crown ether clearly distinguishes all foreign ions (irrespective of size and charge) it is called "peak selectivity". Generally one can expect spatially rigid crown ether with a well defined cavity to show peak selectivity behavior.

1. Theoretical Background

Table 1.2.: Uncomplexed ion and crown ether cavity diameters



cation	cation diameter [Å]	crown ether	cavity diameter [Å]
Li ⁺	1.36	[12]crown-4	1.2-1.5
Na ⁺	1.90	[15]crown-5	1.7-2.2
K ⁺	2.66	[18]crown-6	2.6-3.2
NH ₄ ⁺	2.68		
Cs ⁺	3.38	[21]crown-7	3.4-4.3

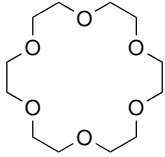
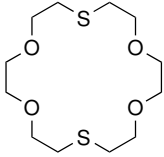
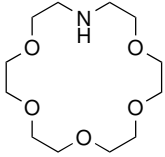
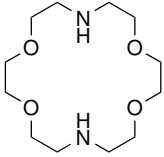
The Concept of Donor-Site Variation

The cavity geometry is not the only factor playing a big part in complexation selectivity.³⁴ An example for this is the incorporation of (soft) sulfur atoms which enhances the complexation of transition metal ions such as Ag⁺ and simultaneously hinders that of alkali metal ions. On the other hand nitrogen plays a mediator role increases the complexation stability of transition metal ions while not drastically decreasing the complexation of alkali metals (see fig. 1.16 for comparison of K_s values). Nitrogen incorporated in the form a pyridine unit seems to favor the complexation of Na⁺ over K⁺.^{36,37} Another example are carbonyl groups of esters and amides which show an affinity towards earth alkali metal ions (Ca²⁺, Sr²⁺). This is in agreement with the higher electrostatic attraction between a twice positively charged ion and the electronegative center of this carbonyl group.^{38,39}

Kinetics and Dynamics of Complexation

The kinetics of complexation are an important factor in understanding the stability and selectivity of crown ether complexes. Complexation and decom-

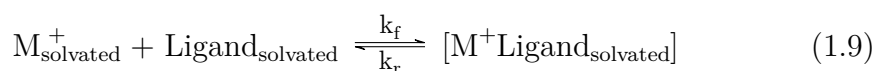
1.2. Host Guest Chemistry

Ligand				
K ⁺ [a]	6.10	1.15	3.90	2.04
Ag ⁺ [b]	1.60	4.34	3.30	7.80

[a] = in metanol, [b] = in water

Figure 1.16.: A comparison of log K_s values of K⁺ and Ag⁺ of 18-crown-6 and its sulfur and nitrogen analogues⁴⁰

plexation in a system composed of ligand, metal and cation can be described by



with k_f being the rate of complex formation and k_r the rate of decomplexation. These two rate constants are directly connected with each other through the stability constant $K_s = \frac{k_f}{k_r}$.

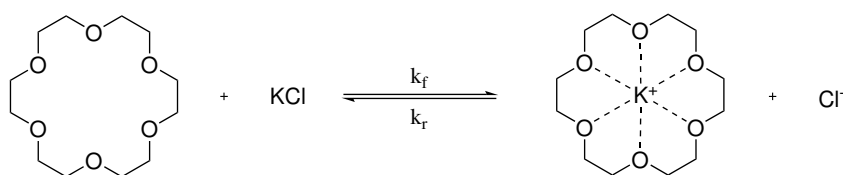


Figure 1.17.: 18-crown-6 complexation of a potassium ion

The process of metal complex formation generally is very fast. However complex formation is not a simple one step reaction between ligand and cation⁴¹ and is often preceded by conformation changes of the ligand and changes in the solvation shell of the ion and within the ligand cavity. A low cation binding

1. Theoretical Background

energy, ligand flexibility and a not too high complex stability favor fast exchange rates. Therefore some of the most stable cryptands bind cations very strongly while also releasing them only slowly.⁴² This is because cryptands envelop the cation three-dimensionally which causes the access of the solvent to be limited. Crown ethers form two-dimensional complex structures and can provide a suitable balance between complex stability and exchange rates / reversibility.⁴³ A comparison of the complexation kinetics of a crown ether and a cryptand can be found in table 1.3.

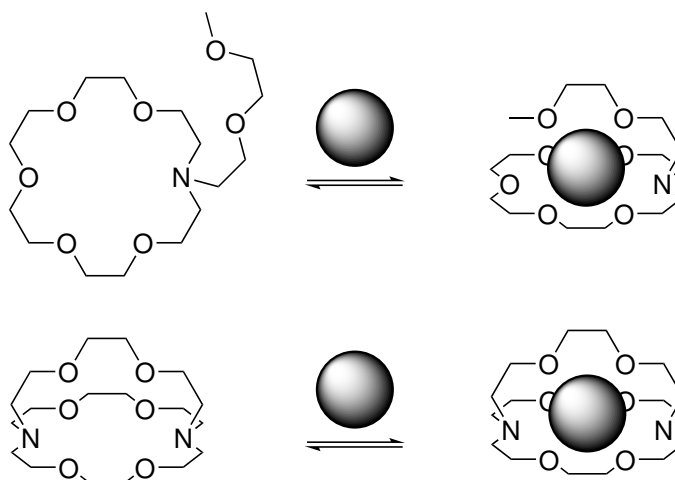


Figure 1.18.: Top: Lariat ether Bottom: Cryptand

Table 1.3.: Complexation and decomplexation rates of 18-crown-6 and [2.2.2]-cryptand compared (KCl in H₂O)¹⁴

Ligand	$k_1 \text{ mol}^{-1} \text{ s}^{-1}$	$k_{-1} \text{ s}^{-1}$	$K_s \text{ mol}^{-1}$	$\log K_s$
18-crown-6	4.8×10^8	3.7×10^6	115	2.06
2.2.2-cryptand	7.5×10^6	38	2.0×10^5	5.3

Lariat ether are modeled to be flexible and dynamic when unbound while also incorporating an enveloping character while complexated (fig. 1.18). Binding constant studies showed clearly that through introduction of a side arm with appropriately placed donors the equilibrium constants were significantly increased.³¹ Another important factor for complexation is the topology. For

1.2. Host Guest Chemistry

example, the smallest molecular cation NH_4^+ is very similar to K^+ in size⁴⁴ (see table 1.2). However there is clear difference in charge distribution between those two. While the charge distribution for K^+ is obviously uniform and spherical the charge distribution of the ammonium ion is tetrahedral accord to its geometry. For 18-crown-6 there is clear difference in selectivity and complexation strength between a potassium ion and an ammonium ion. This is due to one of the hydrogen atoms being out of the planar binding plane of a simple 18-crown-6. It is however possible to coordinate the hydrogen out of plane using cryptands or lariat ethers. These ligand types form three-dimensional complex structures and thus can also bind the fourth hydrogen atom efficiently.

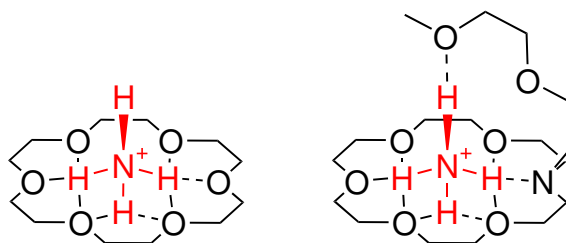


Figure 1.19.: NH_4^+ complexation - Left: planar 18-crown-6 Right: three-dimensional lariat ether

1. Theoretical Background

1.3. Concepts of Sensors

1.3.1. Fluorescent PET Cation Sensors

Sensors of this particular type have been extensively researched and studied.^{45–49} The attachment of a functional group (PET-group) can initiate a redox process between the excited fluorophore and the PET-group thus quenching the fluorophore's fluorescence.

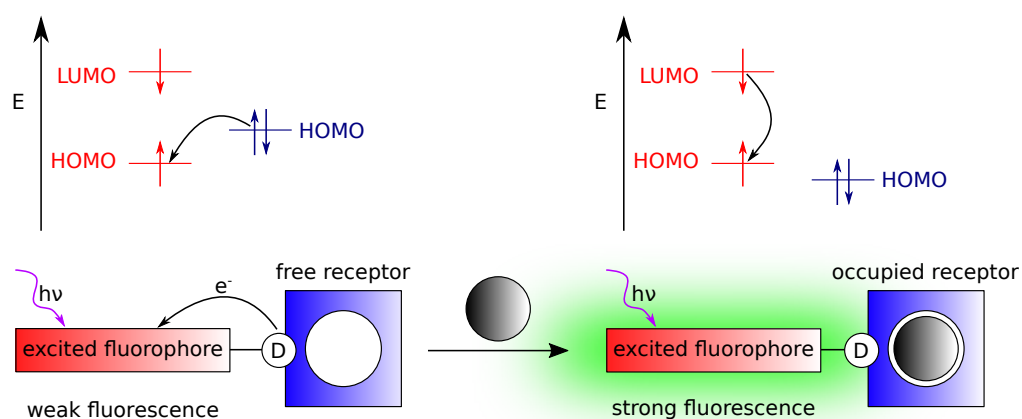


Figure 1.20.: Sensor utilizing PET to increase its fluorescence upon complexation

Usually the receptor acts as donor (e.g. amino group) and the fluorophore is the acceptor. During excitation of the fluorophore an electron is promoted from the HOMO to its LUMO. This enables an uncomplexed receptor to donate one of its electrons in the HOMO to the partially occupied HOMO of the fluorophore. Since radiative de-excitation of the excited fluorophore electron to its ground state is not possible it undergoes the non-radiative process of back electron transfer (BET) to the singly occupied receptor orbital. This in turn results in an effective quenching of the fluorescence. Upon binding of a cation the HOMO of the receptor is lowered so that it is lower in energy than that of the fluorophore. PET is not possible anymore and the can fluorophore de-excite radiatively thus emitting fluorescence. Usually a PET sensor's cation receptor is based on aliphatic or aromatic amines that can act as quenchers. A large variety of PET based sensor system have already been proposed ranging from

1.3. Concepts of Sensors

simple anthracene fluorophore⁵⁰ to more sophisticated and tunable BODIPY fluorophores.⁵¹

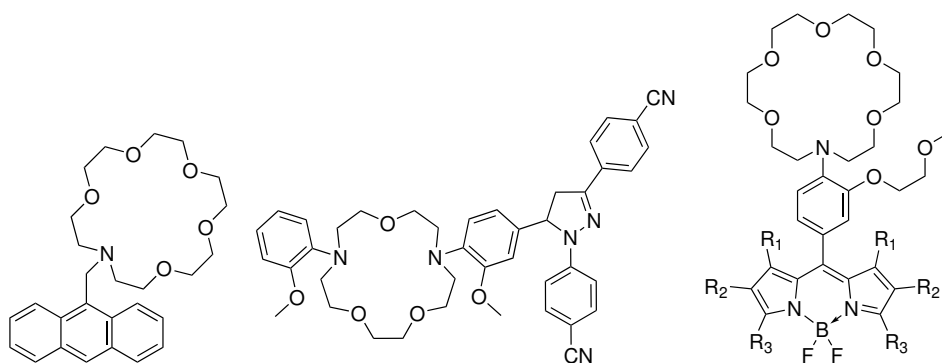


Figure 1.21.: PET sensors - Left: Anthracene fluorophore⁵⁰ Middle: Lariat ether fluorophore⁵² Right: Tunable BODIPY fluorophore⁵¹

1.3.2. Fluorescent PCT Cation Sensors

Aside from electron transfer (PET) fluorophores can also undergo photoinduced charge transfer (PCT). A fluorophore that contains an electron donating (e.g. amino group) and an electron withdrawing group conjugated to it can undergo intramolecular charge transfer when excited by photons. This results in a change of the dipole moment and consequently also a Stokes shift depending on the microenvironment. This effect can also be utilized in polarity probes.⁵³ Furthermore it can be expected that a cation that is in interaction with a donating or accepting moiety also affects the photophysical properties of the fluorophore. When a cation interacts with a donating group of a fluorophore such as an amine it reduces the electron donating character of said group. This results in lowering of the HOMO which in turn causes a blue shift in the absorption spectrum due to the higher energy difference between donor and acceptor orbitals. Conversely, an interaction of a cation with the accepting group reduced its electron-withdrawing character even more. The result is a lowering of the LUMO orbital thus reducing the energy needed to promote an electron. A red-shift in the absorption spectrum can then be expected. Generally, the fluorescence spectra are also shifted in the same directions as the absorption spectra. However the fluorescence shifts are much smaller than

1. Theoretical Background

those in the absorption spectra. This can be explained by the fact that a charge transfer makes an electron donating group more positively polarized. A disruption in the bond between cation and receptor can be the result thus breaking the coordination bond between both. Since the complex between receptor and cation then is not or barely present anymore the fluorescence is only slightly effected and the shift is much weaker than that of the absorption spectrum. Obviously a photoinduced de-complexation can only be possible if the time for the total release of the cation is lower than the lifetime τ of the excited state.

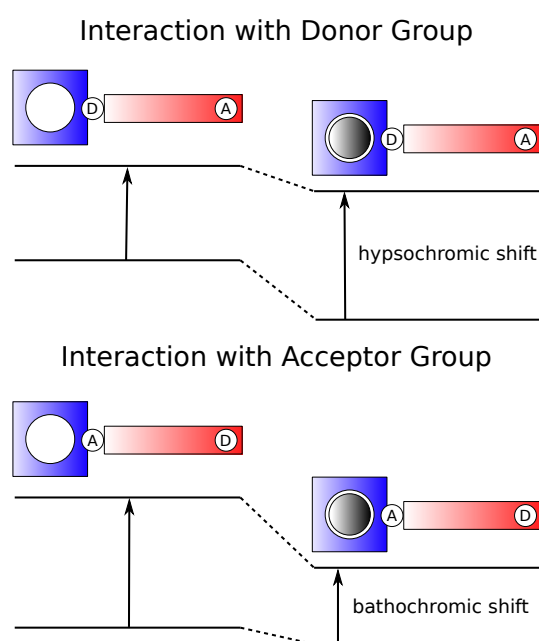


Figure 1.22.: PCT sensors - Spectral shifts due to interactions of electron withdrawing and donating groups with cation

1.3.3. Fluorescent RET Sensors

Resonance Energy Transfer is a non-radiative energy transfer between a donating and an accepting molecule. Often the term FRET (Fluorescence Resonance Energy Transfer) is used, however this term is incorrect since it is not fluorescence that is transferred. This type of energy transfer can occur if the

1.3. Concepts of Sensors

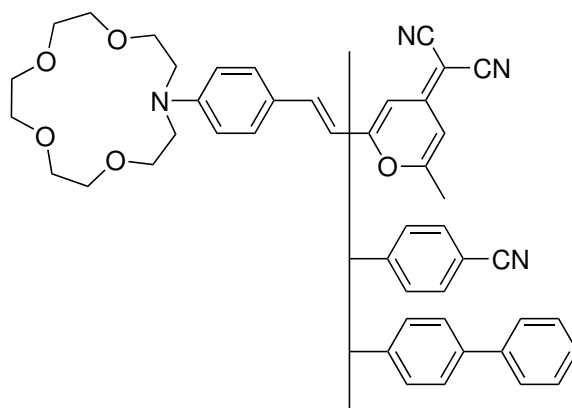


Figure 1.23.: PCT sensors - Various examples of PCT based sensors in which the donor group interacts with the cation

emission spectrum of the donor overlaps with the absorption spectrum of the acceptor. The spectral overlap implies that the donor possesses several vibronic transitions which have the same energy as the transitions of the acceptor - they are thus in *resonance* with each other (fig. 1.24).

RET can arise when an excited state donor interacts with an acceptor molecule which returns the donor to its ground state and the emission may arise from the acceptor molecule. The efficiency of RET generally depends on the three factors: distance between donor and acceptor, spectral overlap of donor and acceptor and the relative orientations of the emission dipole moment of the donor and the acceptor absorption moment.² One example of a RET based sensor is the calixarene based Na^+ sensor developed by Jin.⁵⁴

In the depicted FRET sensor (see fig. 1.25) the emission spectrum of the pyrene group (donor) overlaps with the absorption band of the anthroyloxy group (acceptor). Upon complexation of a Na^+ ion the emission intensity of the anthroyloxy group increase 10-fold confirming an effective energy transfer between the (complexating) ligands. This increase in emission intensity can be explained by the donor and acceptor substituents moving closer in distance upon Na^+ complexation. This allows for a more efficient energy transfer as this mechanism is distance dependent. Other RET sensor system such as the utilization of gold nanoparticles using linked recognition molecules such as proteins or nucleic acids have also been proposed.⁵⁵ Additionally, RET based

1. Theoretical Background

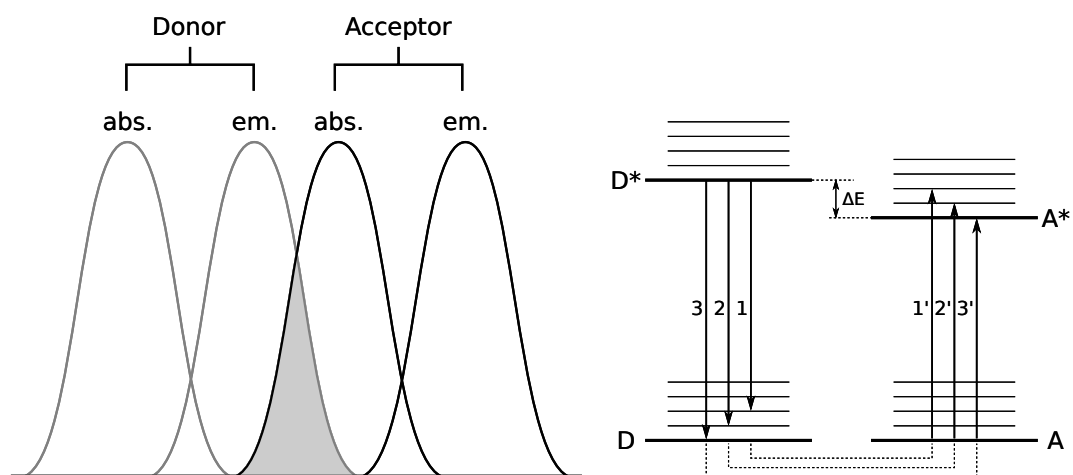


Figure 1.24.: RET - Left: Overlap of absorption and emission spectra between donor and acceptor Right: Resonance transitions between donor and acceptor

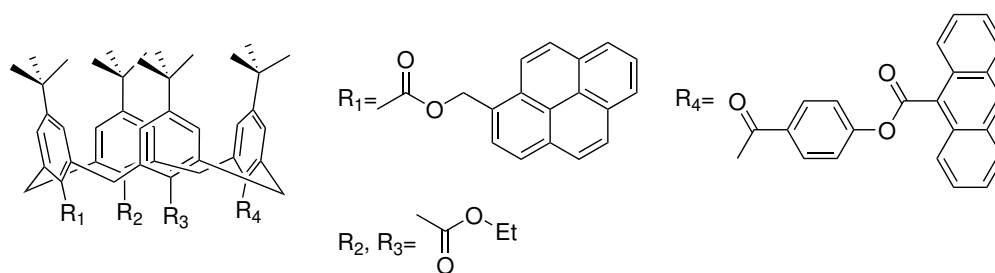


Figure 1.25.: RET sensor - Calixarene based RET sensor with donor (R₁) and acceptor (R₄) moieties

system or often used as a molecular ruler⁵⁶ for detecting structural changes in peptides.

1.4. Determination of Stability Constants

1.4. Determination of Stability Constants

One of the most important characteristics of a supramolecular complex is its complex stability. Therefore the right choice of method to determine this stability constant K_s is of high significance. The first step towards determining a stability constant is to understand how a typical equilibrium in supramolecular chemistry is defined. For the simple case of a 1:1 host-guest stoichiometry the equilibrium can be described as

$$K_s = \frac{[HG]}{[H][G]} \quad (1.10)$$

with $[HG]$ being the concentration of the host-guest complex, $[H]$ being the free host concentration and $[G]$ being the free guest concentration. Often K_s is also often substituted with K_a which stand for association constant. In this case $K_a = \frac{k_f}{k_{-f}}$ with k_f being the forward (formation) rate constant and k_{-f} being the backwards rate constant. For a typical 1:1 host-guest system the equations

$$[H]_0 = [H] + [HG] \quad (1.11)$$

$$[G]_0 = [G] + [HG] \quad (1.12)$$

describe the mass balance between host, guest and host-guest complex. If $[HG]$ was known the remaining concentrations could be determined and thus K_s could easily be obtained by using eq. (1.10). Unfortunately it is generally not possible to determine $[HG]$ in supramolecular complex chemistry experiments. However, there are a few accurate methods to indirectly determine $[HG]$ and thus K_s via titration experiments. Usually this is done by keeping the host concentration $[H]$ constant while varying the guest concentration $[G]$. During the process of this titration the physical properties of the measured system change and are monitored (commonly via spectroscopy). This change can then be plotted as function of guest added to host. The resulting titration curve is generally referred to as *binding isotherm*. This binding isotherm can be fitted with a

1. Theoretical Background

mathematical model based on the (assumed) equilibrium to calculate K_s . The mathematical models are generally based on the idea that a change in $[HG]$ (and therefore also $[H]$ and $[G]$) will induce a change in the physical properties ΔY of the medium.

$$Y = Y_H[H] + Y_G[G] + Y_{HG}[HG] \quad (1.13)$$

$$Y = Y_H f_H + Y_G f_G + Y_{HG} f_{HG} \quad (1.14)$$

When combining eq. (1.14), eqs. (1.11) and (1.12) with the equation for the stability constant (eq. (1.10)) the *general binding isotherm* for a 1:1 host-guest system is received.

$$f_{HG} = \frac{K_a[G]}{1 + K_a[G]} \quad (1.15)$$

Furthermore, assuming $f_{HG} = \frac{[HG]}{[H]_0}$, eq. (1.15) can also be written as

$$[HG] = \frac{[H]_0 K_a [G]}{1 + K_a [G]} \quad (1.16)$$

It is not uncommon to have non-absorbing guest $[G]$ which is also referred to as *silent* guest. This circumstance can be used to simplify eq. (1.14) by substituting $[H]_0 = [H] + [HG]$ as well as $f_{HG} = \frac{[HG]}{[H]_0}$. The resulting equation can be simplified further to

$$\begin{aligned} \Delta Y &= Y_H + \left(\frac{[HG]}{[H]_0} \right) (Y_{HG} - Y_H) \\ &= Y_{\Delta HG} \left(\frac{[HG]}{[H]_0} \right) \end{aligned} \quad (1.17)$$

1.4. Determination of Stability Constants

This is the general equation for a *change in the mole fraction depending on the physical property Y during titration*. Conversely, if the change of ΔY is based on absolute concentrations eq. (1.13) can similarly be rearranged to yield

$$\Delta Y = Y_{\Delta HG} ([HG]) \quad (1.18)$$

Those two equations (eqs. (1.17) and (1.18)) are the basis which can be used to calculate the two unknown parameters (K_s and $Y_{\Delta HG}$) from the two known parameters $[H]_0$ and $[G]_0$. This is done via a non-linear regression of the experimental data. For non-linear regression a computer algorithm guesses values for K_s and $Y_{\Delta HG}$ until the desired fit between the experimental data and eq. (1.18) is obtained. Various technique specific equations are directly derived from eqs. (1.17) and (1.18).⁵⁷⁻⁵⁹

NMR: Changes upon titration

$$\Delta\delta = \delta_{\Delta HG} \left(\frac{[HG]}{[H]_0} \right) \quad (1.19)$$

UV-Vis: Changes upon titration

$$\Delta A_{obs} = \epsilon_{\Delta HG} ([HG]) \quad (1.20)$$

Fluorescence: Changes in fluorescence of host-complex (no dynamic quenching)

$$\Delta F_{obs} = k_{\Delta HG} ([HG]) \quad (1.21)$$

Calorimetry: Heat of transformation upon titration

$$Q = \Delta H_{HG} V ([HG]) \quad (1.22)$$

There are also various ways how to transform the aforementioned equations and expressions can be transformed into linear equations that can then be plotted to obtain K_s via the the knowledge slopes and intercepts. Although these methods have some drawbacks such as distorting the experimental error through linear

1. Theoretical Background

regression^{60,61} or implementing assumptions such as $[G] = [G]_0$ they are still widely used as they can be utilized without the use of advanced computer based algorithms. Among those methods are the popular Benesi-Hildebrandt plot⁶² (known as Lineweaver-Burk plot⁶³ in enzyme kinetics), the Scott / Hanse-Woolf transformations^{64,65} and the Scatchard plot.⁶⁶

Benesi-Hildebrandt plot / Lineweaver-Burk plot:

$$\frac{1}{f_{HG}} = 1 + \frac{1}{K_a[G]} \quad (1.23)$$

$$\frac{1}{\Delta Y} = \frac{1}{Y_{\Delta HG} K_a [G]} + \frac{1}{Y_{\Delta HG}} \quad (1.24)$$

Scott / Hanse-Woolf transformation:

$$\frac{[G]}{f_{HG}} = [G] + \frac{1}{K_a} \quad (1.25)$$

$$\frac{[G]}{\Delta Y} = \frac{1}{Y_{\Delta HG} K_a} + \frac{[G]}{Y_0} \quad (1.26)$$

Scatchard plot:

$$\frac{f_{HG}}{[G]} = K_a - K_a f_{HG} \quad (1.27)$$

$$\frac{\Delta Y}{G} = -K_a [G] + K_a Y_{\Delta HG} \quad (1.28)$$

1.4.1. NMR Titrations

H^1 -NMR counts among the most informative techniques for most situations. Not only can an NMR titration give quantitative information but the relative shifts and the symmetry changes can give information about the interaction between host and guest as well as the stoichiometry of the reaction. For a classical NMR titration experiment it is assumed that the resonance of interest is a weighted average between the free host H and the host-guest complex HG . That is assuming the simple case of a 1:1 host-guest stoichiometry. A

1.4. Determination of Stability Constants

modern NMR-instrument can obtain good quality spectra in the sub-millimolar concentration range.⁶⁷ The real limiting factor for NMR titration experiments are the rate constants k_1 and k_{-1} between the host and guest and the time scale of the NMR experiment.

1.4.2. UV-Vis Titrations

Another very common titration technique in supramolecular chemistry is the UV-Vis titration technique. With this method, even concentrations down to 10^{-7} mol can be measured granted the right chromophore is used. The concentrations ranges must lie within a region where the absorption peaks of both guest and host are within the limits of the Lambert-Beer law. Usually this means absorption peaks between 0.3 Å to 1 Å. It is also desirable that the added guest does not have an absorption of its own in the region of interest. This is usually the case for simple host-guest complexes with cations and anions added. Additionally, there has to be a noticeable change in the molar absorptivity (ϵ) upon complexation. UV-Vis titration is particularly sensitive to impurities as well as dilution effects and temperature changes.⁶⁷

1.4.3. Fluorescence Titrations

The third most popular technique is fluorescence spectroscopy. Especially notable is this technique's outstanding sensitivity which makes it possible to determine concentrations down to the nanomolar range. This makes fluorescence spectroscopy particularly well suited to determine large K_s (or very small K_d) values. For a suitable linear response it is necessary that the absorbance at the excitation wavelength does not exceed 0.05 Å. Above this absorbance value the fluorescence response F is not linear anymore. This is due to the absorption of the excitation light before it can reach the heart of the cell where the emission is detected. Therefore the concentrations used or the excitation wavelengths have to be adjusted to keep the absorbance below the mentioned target value. Fluorescence is especially useful when there is only one fluorescent species in the system. This is the case when either the host or guest are "silent" / inactive and the other remaining species' fluorescence is turned "off" (quenched) or "on" upon complexation.

1. Theoretical Background

1.4.4. Other Titration Techniques

There are also other titration techniques such as ESI / MS based titration¹⁹ or calorimetric titration^{18,67} which will not be discussed in more detail in this thesis.

Part II.

Experimental

2. Materials and Methods

2.1. Chemicals

All chemicals and solvents that were used during the experimental work for this thesis are listed in table 2.1.

2.2. Nuclear Magnetic Resonance Spectrometry

The ^1H -NMR spectra were measured using a *Bruker AVANCE III* (300.36 MHz) equipped with an autosampler. As reference for the chemical shifts either the signal of the deuterated solvent itself or the (in the deut. solvent premixed) standard Tetramethylsilane was used. For analysis of the record NMR spectra the software *MestReNova NMR* was used.

NMR solvents:

Chloroform D: + 0.03 % TMS, 99.80 % D, supplier: Eurisotop

2.3. Mass Spectrometry

The mass spectra to check reaction yields and products were performed using an *Advion expression L* mass spectrometer. The device was used in APCI mode with default preset.

2. Materials and Methods

2.4. Absorption Spectra

The absorption spectra were measured using a *Varian Cary 50 conc* UV-Vis spectrometer. The cuvette used was a precision cell of quartz glass by Hellma Analytics (type 100-QS 10mm, art. no. 100-10-40). All spectra were recorded in “fast” mode and the spectra were baseline corrected by a sample containing only solvent (blank sample).

2.5. Emission and Excitation Spectra

The emission and excitation spectra were recorded using a Hitachi-F7000 spectrofluorometer. The cuvettes used were high precision cells by Hellma Analytics (type 100-QS 10mm, art. no. 100-10-40). The software used to operate the spectrofluorometer was the company’s own *Fluorescence* software.

2.6. Thin Layer Chromatography (TLC)

For thin layer chromatography, TLC plates from Merck (silica gel 60, F254) were used. The eluent was varied depending on the product. For detection a UV lamp ($\lambda=254$ nm and $\lambda=366$ nm) was used. Additionally, standard staining agents were occasionally used to highlight and indicate certain functional groups.

2.7. Flash Column Chromatography

The silica gel used for packing the columns was purchased from Roth (0.04-0.063 mm, 60 Å). The amounts of silica used for separating the products were varied depending on the separation difficulty. Generally, a silica amount of 80-100 times the weight of the crude product was used for preparative flash column chromatography. During elution a polarity gradient was applied to improve the separations of the products.

2.7. Flash Column Chromatography

Table 2.1.: List of all chemicals used

Name	CAS	Supplier
N,N-bis-(2-hydroxyethyl)aniline	120-07-0	TCI
2-Methylbenzenamine	95-53-4	TCI
2-Methoxybenzenamine	90-04-0	TCI
2-Chlorobenzenamine	95-51-2	TCI
2-Methoxy-6-methylbenzenamine	50868-73-0	TCI
Anthrilic acid	118-92-3	Aldrich
p-Anisidin	104-94-9	TCI
2-Methoxyethyl chloride	627-42-9	TCI
2-Nitroresorcinol	601-89-8	TCI
2-Bromoethanol	540-51-2	TCI
Tetraethylenglycol	112-60-7	Aldrich
Tosylchloride	98-59-9	TCI
TRIS	77-86-1	Roth
KOH	1310-58-3	Merck
NaH	7646-69-7	TCI
Fe (powder)	7439-89-6	Merck
HCl, 37%	7647-01-0	VWR
CaCO ₃	471-34-1	Merck
KI	7681-11-0	Roth
KCl	7447-40-7	Roth
NH ₄ Cl	12125-02-9	Aldrich
MgCl ₂	7786-30-3	Roth
NaCl	7647-14-5	VWR
CaCl ₂	10043-52-4	Roth
LiCl	7447-41-8	LiCl
Tetrahydrofurane	109-99-9	Roth
Ethanol	64-17-5	Fisher
Dimethylformamide	68-12-2	Roth
Methanol	67-56-1	VWR
Dichloromethane	75-09-2	Fisher
Cyclohexane	110-82-7	VWR
Ethyl acetate	141-78-6	VWR

3. Synthesis

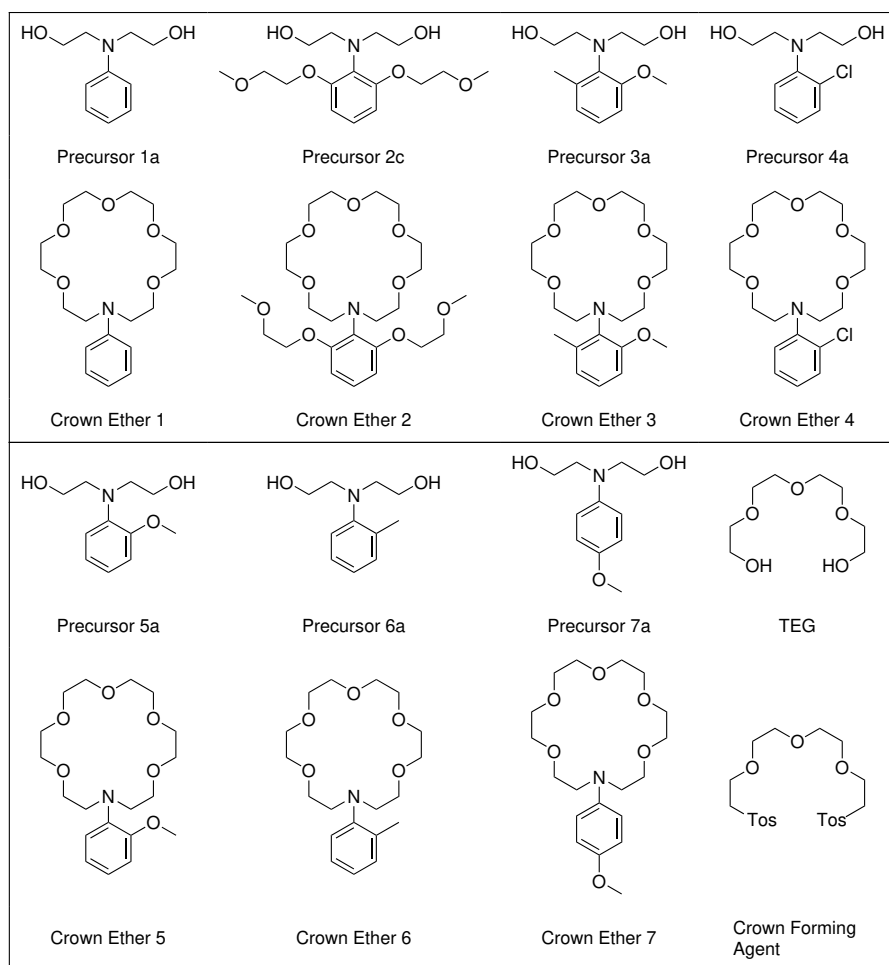


Figure 3.1.: Compound Overview

3. Synthesis

3.1. Crown Ether 1

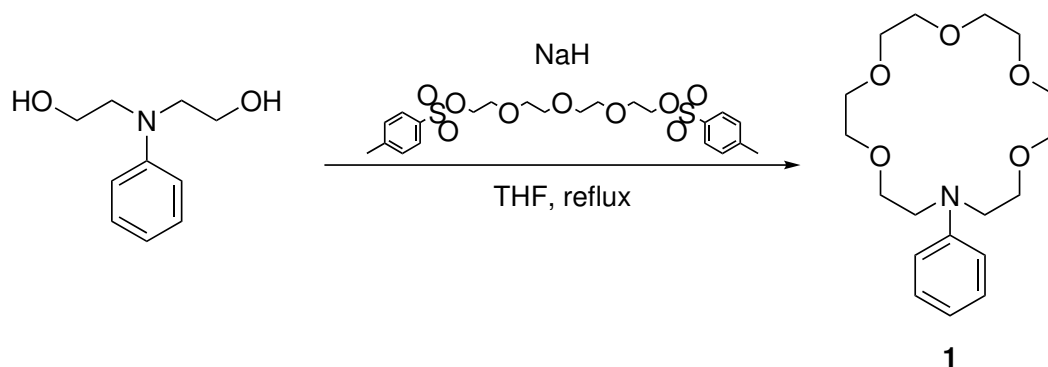


Figure 3.2.: Synthesis of Crown Ether 1

N,N-Bis(2-hydroxyethyl)aniline (1.00 g, 5.52 mmol) was dissolved in 60 mL THF. NaH (827 mg, 40 wt%, 2.5 eq) was added carefully while stirring and using an ice bath to control the solution's temperature. The mixture was then heated to reflux. 1,17-ditosyl-3,6,9,12,15-pentaoxaheptadecane (2.77 g, 5.52 mmol, 1.00 eq) was dissolved in THF and slowly added to the solution while stirring. The mixture was then stirred for 4 h at reflux. The product was purified by column chromatography (silica) using ethyl acetate as eluent.

Yield: 450 mg (24%)

^1H NMR (300 MHz, Chloroform-d) δ 7.20 (t, 2H), 6.80 – 6.60 (m, 3H), 3.73 – 3.55 (m, 24H).

3.2. Crown Ether 3

3.2.1. Synthesis of Precursor 3a

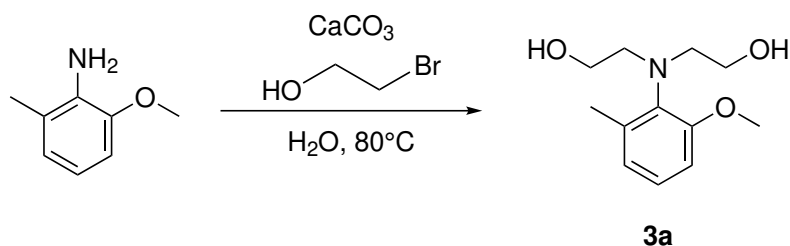


Figure 3.3.: Synthesis of Precursor **3a**

2-Methoxy-6-methylaniline (1.00g, 7.29 mmol) was mixed with 2-Bromoethanol (2.73 g, 21.87 mmol, 3 eq) and CaCO_3 (1.46 g, 14.58 mmol, 2 eq) in purified water and stirred at overnight at 80 °C. The mixture was filtrated and the solid phase washed with DCM. Sat. NaCl (brine) was added to the H_2O phase and extracted with DCM (3x). The organic phase was dried over NaSO_4 and evaporated. Purification by column chromatography (silica): ethyl acetate as eluent.

Yield: 1.24 g (76 %)

^1H NMR (300 MHz, Chloroform-d) δ 7.10 (t, $J = 7.9$ Hz, 1H), 6.80 (dd, $J = 20.0, 8.0$ Hz, 2H), 3.87 (s, 3H), 3.51 (d, $J = 29.1$ Hz, 4H), 3.30 – 3.13 (m, 6H), 2.33 (s, 3H).

3. Synthesis

3.2.2. Synthesis of Crown Ether **3**

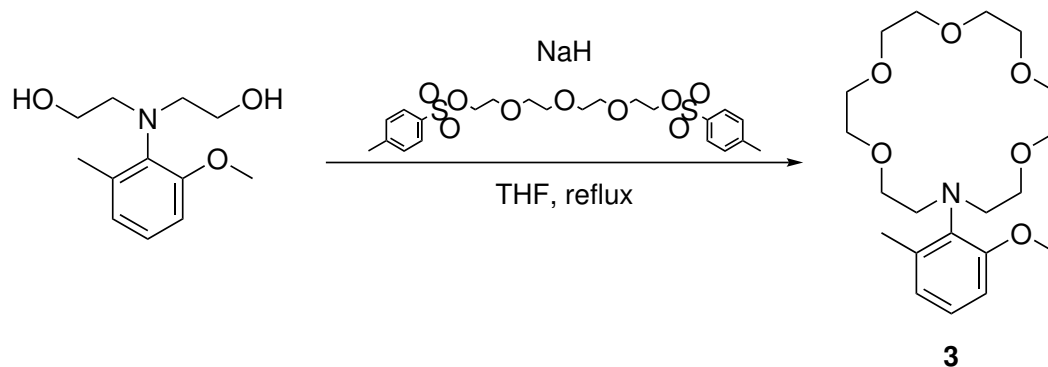


Figure 3.4.: Synthesis of Crown Ether **3**

2,2'-((2-methoxy-6-methylphenyl)azanediyl)bis(ethan-1-ol) (250 mg, 1.11 mmol) was dissolved in dry THF and transferred into a Schlenk under Ar atmosphere. NaH (111 mg, 2.77 mmol, 60 wt%, 2.50 eq) was slowly added while stirring. After addition of NaH the solution was stirred for 30 min. 1,17-ditosyl-3,6,9,12,15-pentaoxaheptadecane (558 mg, 1.11 mmol, 1 eq) was dissolved in dry THF and slowly added to the solution while stirring. The solution was stirred for 3 h at reflux. Afterwards, the solution was filtrated and the organic solvent evaporated. The product was extracted with DCM/brine (3x) and the organic solvent was again evaporated. Purification via column chromatography (silica): MeOH in DCM (0-5 v%) as eluent.

Yield: 70.0 mg (16 %)

^1H NMR (300 MHz, Chloroform-d) δ 7.02 (t, $J = 7.9$ Hz, 1H), 6.73 (dd, $J = 23.4, 7.9$ Hz, 2H), 3.79 (s, 3H), 3.74 – 3.13 (m, 24H), 2.34 (s, 3H).

3.3. Crown Ether 4

3.3.1. Synthesis of Precursor 4a

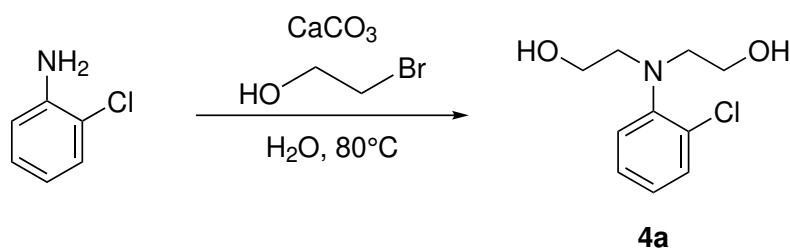


Figure 3.5.: Synthesis of Precursor 4a

2-Chlorobenzeneamine (1.00g, 7.84 mmol) was mixed with 2-Bromoethanol (3.92 g, 31.36 mmol, 4 eq) and CaCO_3 (2.35 g, 23.52 mmol, 3 eq) in purified water and stirred at overnight at 80 °C. The mixture was filtrated and the solid phase washed with DCM. Sat. NaCl (brine) was added to the H_2O phase and extracted with DCM (3x). The organic phase was dried over NaSO_4 and evaporated. Purification by column chromatography (silica): ethyl acetate as eluent.

Yield: 637 mg (38 %)

^1H NMR (300 MHz, Chloroform- d) δ 7.40 (d, 1H), 7.34 – 7.21 (m, 2H), 7.10 (t, 1H), 3.59 (t, $J = 5.2$ Hz, 4H), 3.27 (t, $J = 5.3$ Hz, 4H), 2.87 (d, $J = 20.9$ Hz, 2H).

3. Synthesis

3.3.2. Synthesis of Crown Ether 4

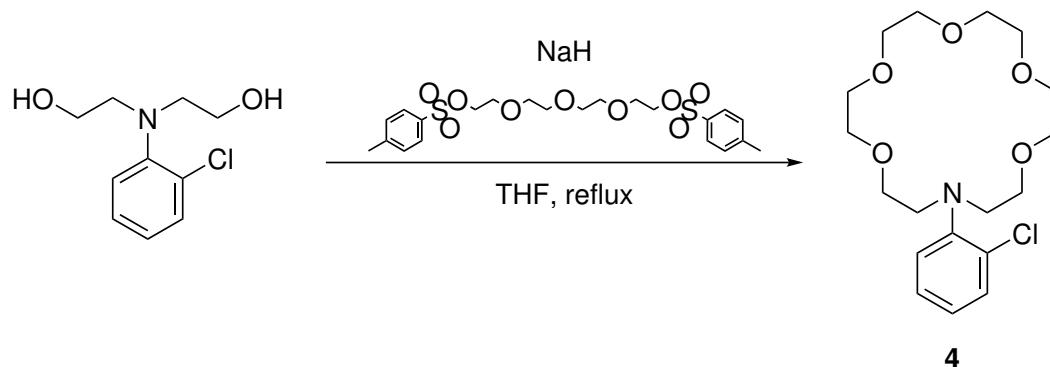


Figure 3.6.: Synthesis of Crown Ether 4

2,2'-((2-chlorophenyl)azanediyl)bis(ethan-1-ol) (300 mg, 1.39 mmol) was dissolved in dry THF and transferred into a Schlenk under Ar atmosphere. NaH (139 mg, 3.48 mmol, 60 wt%, 2.50 eq) was slowly added while stirring. After addition of NaH the solution was stirred for 30 min. 1,17-ditosyl-3,6,9,12,15-pentaoxaheptadecane (699 mg, 1.39 mmol, 1 eq) was dissolved in dry THF and slowly added to the solution while stirring. The solution was stirred for 4.5 h at reflux. Afterwards, the solution was filtrated and the organic solvent evaporated. The product was extracted with DCM/brine (3x) and the organic solvent was again evaporated. Purification via column chromatography (silica): MeOH in DCM (0-5 v%) as eluent.

Yield: 125 mg (24 %)

^1H NMR (300 MHz, Chloroform- d) δ 7.30 (dd, $J = 16.4, 7.3$ Hz, 2H), 7.19 (t, $J = 7.6$ Hz, 1H), 6.95 (t, $J = 7.6$ Hz, 1H), 3.77 – 3.40 (m, 24H).

3.4. Crown Ether 5

3.4.1. Synthesis of Precursor 5a

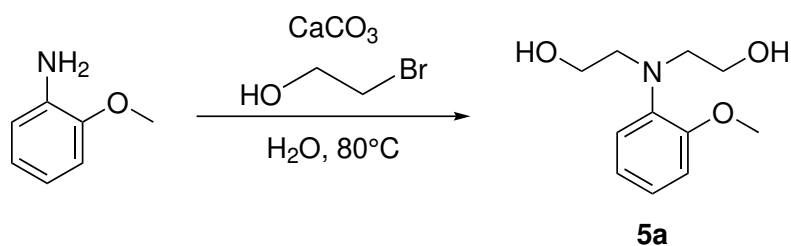


Figure 3.7.: Synthesis of Precursor **5a**

2-Methoxybenzenamine (1.00g, 8.12 mmol) was mixed with 2-Bromoethanol (4.06 g, 32.48 mmol, 4 eq) and CaCO_3 (1.63 g, 16.24 mmol, 2 eq) in purified water and stirred at overnight at 80 °C. The mixture was filtrated and the solid phase washed with DCM. Sat. NaCl (brine) was added to the H_2O phase and extracted with DCM (3x). The organic phase was dried over NaSO_4 and evaporated. Purification by column chromatography (silica): ethyl acetate as eluent.

Yield: 857 mg (50 %)

^1H NMR (300 MHz, Chloroform-d) δ 7.26 – 6.87 (m, 4H), 3.88 (s, 3H), 3.50 (t, $J = 5.1$ Hz, 4H), 3.20 (t, $J = 5.0$ Hz, 4H).

3. Synthesis

3.4.2. Synthesis of Crown Ether **5**

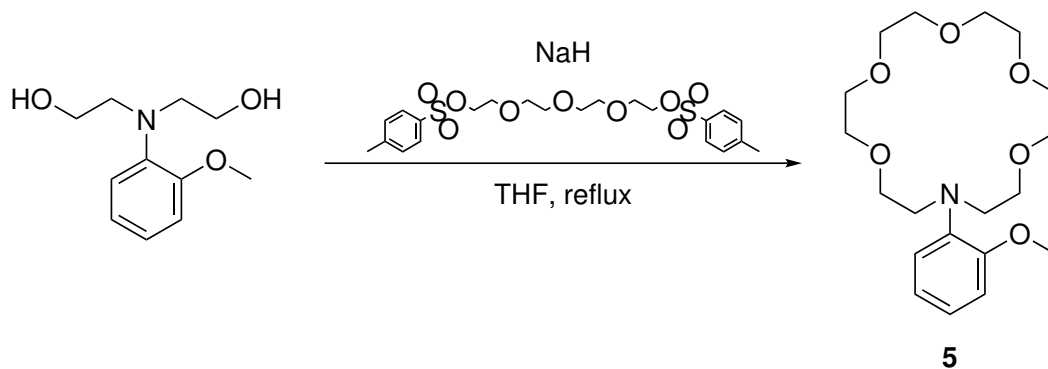


Figure 3.8.: Synthesis of Crown Ether **5**

2,2'-((2-methoxyphenyl)azanediyl)bis(ethan-1-ol) (250 mg, 1.18 mmol) was dissolved in dry THF and transferred into a Schlenk under Ar atmosphere. NaH (118 mg, 2.96 mmol, 60 wt%, 2.50 eq) was slowly added while stirring. After addition of NaH the solution was stirred for 30 min. 1,17-ditosyl-3,6,9,12,15-pentaoxaheptadecane (595 mg, 1.18 mmol, 1 eq) was dissolved in dry THF and slowly added to the solution while stirring. The solution was stirred for 3 h at reflux. Afterwards, the solution was filtrated and the organic solvent evaporated. The product was extracted with DCM/brine (3x) and the organic solvent was again evaporated. Purification via column chromatography (silica): MeOH in DCM (15 v%) as eluent. Filtration of eluated silica afterwards was necessary.

Yield: 67 mg (15 %)

^1H NMR (300 MHz, Chloroform-*d*) δ 7.19 – 6.80 (m, 4H), 3.82 (s, 3H), 3.75 – 3.13 (m, 24H).

3.5. Crown Ether 6

3.5.1. Synthesis of Precursor 6a

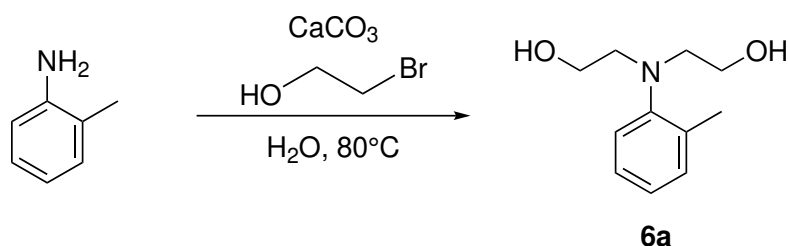


Figure 3.9.: Synthesis of Precursor 6a

2-Methylbenzenamine (1.00g, 9.33 mmol) was mixed with 2-Bromoethanol (4.66 g, 37.33 mmol, 4 eq) and CaCO₃ (2.80 g, 28.00 mmol, 3 eq) in purified water and stirred at overnight at 80 °C. The mixture was filtrated and the solid phase washed with DCM. Sat. NaCl (brine) was added to the H₂O phase and extracted with DCM (3x). The organic phase was dried over NaSO₄ and evaporated. Purification by column chromatography (silica): ethyl acetate as eluent.

Yield: 905 mg (49 %)

¹H NMR (300 MHz, Chloroform-d) δ 7.25 – 6.98 (m, 4H), 3.60 (t, J = 5.4 Hz, 4H), 3.17 (t, J = 5.4 Hz, 4H), 2.83 (s, 2H), 2.35 (s, 3H).

3. Synthesis

3.5.2. Synthesis of Crown Ether **6**

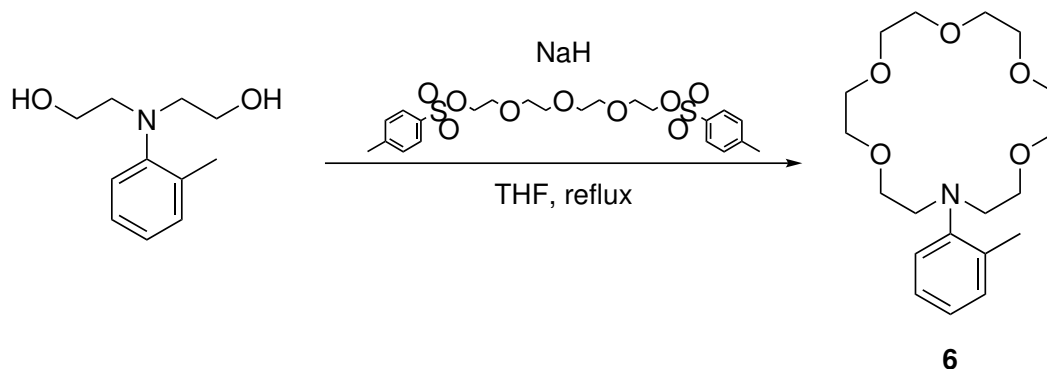


Figure 3.10.: Synthesis of Crown Ether **6**

2,2'-(o-tolylazanediyl)bis(ethan-1-ol) (320 mg, 1.64 mmol) was dissolved in dry THF and transferred into a Schlenk under Ar atmosphere. NaH (164 mg, 4.10 mmol, 60 wt%, 2.50 eq) was slowly added while stirring. After addition of NaH the solution was stirred for 30 min. 1,17-ditosyl-3,6,9,12,15-pentaoxaheptadecane (824 mg, 1.64 mmol, 1 eq) was dissolved in dry THF and slowly added to the solution while stirring. The solution was stirred for 3 h at reflux. Afterwards, the solution was filtrated and the organic solvent evaporated. The product was extracted with DCM/brine (3x) and the organic solvent was again evaporated. Purification via column chromatography (silica): ethyl acetate.

Yield: 160 mg (32 %)

^1H NMR (300 MHz, Chloroform-d) δ 7.24 – 6.93 (m, 4H), 3.76 – 3.26 (m, 24H), 2.29 (s, 3H).

3.6. Crown Ether 7

3.6.1. Synthesis of Precursor 7a

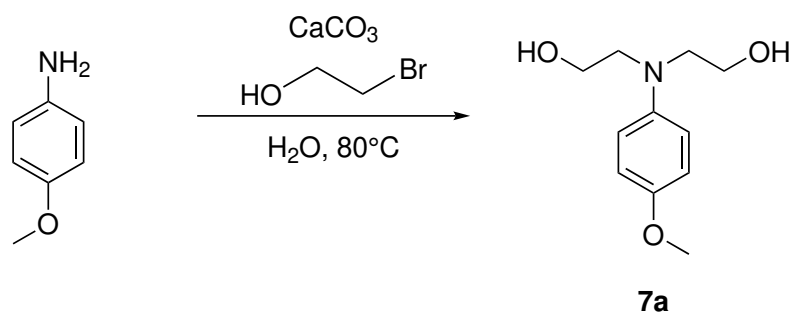


Figure 3.11.: Synthesis of Precursor **7a**

p-Anisidin (1.00g, 8.12 mmol) was mixed with 2-Bromoethanol (3.04 g, 24.36 mmol, 3 eq) and CaCO_3 (1.63 g, 16.14 mmol, 2 eq) in purified water and stirred at overnight at 80°C . The mixture was filtrated and the solid phase washed with DCM. Sat. NaCl (brine) was added to the H_2O phase and extracted with DCM (3x). The organic phase was dried over NaSO_4 and evaporated. Purification by column chromatography (silica): ethyl acetate as eluent.

Yield: 678 mg (40 %)

^1H NMR (300 MHz, Chloroform-d) δ 6.77 (dd, 4H), 3.82 – 3.68 (m, 7H), 3.44 (t, $J = 5.0$ Hz, 4H), 3.14 (s, 2H).

3. Synthesis

3.6.2. Synthesis of Crown Ether **7**

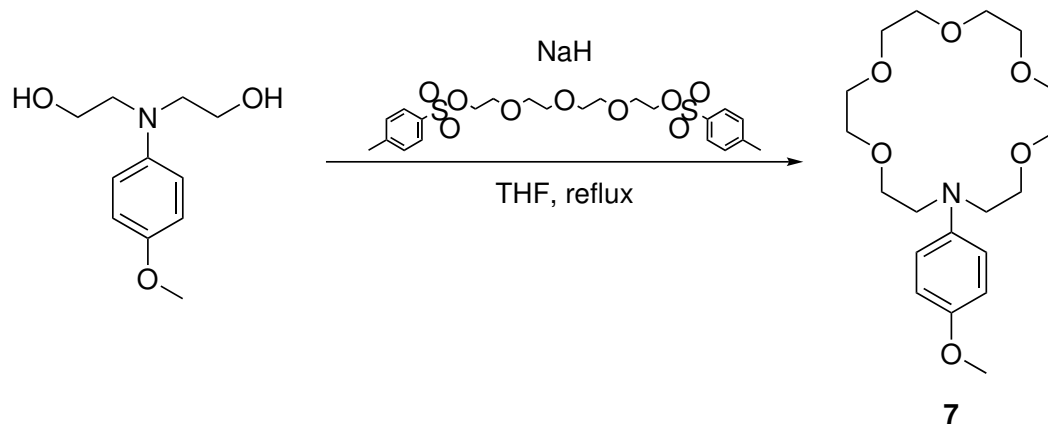


Figure 3.12.: Synthesis of Crown ether **7**

2,2'-((4-methoxyphenyl)azanediyl)bis(ethan-1-ol) (250 mg, 1.18 mmol) was dissolved in dry THF and transferred into a Schlenk under Ar atmosphere. NaH (118 mg, 2.96 mmol, 60 wt%, 2.50 eq) was slowly added while stirring. After addition of NaH the solution was stirred for 30 min. 1,17-ditosyl-3,6,9,12,15-pentaoxaheptadecane (595 mg, 1.18 mmol, 1 eq) was dissolved in dry THF and slowly added to the solution while stirring. The solution was stirred for 3.5 h at reflux. Afterwards, the solution was filtrated and the organic solvent evaporated. The product was extracted with DCM/brine (3x) and the organic solvent was again evaporated. Purification via column chromatography (silica): MeOH in DCM (15 v%) as eluent. Filtration of eluated silica afterwards was necessary.

Yield: 13 mg (3 %)

^1H NMR (300 MHz, Chloroform-d) δ 6.83 (d, J =8.8 Hz, 4H), 3.75 (s, 3H), 3.70 – 3.50 (m, 24H).

3.7. Synthesis of Crown Forming Agent

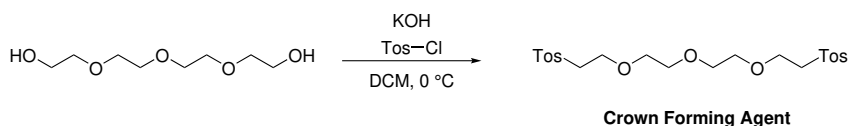


Figure 3.13.: Synthesis of **Crown Forming Agent**

Tetraethylene glycol (20 g, 103 mmol) was dissolved in 300 mL DCM and cooled to 0 °C. Tosylchloride (58.9 g, 309 mmol, 3 eq) was slowly added followed by the slow addition of KOH (46.22 g, 824 mmol, 8 eq) over 60 min while stirring. After 2 h of stirring the solution was extracted with H₂O (3x) and the organic phase was dried over NaSO₄ followed by evaporation of the organic solvent. Purification via column chromatography (silica): (CH+EA 1+2) as eluent.

Yield: 43 g (83 %)

¹H NMR (300 MHz, Chloroform-d) δ 7.79 (d, J = 8.2 Hz, 4H), 7.34 (d, J = 8.0 Hz, 4H), 4.15 (dd, J = 5.9, 3.7 Hz, 4H), 3.68 (dd, J = 5.7, 3.9 Hz, 4H), 3.56 (s, 8H), 2.44 (s, 6H).

3. Synthesis

3.8. Synthesis of Crown Ether 2

3.8.1. Synthesis of Precursor 2a

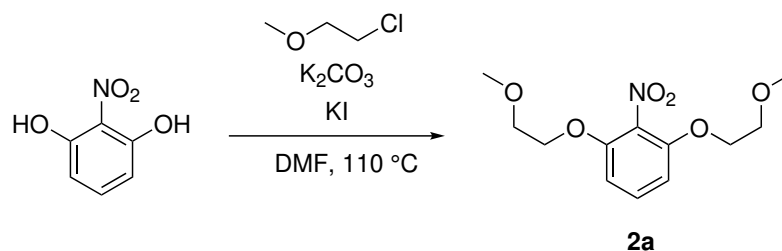


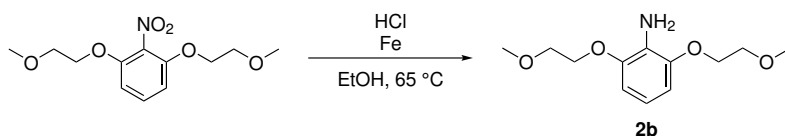
Figure 3.14.: Synthesis of Precursor **2a**

2-Nitroresorcinol (2.00g, 12.89 mmol), KI (1.07 g, 6.45 mmol, 0.50 eq), K_2CO_3 (3.74 g, 27.08 mmol, 2.10 eq) and chloroethyl methyl ether (2.56 g, 27.08 mmol, 2.10 eq) were mixed in DMF. The mixture was heated to 110 °C and stirred for 6 h. Afterwards the mixture was filtrated and the solvent evaporated. The product was dissolved in DCM / H_2O and extracted with 2.5 v% Na_2CO_3 solution and brine. The organic solvent was evaporated. Purification via column chromatography (silica): EA in CH 10-80 v% as eluent.

Yield: 2.06 g (59 %)

1H NMR (300 MHz, Chloroform-d) δ 7.29 (t, 1H), 6.65 (d, $J = 8.4$ Hz, 2H), 4.19 (t, $J = 4.9$ Hz, 4H), 3.72 (t, $J = 5.7, 4.0$ Hz, 4H), 3.41 (s, 6H).

3.8.2. Synthesis of Precursor 2b

Figure 3.15.: Synthesis of Precursor **2b**

Fe (1.65 g, 29.49 mmol, 5eq) was added to 170 mL EtOH in a round bottom flask and stirring bar was added. HCl (290.6 mg, 2.95 mmol, 37 wt%, 0.5 eq) was added and the mixture was stirred at 65 °C for 1 h. The mixture / solution turned from clear / yellowish to orange / red. 50 mL of 25 wt% NH₄Cl were added to the mixture and the heating bath was removed while still stirring. After 5 min 1,3-bis(2-methoxyethoxy)-2-nitrobenzene (1.60 g, 5.90 mmol) was added to the mixture and heated again to 65 °C while stirring. After 3 h the reaction was stopped and the solids filtered off. The solvent was evaporated. Extraction with EA / sat. NaHCO₃ and brine. The organic solution was dried over NaSO₄ and the solvent evaporated. Purification via column chromatography (silica): EE in CH 20-80 v% as eluent.

Yield: 900 mg (63 %)

¹H NMR (300 MHz, Chloroform-d) δ 6.72 – 6.47(m, 3H), 4.13 (dt, J = 9.3, 4.5 Hz, 4H), 3.78 – 3.71(m, 4H), 3.44 (d, J = 2.4 Hz, 6H).

3. Synthesis

3.8.3. Synthesis of Precursor **2c**

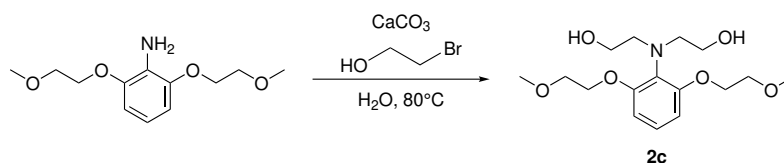


Figure 3.16.: Synthesis of Precursor **2c**

2,6-bis(2-methoxyethoxy)aniline (500 mg, 2.07 mmol) was dissolved in purified water and 2-Bromoethanol (777 mg, 6.22 mmol, 3 eq) and CaCO_3 (415 mg, 4.14 mmol, 2 eq) were added. The mixture was stirred overnight at 80°C . The mixture was filtrated and the solid phase washed with DCM. Sat. NaCl (brine) was added to the H_2O phase and extracted with DCM (3x). The organic phase was dried over NaSO_4 and evaporated. Purification by column chromatography (silica): EtOH in EA 0-15 v% as eluent.

Yield: 487 mg (71 %)

^1H NMR (300 MHz, Chloroform-d) δ 7.10 (t, $J = 8.4\text{Hz}$, 1H), 6.54 (d, $J = 8.4\text{ Hz}$, 2H), 4.10 (t, 4H), 3.75 (t, $J = 5.4, 3.7\text{ Hz}$, 4H), 3.48 – 3.35 (m, 10H), 3.20 (t, $J = 5.6, 3.7\text{ Hz}$, 4H).

3.8.4. Synthesis of Crown Ether 2

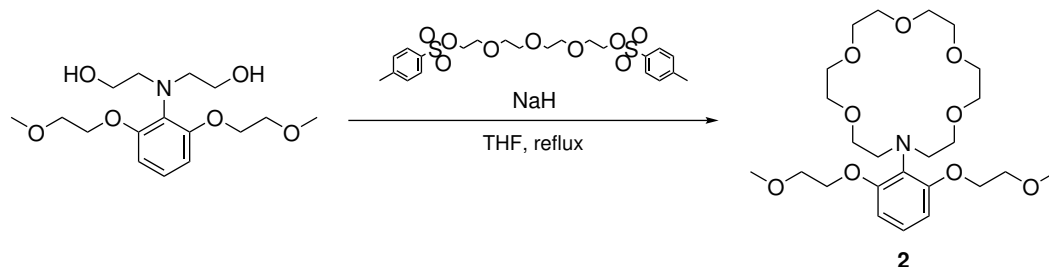


Figure 3.17.: Synthesis of Crown Ether 2

2,2'-((2,6-bis(2-methoxyethoxy)phenyl)azanediyl)bis(ethan-1-ol) (250 mg, 759 μmol) was dissolved in dry THF and transferred into a Schlenk under Ar atmosphere. NaH (66.78 mg, 1.67 mmol, 60 wt%, 2.20 eq) was slowly added while stirring. After addition of NaH the solution was stirred for 30 min. 1,17-ditosyl-3,6,9,12,15-pentaoxaheptadecane (595 mg, 1.18 mmol, 1 eq) was dissolved in dry THF and slowly added to the solution while stirring. The solution was stirred for 2 h at reflux. Afterwards, the solution was filtrated and the organic solvent evaporated. Purification via column chromatography (silica): MeOH in DCM (10-40 v%) as eluent. Filtration of eluated silica afterwards was necessary. **Product could not be isolated purely!**

Part III.
Results and Discussion

4. Synthetic Considerations

One of the goals of this thesis was, on the one hand, the synthesis of an improved potassium ion receptor based on phenyl aza crown ethers. On the other hand, we wanted to further investigate the influence of the side groups on the phenyl moiety and how it affects the complexation ability of the crown ether. The main assumption was that the more electron density is present in the crown ether ring, specifically the nitrogen atom, the higher the complexation stability will be. Provided with a higher electron density at the lone pairs of the nitrogen and oxygen atoms of the crown ether a stronger interaction between the positively charged guest (K^+) and the electron rich crown ether is formed. Therefore we expected improved complexation characteristics when incorporating electron donating side groups such as methyl or methoxy groups into the phenyl moiety. Aside from Crown Ether **2** all crown ethers were synthesized in a two step synthesis. The first step of the crown ether synthesis involves using the phenyl amines with the corresponding side groups already attached. Most of these phenyl amines are readily commercially available and quite cheap. The reaction is performed in aqueous medium at 80 °C using 2-Bromoethanol and $CaCO_3$ as reagents. The nucleophilic nitrogen undergoes nucleophilic substitution with the bromine atom of the 2-Bromoethanol. Since the bromine ion is a good leaving group this reaction usually shows high yields and short reaction times. The workup consists of a filtration (of the insoluble salts) and an extraction followed by purification via column chromatography. This reaction step converts the primary amine into a tertiary amine with two ethanol groups attached.

The second synthesis step has to be performed using dry solvent and under inert atmosphere. This is mainly due to the high reactivity of NaH as both the educt and the reagent are stable under normal atmosphere. The previously synthesized diol is dissolved in dry THF and activated by deprotonating the hydroxy groups using NaH. This results in highly reactive and nucleophilic alkoxides. Upon addition of the tosyl substituted reagent the alkoxide groups

4. Synthetic Considerations

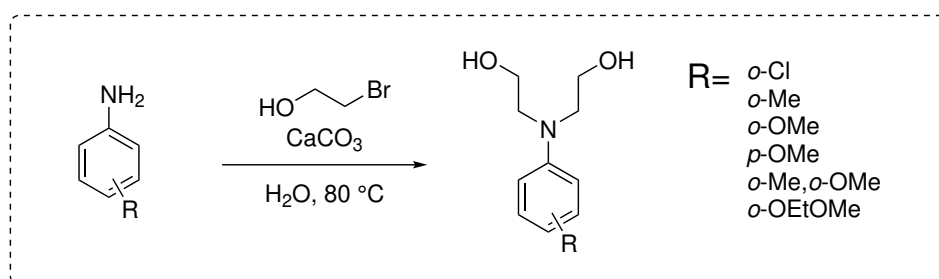


Figure 4.1.: General scheme for the first step of the crown ether synthesis

undergo nucleophilic substitution with the tosyl groups. To prevent polymerization only one equivalent of tosylated reagent is used. Additionally, the tosylated reagent is dissolved beforehand and only added dropwise. The resulting dilution prevents the polymerization from occurring. This solution was performed in dry THF at reflux temperature. Depending on the reactivity of the educt (more electron density at the hydroxy groups means higher reactivity) the reaction time was between 3 and 4.5 hours. The workup consists of an extraction following by column chromatography. This reaction converts the diol educt into an 18-crown-6 phenyl aza crown ether.

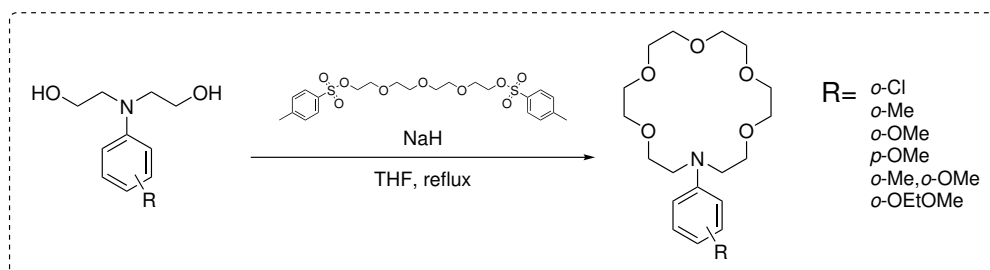


Figure 4.2.: General scheme for the second step of the crown ether synthesis

The purification of the yielded crown ethers via column chromatography proved to be tricky. One of the reasons for that is the fact that crown ether tend to “drag” down the column which means that clear separation is hard to achieve. This behavior is most likely caused by the interactions of the crown ether oxygen atoms that interact with silica forming hydrogen bonds. Subsequently, the product cannot be efficiently eluated as one concentrated fraction but it is rather dragged out throughout the column. This results in several difficulties.

First of all, the yield is decreased significantly as the product cannot be gathered as one pure concentrated fraction and some fractions are mixed with impurities. Due to the high dilution of the product caused by the “dragging” it is hard to detect the product. Additionally, the crown ethers can only be detected under UV light. In this case the product could not be seen even when shining UV light onto the column. In order to eluate the products a methanol amount of at least 2 v% has to be used. This amount has to be increased when additional oxygen containing side groups such as a methoxy group are present on the crown ether. To effectively eluate these crown ethers often 10 v% of methanol was necessary. At this point the silica used for packing the column also dissolves and is eluated. This silica then has to be removed after evaporation via filtration of the solvent.

Despite these difficulties it was possible to purely yield all crown ethers except for Crown Ether **2**. This receptor is also the only one that was not synthesized in two but rather in four steps. The main reason for this was the fact that the corresponding amine was not commercially available. This resulted in two additional synthesis steps in which both the desired side groups and the amine had to be incorporated.

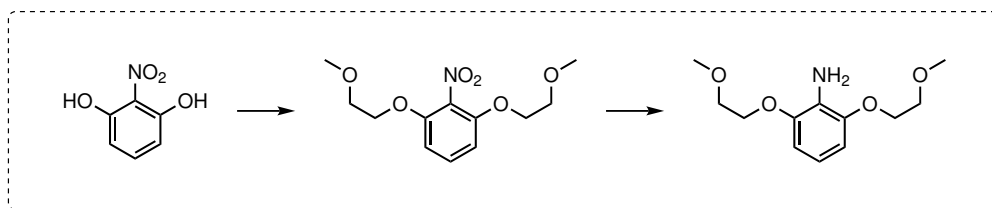


Figure 4.3.: Two additional synthetic steps that were necessary for the synthesis of Crown Ether **2**. See section 3.8 for detailed description.

Even after multiple attempts starting from scratch the product of the last step for Crown Ether **2** was not isolated purely. This can be explained by the additional interaction of the ether groups on the phenyl moiety with the silica. This made the eluation process very difficult as the product spread over a large amount of fractions that were contaminated with dissolved silica and byproducts.

5. Stability Constants

The specific stability constants / dissociation constants were measured using UV-Vis spectrometry in combination with a K^+ titration. As medium a solution of ethanol + water 8 + 2 was utilized. Using only water was not possible due to the crown ether's low solubility in water. However the crown ethers are decently soluble in ethanol which makes a mixture of ethanol and water a viable choice. All samples were measured with a buffer system of 20 mM Tris at pH 7.4. For the measurements potassium chloride was chose to be the titration agent. The crown ether (receptor) concentration was adapted to the specific absorption intensities to stay in the optimal absorption range of 0.3 - 0.8. The concentration of all receptors ranged between 10^{-6} and 10^{-7} M. All spectra were background corrected against a blank sample (containing the 20 mM Tris pH 7.4 buffer). To calculate the specific K_d values a double logarithmic Benesi-Hildebrand⁶² plot was utilized.

Aside from all the synthesized crown ethers two additional receptors were measured for better comparison: an *ortho*-methoxyethoxy substituted phenyl aza crown ether (Müller et al. [51] proposed a potassium sensor based on this receptor) as well as a cryptand called triazacryptand (TAC) that is commonly used as a potassium receptor.

5.1. Calibration Method

In order to determine the stability constants a KCl titration has to be performed. This is done by varying the KCl concentration in the measurement sample while keeping the solvent mixture as well as the buffer concentrations the same. Crown ethers, similarly to most other detection systems, have a dynamic range. This means that the crown ether can only be used as a receptor for certain

5. Stability Constants

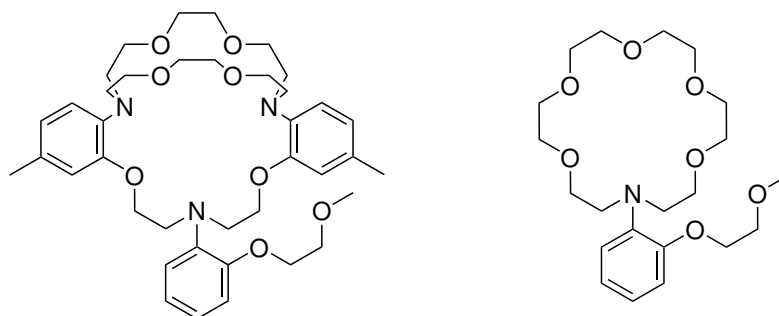


Figure 5.1.: Left: Triazacryptand (TAC) Right: Methoxyethoxy Crown Ether

potassium concentration ranges. This dynamic range revolves around the K_d as can be seen in

$$K_d = \frac{[H]_{eq}[G]_{eq}}{[HG]_{eq}} \quad (5.1)$$

The dissociation constant K_d is the inverse of the stability constant K_s . It is particularly useful as it directly relates to a specific guest concentration. When assuming that the concentrations of both the host molecule H and the formed complex HG are equal the free guest concentration directly correlates to the dissociation constant K_d . This also implies that K_d represents the middle of the dynamic range of the host molecule. Outside of this dynamic range, at both too high and too low guest concentrations, no measurements can be performed.

The nitrogen lone pair of an uncoordinated phenyl aza crown ether plays a crucial role for measuring using UV-Vis. It can be assumed that this lone pair occupies the HOMO of the receptor molecule. When excited by light the electrons of this lone pair undergo an electronic transition followed by relaxation back to the HOMO. Since this transition originates from the HOMO it exhibits the highest wavelengths of all observed transitions. Upon complexation the nitrogen lone pair coordinates to the potassium ion. Due to the fact that it is coordinated the lone pair is not readily available for the aforementioned electronic transitions. This results in a decrease of absorption intensity. By varying the guest concentration within the dynamic range the receptor responds by matching the concentration change with a decrease or increase in absorption

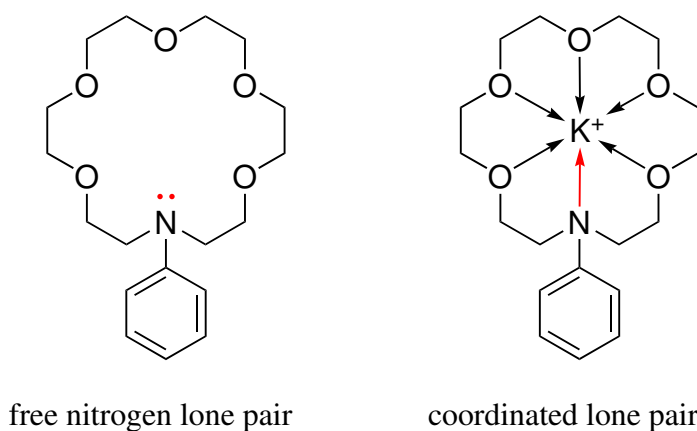


Figure 5.2.: Left: The uncoordinated nitrogen lone pair is available for an electronic transition upon excitation Right: The nitrogen lone pair is coordinated and not available for an electronic transition upon excitation

intensity. Additionally, upon coordination the nitrogen lone pair's energy is lowered by a small amount. This results in a slight blue shift in the absorption spectrum.

After performing a K^+ titration the data can be displayed by plotting the absorption against the wavelength. In case the receptor responds to the titration a pattern will develop with different KCl concentrations. The titration spectra from the unsubstituted receptor Crown Ether 4 can be seen in fig. 5.3. Looking at the figure there are two distinct peaks that respond to the KCl titration. However, for the determination of the dissociation constants only one the peak at the highest wavelength was utilized. It can be seen that by increasing the KCl concentration the receptor exhibits a lowered absorption value for the responsive peak. This confirms that the receptor can effectively coordinate the potassium ion. During these titrations the limits of solubility for the guest and the host moieties at the specific temperature have to be considered. A concentration of 0.1 M KCl in an ethanol + water 8 + 2 mixture at room temperature is very close to its saturation point. Increasing the KCl concentration by another factor of 10 resulted in precipitation of the salt. These particles interfere with the UV-Vis measurement causing scattering and additional absorption thus rendering the data useless. However, the range of solubility of KCl in the used sample medium was sufficient to effectively determine the K_d values. After

5. Stability Constants

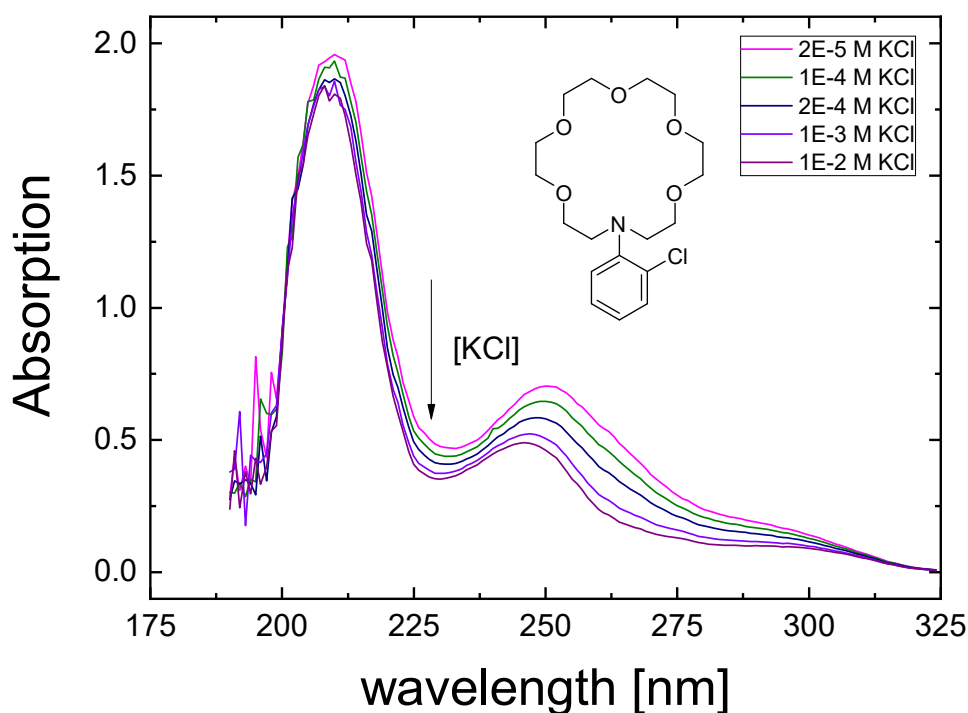


Figure 5.3.: Absorption KCl titration spectra for Crown Ether 4

plotting the measured spectra the absorption maxima of the respective graphs are noted. These can now be plotted in a double logarithmic Benesi-Hildebrand plot (see fig. 5.4).⁶² In this plot

$$\log \left(\frac{A - A_{min}}{A_{max} - A} \right)$$

is plotted against $\log[KCl]$. Since the this titration can only be performed in the dynamic range of the specific receptor data points outside of that range need to be omitted from this plot. After plotting the data points they should, assuming the measurements were performed correctly, form a linear line. These data plots are then fitted using a standard $y = kd + d$ linear fit. The intercept of this linear fit at $y = 0$ is directly correlated to $\log K_d$. This value can easily be converted to a K_d value in mol L^{-1} . For this example case of Crown Ether 4 the measured K_d value is 0.21 mM KCl.

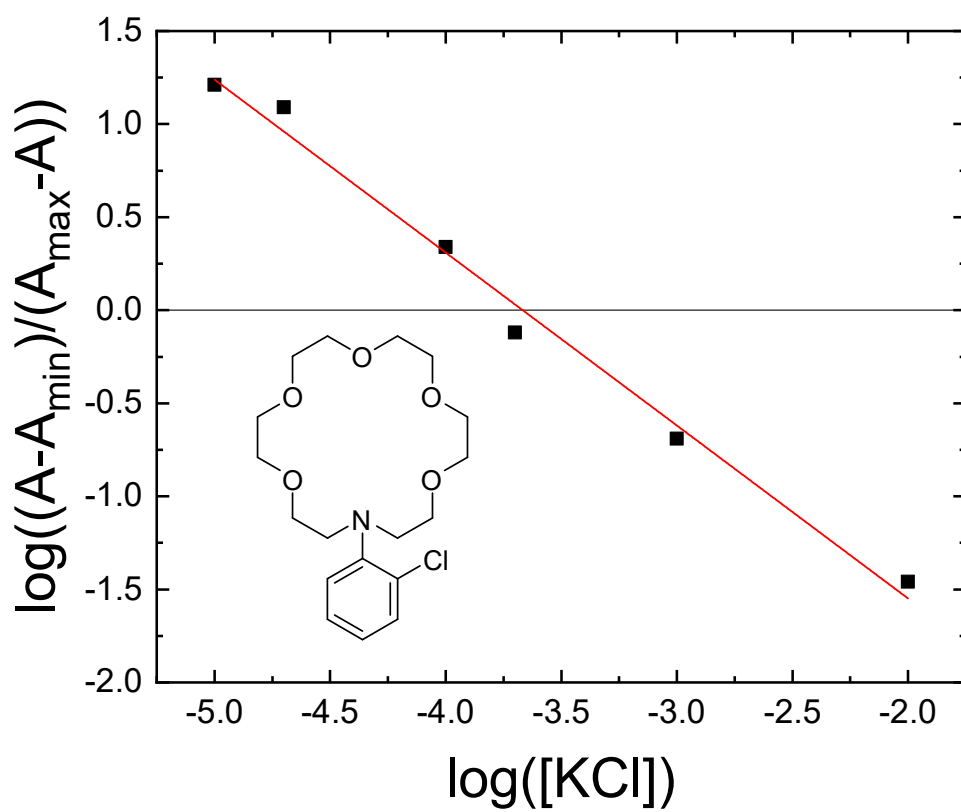


Figure 5.4.: Double logarithmic Benesi-Hildebrand plot for Crown Ether 4

5. Stability Constants

5.2. Crown Ether 1

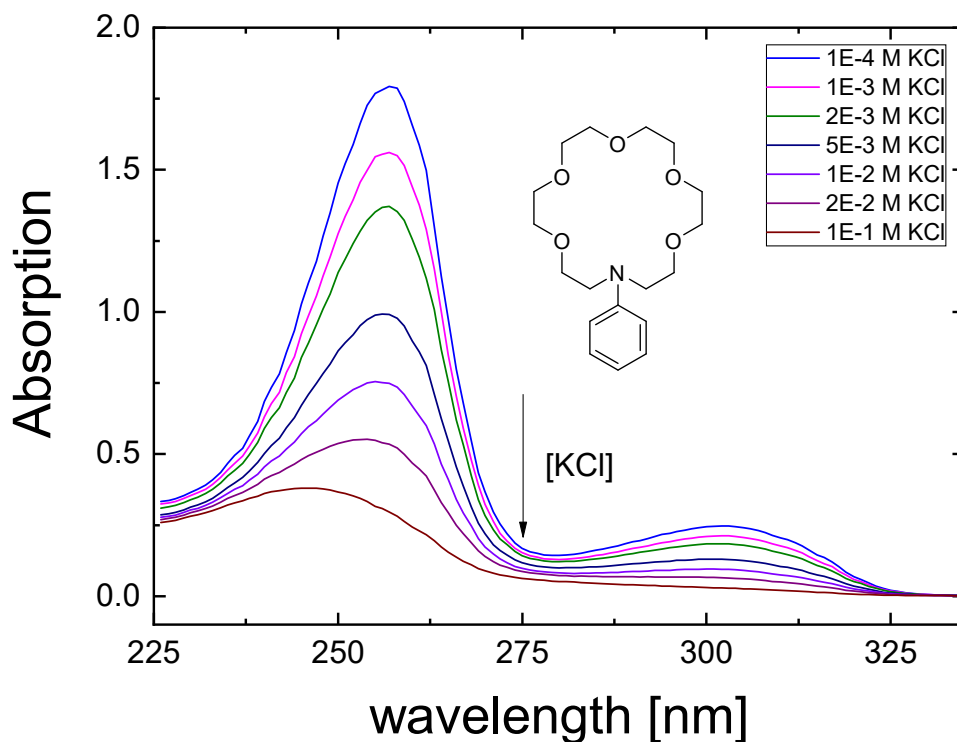


Figure 5.5.: Absorption KCl titration spectra for Crown Ether 1

As expected the unsubstituted version of the 18-crown-6 ether exhibits the lowest complex stability constant of all measured crown ethers. This is due to the missing *ortho* substituents at the phenyl moiety that provide the coordinating crown ether with more electron density. It also exhibits an additional absorption peak that responds to KCl titration which is not present for all other crown ethers. **Substitution:** none; **Absorption peak:** 302 nm; K_d for \mathbf{K}^+ : 4.2 mM

5.3. Crown Ether 3

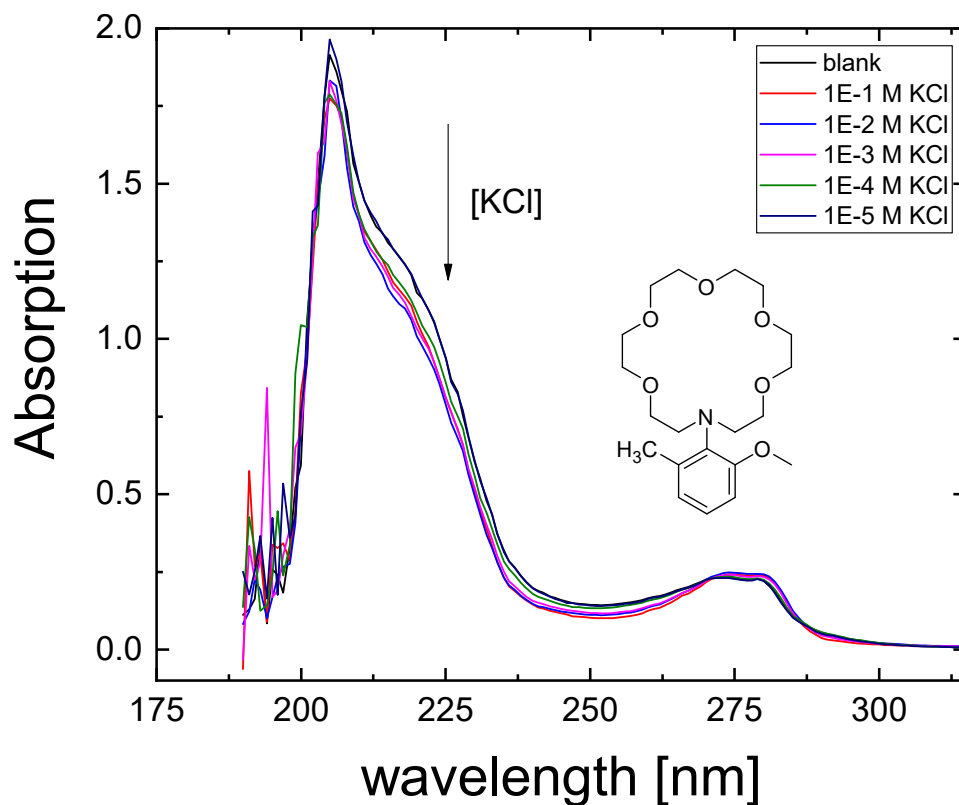


Figure 5.6.: Absorption KCl titration spectra for Crown Ether 3

Crown Ether **3** exhibits no apparent response to the KCl titration. A reason for the optical inactivity of this receptor is its substituents located on both *ortho* positions of the phenyl moiety. The substitution at both *ortho* positions induces a change in the molecules geometry due to steric hindrance. This results in the fact that there is no photophysical response upon complexation. Thus it was not possible to determine the dissociation constant of Crown Ether **3** by using UV-Vis spectrometry. **Substitution:** *ortho*-methoxy, *ortho*-methyl; **Absorption peak:** 275 nm; K_d for K^+ : n.a.

5. Stability Constants

5.4. Crown Ether 4

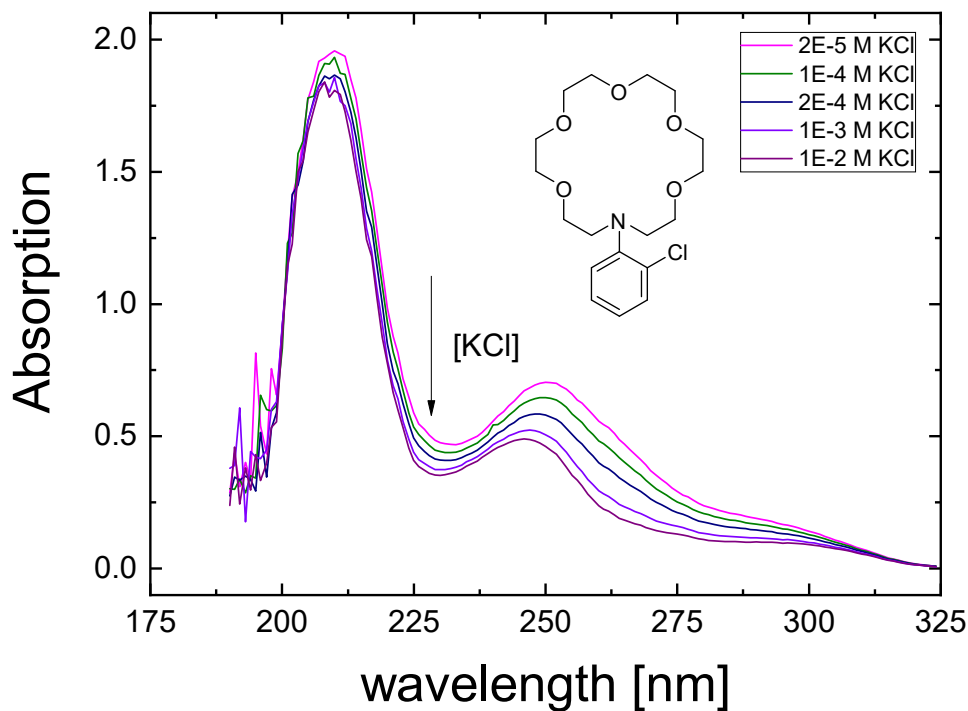


Figure 5.7.: Absorption KCl titration spectra for Crown Ether 4

The chloro-substituted version of the receptor has an absorption peak that has a much smaller wavelength compared to the unsubstituted Crown Ether 1. This agrees with the assumption that electron drawing substituents lower the energy of the HOMO thus resulting in a higher energy necessary to excite the electrons that occupy this orbital. However, the dissociation constant is lower than that of Crown Ether 1 which makes the chloro-substituted receptor a better host for potassium. A possible explanation could be that the relatively big chlorine atom additionally interacts with the complexed K^+ thus stabilizing it further. **Substitution:** *ortho*-chloro; **Absorption peak:** 250 nm; K_d for K^+ : 0.21 mM

5.5. Crown Ether 5

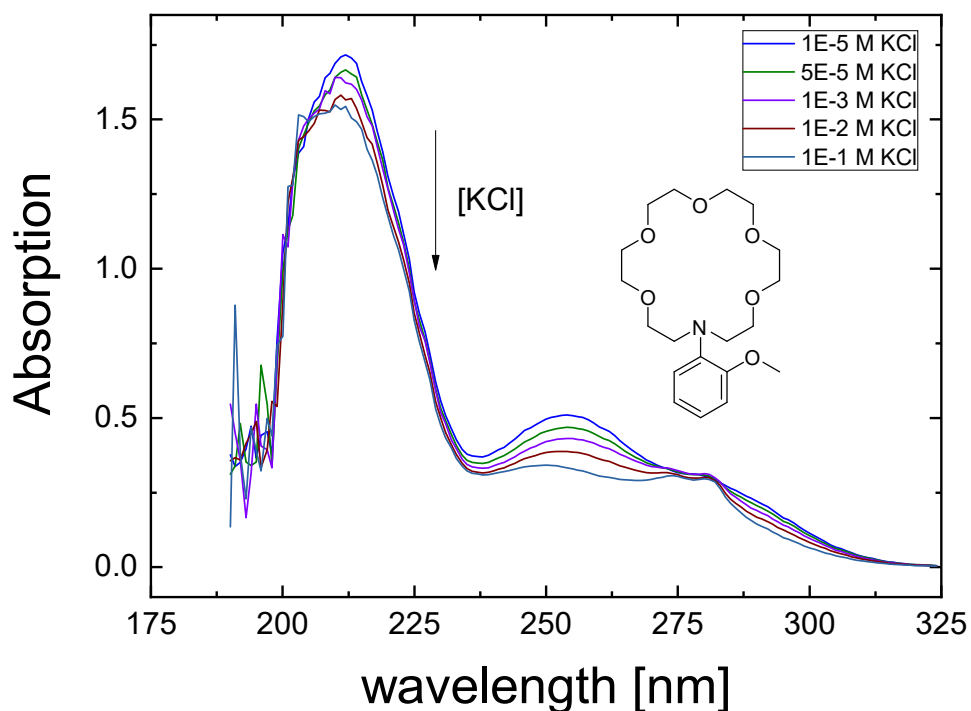


Figure 5.8.: Absorption KCl titration spectra for Crown Ether 5

The *ortho*-methoxy substituted crown ether is expected to have higher complex stability due to the methoxy group donating electron density into the crown ether ring. This in turn results in a stronger interaction between guest and host molecule. Interestingly, this crown ether's stability constant is not higher than the chloro-substituted version. Consequently it can be assumed that not only a higher electron density but also the right placement of additionally coordinating atoms plays a role in forming a good host guest interaction. Apparently the oxygen from the methoxy group cannot contribute to the additional complexation due to its position close to the phenyl ring. **Substitution:** *ortho*-methoxy; **Absorption peak:** 253 nm; K_d for K^+ : 0.65 mM

5. Stability Constants

5.6. Crown Ether 6

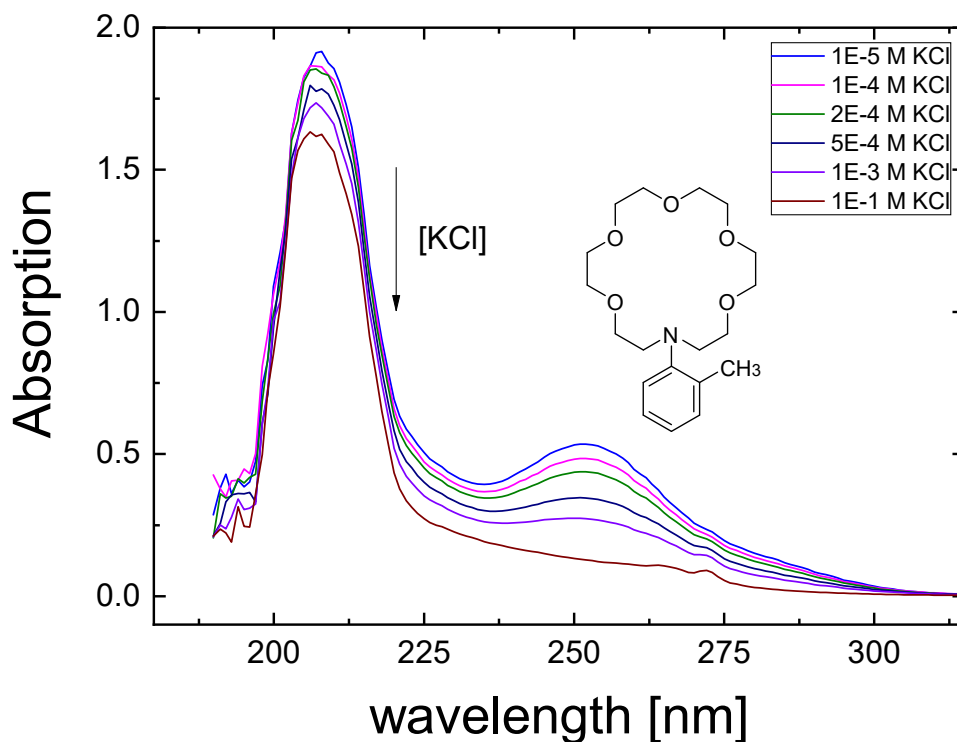


Figure 5.9.: Absorption KCl titration spectra for Crown Ether 6

Crown Ether **6** is the *ortho*-methyl substituted phenyl aza crown ether. Generally, we can expect a higher complex stability compared to the unsubstituted receptor and a lower complex stability compared to the methoxy substituted crown ether. Using UV-Vis spectrometry a slightly higher complex stability was measured for the methyl substituted receptor compared to the methoxy substituted version. This difference might be caused by the inaccuracies of the linear regression in the plotting method. However, it also confirms the assumption that electron density does not play that big of a role when trying to improve the host guest complex stability. **Substitution:** *ortho*-methyl; **Absorption peak:** 252 nm; K_d for K^+ : 0.49 mM

5.7. Crown Ether 7

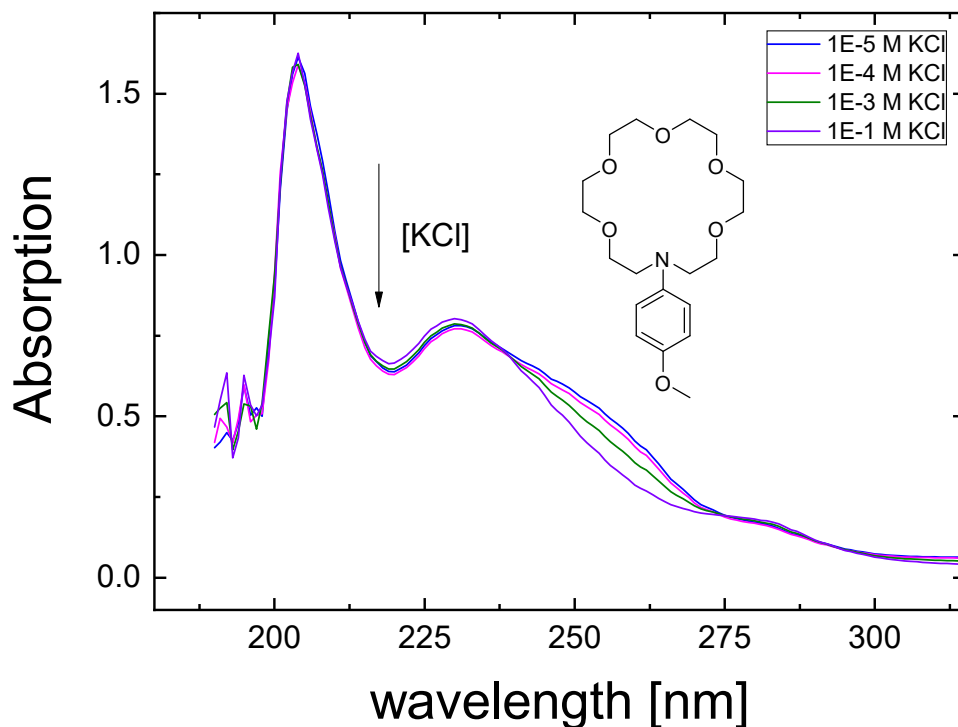


Figure 5.10.: Absorption KCl titration spectra for Crown Ether 7

The *para*-methoxy substituted version of the crown ether exhibits an absorption maximum of 230 nm which is around 20 nm lower than all the other measured crown ethers. Additionally, the absorption peak does not respond to KCl titration apart from an area around the peak's shoulder. The low absorption peak can be explained by the methoxy substituent being in *para* position. This results in a change in the conjugated electronic system and thus also in a change in its photophysical properties. It can also be expected that a methoxy substituent in *para* position does not increase the crown ether's complexation ability that much as it cannot directly interact with the guest molecule. **Substitution:** *para*-methoxy; **Absorption peak:** 230 nm; K_d for K^+ : n.a.

5. Stability Constants

5.8. Methoxyethoxy Crown Ether

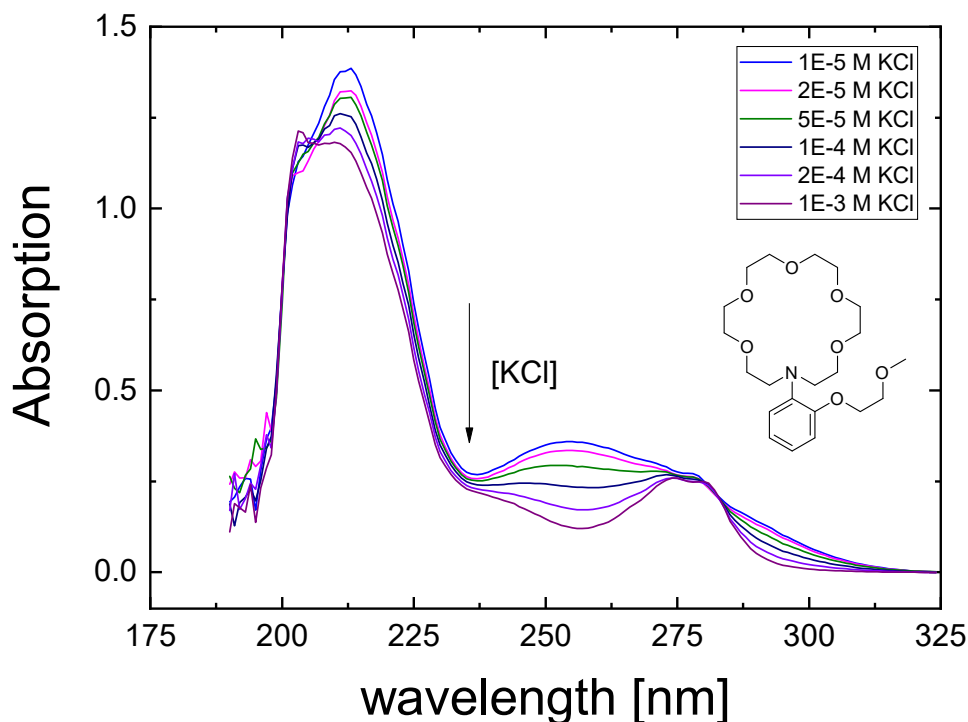


Figure 5.11.: Absorption KCl titration spectra for Methoxyethoxy Crown Ether

The *ortho*-methoxyethoxy shows a KCl titration responsive peak at 255 nm. Upon titration this peak decreases and a second higher wavelength peak develops. Interestingly, this second peak at 275 nm is very similar in both shape and wavelength to that of Crown Ether **3** (*ortho*-methoxy). Similarly to Crown Ether **3** this peak does not change its shape upon titration. The spectra of this crown ether also confirm the assumption that the incorporation of additional complexating atoms significantly increase the crown ether's complexation ability. **Substitution:** *ortho*-methoxyethoxy; **Absorption peak:** 255 nm; K_d for K^+ : 0.09 mM

5.9. Triazacryptand

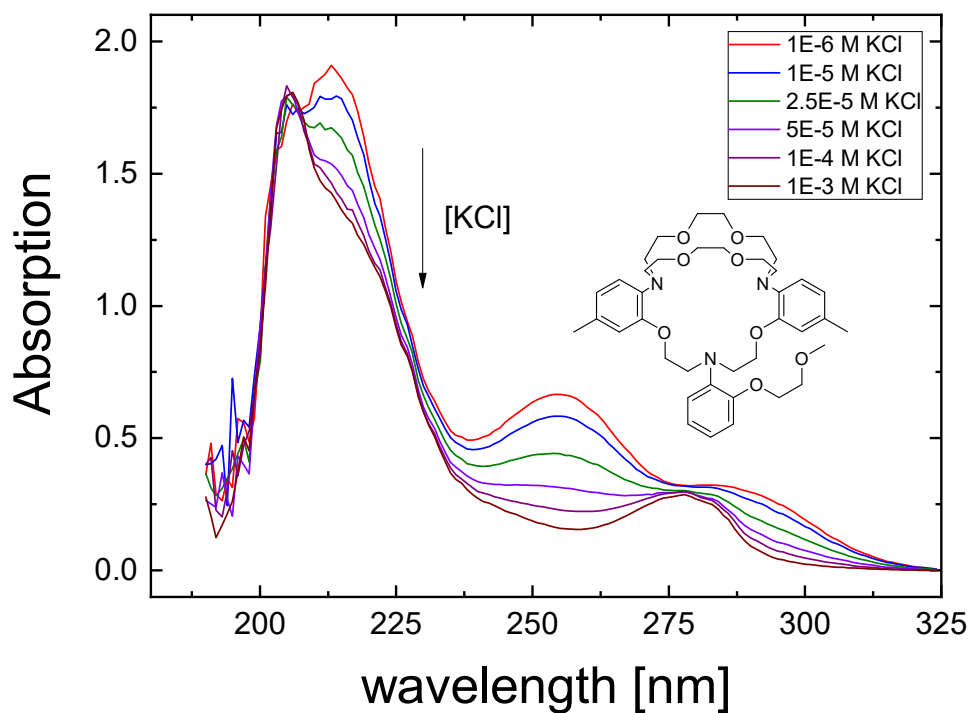


Figure 5.12.: Absorption Absorption KCl titration spectra for Triazacryptand

As expected the triazacryptand exhibits the highest complexation stability of all measured receptors. This is no surprise as its structural features allow for a much stronger host guest interaction. The cryptand's three bridge design enable it to effectively "trap" the potassium inside its cavity. With a response peak at 254 nm it exhibits a spectral properties that are very similar to that of the other measured crown ethers. **Substitution:** cryptand specific; **Absorption peak:** 254 nm; K_d for K^+ : 0.02 mM

5. Stability Constants

Table 5.1.: Absorption KCl titration - Overview of substitutions, absorption peaks and dissociation constants. Sample medium: ethanol+water 8+2 (20 mM Tris pH 7.4)

Name	Substitution	Absorption peak	K_d for K^+
Crown Ether 1	none	320 nm	4.2 mM
Crown Ether 3	<i>ortho</i> -methyl <i>ortho</i> -methoxy	275 nm	n.a.
Crown Ether 4	<i>ortho</i> -chloro	250 nm	0.21 mM
Crown Ether 5	<i>ortho</i> -methoxy	253 nm	0.65 mM
Crown Ether 6	<i>ortho</i> -methyl	252 nm	0.49 mM
Crown Ether 7	<i>para</i> -methoxy	230 nm	n.a.
MECE	<i>ortho</i> -methoxyethoxy	255 nm	0.09 mM
Triazacryptand	cryptand specific	254 nm	0.02 mM

5.10. Cross Sensitivity

In addition to the KCl titrations the crown ethers were also measured against their cross sensitivities towards other alkali and earth alkali ions as well as the ammonium ion. It is known that the NH_4^+ ion is very similar to K^+ in size which causes cross sensitivity, particularly for the 18-crown-6 ether. For this, the crown ethers were measured with a constant background of 10 mM of the specific ion. To remain consistent the chloride ion was chosen to be the counter ion for all measurements. The measurement medium also stayed the same as with the KCl titrations which was 8+2 ethanol+water (20 mM Tris pH 7.4).

Using the size exclusion theory the cross sensitivities can roughly be predicted. Based on ion diameters it is expected that the NH_4^+ (2.68 Å) ion will show the biggest cross sensitivity since it is very similar in diameter to that of K^+ (2.66 Å). This is followed by the Na^+ ion (1.90 Å) which is smaller than the ammonium ion but still big enough to achieve a certain level of coordination. Both Li^+ and Mg^{2+} are a lot smaller than the potassium ion. Based on their sizes they should show very weak to no cross sensitivity as the crown ether cavity is too large to form sufficient coordination. Ca^{2+} is very similar in size to Na^+ however it is double positively charged.

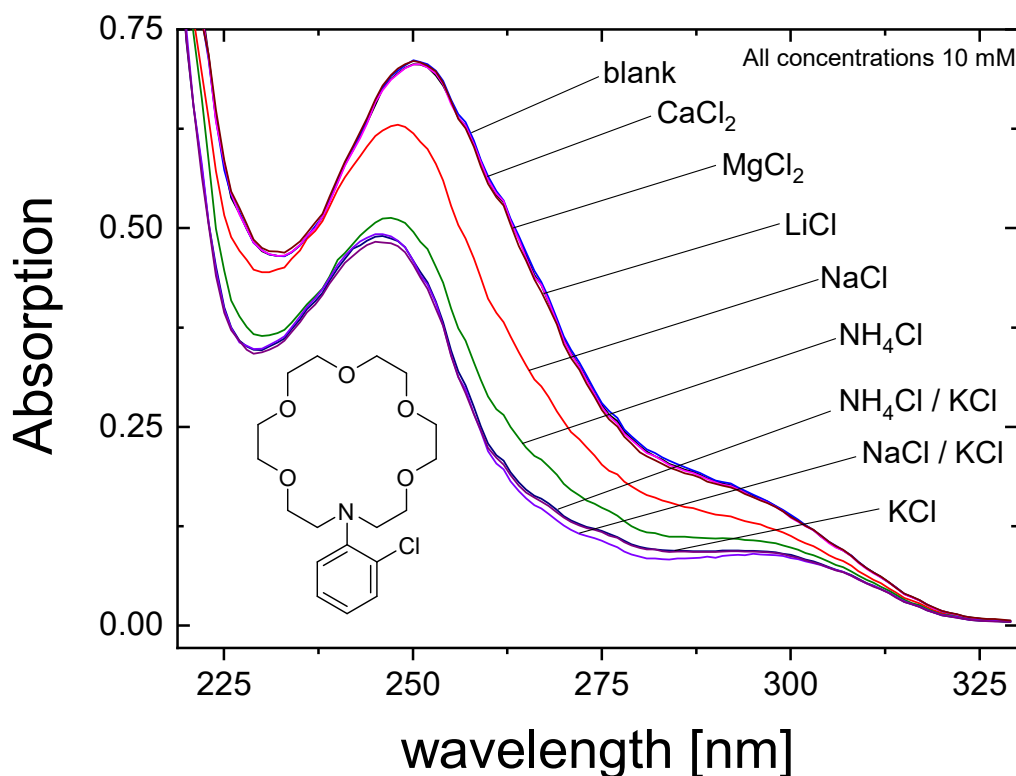


Figure 5.13.: Cross sensitivities for the *chloro*-substituted Crown Ether 4. All other cross sensitivity spectra can be found in the appendix.

In fig. 5.13 the absorption spectra for the chloro-substituted Crown Ether 4 are shown. The spectra for Ca²⁺, Mg²⁺, Li⁺ as well as the blank are very similar and overlap each other. This is in accordance with the predicted cross sensitivities. The Ca²⁺ ion, although very similar in size to Na⁺ exhibits no apparent complexation. A reason for this might be the twice positive charge which separates it from the sodium ion. There is a decent complexation for Na⁺ followed by a strong interaction with the NH₄⁺ ion. All crown ethers / receptors showed the same cross sensitivity behaviors except for two outliers. Both the methoxyethoxy- and methoxy (*ortho*) substituted crown ethers exhibited enhanced complexation towards Ca²⁺ and Na⁺. One explanation for this behavior is an interaction between the ether (oxygen) group and the guest ion. This results in an improved stability constant for both Ca²⁺ and Na⁺.

5. Stability Constants

5.11. Fluorescence Spectrometry

Since a consistent KCl titration using UV-Vis spectrometry was not possible for both Crown Ether **3** and Crown Ether **7** an attempt was made to determine the stability constant using fluorescence spectrometry. The principle and execution is very similar to that of the UV-Vis method. The sample consisted of the identical composition as when used during UV-Vis spectrometry. A wavelength at the area of the lower shoulder end of the absorption peak was selected as excitation wavelength. Just as with the UV-Vis method a decrease of fluorescence emission intensity was expected upon increasing KCl concentration. The process of determining the K_d values was identical to the one that was performed when using UV-Vis spectrometry (Benesi-Hildebrand plot).

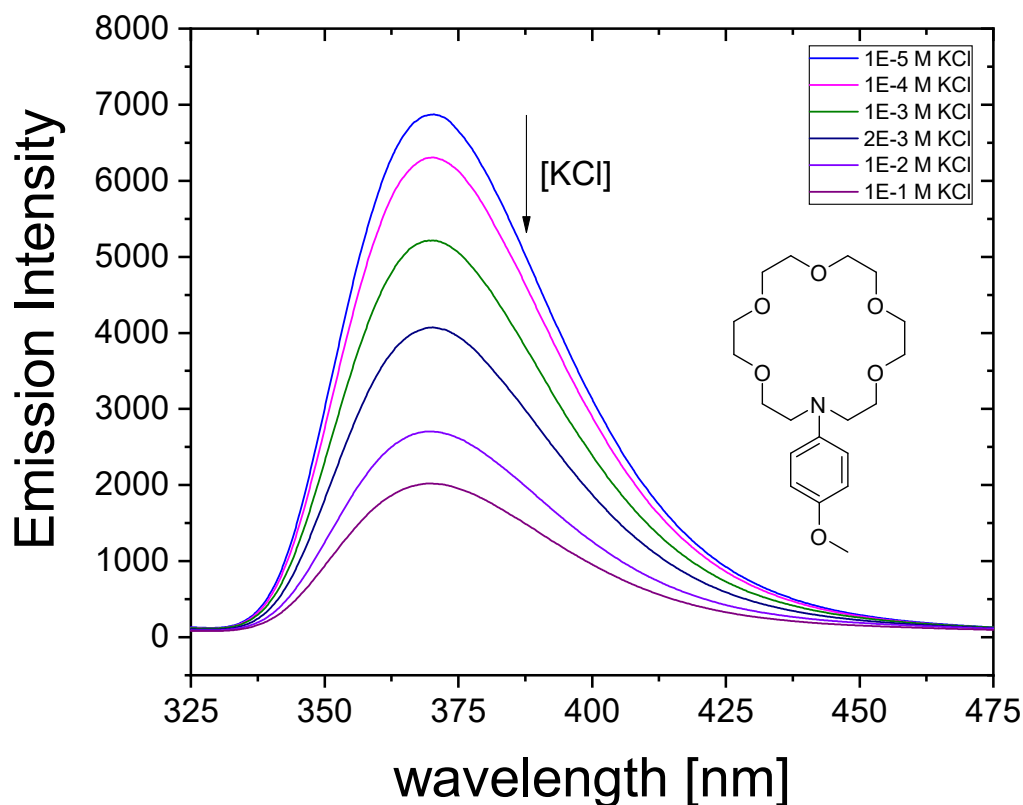


Figure 5.14.: KCl titration using fluorescence spectrometry for Crown Ether **7**. All other fluorescence titration spectra can be found in the appendix.

5.11. Fluorescence Spectrometry

Using fluorescence spectrometry method it was possible to determine the K_d for Crown Ether **7**. However, just as with UV-Vis spectrometry Crown Ether **3** did not yield any usable fluorescence spectra thus preventing us from calculating a K_d for it. A reason for this circumstance might be again, just as with the UV-Vis method, the lack of a planar structure caused by the steric hindrance of the double *ortho*-substituted phenyl moiety. The resulting lack of conjugation changes the receptor's electronic and optical properties which prevents us from gathering usable photometric data upon titration. Also, the emission from the *ortho*-chloro substituted Crown Ether **4** was too low to be used for calculating a K_d . A reason for this might be the heavy and electron drawing chlorine atom that influences the molecule's electronic properties. The other calculated K_d values using fluorescence spectrometry are very similar to those from UV-Vis method. It can therefore be assumed that both measurement methods were performed correctly.

Table 5.2.: Fluorescence KCl titration - Overview of substitutions, absorption peaks and dissociation constants. Sample medium: ethanol+water 8+2 (20 mM Tris pH 7.4)

Name	Substitution	Emission peak	K_d for K^+
Crown Ether 1	none	346 nm	6.3 mM
Crown Ether 5	<i>ortho</i> -methoxy	365 nm	0.07 mM
Crown Ether 6	<i>ortho</i> -methyl	366 nm	1.0 mM
Crown Ether 7	<i>para</i> -methoxy	370 nm	1.6 mM
MECE	<i>ortho</i> -methoxyethoxy	365 nm	0.11 mM
Triazacryptand	specific	370 nm	0.06 mM

6. Conclusion

For this master thesis various phenyl aza crown ethers with different substitutions at the phenyl moiety were synthesized. These crown have proven to be capable potassium ion receptors based on their specific crown ether cavity diameter. The influence of different substituted phenyl moieties were outlined by determining the specific complex stability constants. This was done by conducting a KCl titration using UV-Vis spectrometry to detect changes in the receptors' absorption intensity. Additionally, an attempt was made to conduct the same determination via fluorescence spectrometry. Upon complexation of a potassium ion both the absorption and the fluorescence intensity are decreased as the nitrogen lone pair density decreases. All stability constants were determined in ethanol+water 8+2 including a 20 mM Tris pH 7.4 buffer system. Overall, it can be concluded that by increasing the electron density of the nitrogen lone pair increases the complex stability. This is done by incorporating electron donating side groups such as methyl or methoxy units preferably in *ortho* position of the phenyl moiety. However, another significant increase in complex stability was observed when incorporating additional complexating groups such as ether groups. When these complexating groups were placed in a position where they can interact with the guest directly a significant increase in complex stability was achieved. Since it is known that 18-crown-6 ethers show cross sensitivity towards NH_4^+ a cross sensitivity survey was conducted. This was done by using UV-Vis spectrometry to measure the absorption intensity decrease upon complexation. The crown ethers were measured towards all common alkali, earth alkali ions as well as NH_4^+ . The survey confirmed that there is a significant cross sensitivity towards NH_4^+ . This can be explained by the very similar ion size diameter of both ammonium and potassium ions. Furthermore, a small cross sensitivity towards Na^+ was demonstrated. When a methoxy unit was present at the phenyl moiety a slight increase in cross sensitivity towards Ca^{2+} was also determined. This suggests that the methoxy unit can interact with the double positively charged calcium ion.

6. Conclusion

For an outlook it is worth exploring additional complexating side groups. By incorporating additional complexating side groups in positions where they can interact with the guest ion a significant increase in complex stability can be achieved. This was already demonstrated by Gokel et al. in 1980³¹ where they characterized differently aliphatic substituted crown ethers. This concept can also be transferred to phenyl aza crown ethers where the phenyl moiety provides a lot of freedom for substitutions. The phenyl moiety provides suitable positions for complexating side arms as well as the possibility for in addition of a fluorophore. Some structures that are worth exploring are listed in fig. 6.1. All of these structures have complexating side arms that should be able to interact with the guest ion. Overall, the focus when designing new cation crown ether receptors should be on the placement of complexating side groups that further increase the complex stability.

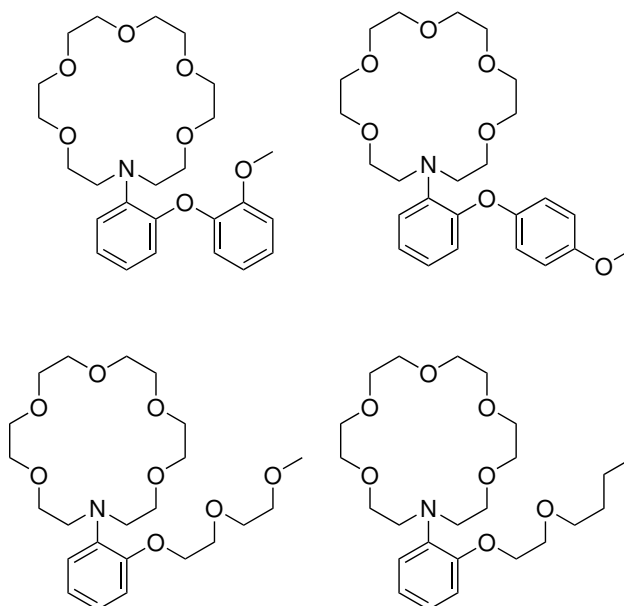


Figure 6.1.: Phenyl aza crown ether structures with additional complexating side arms that should provide strong interaction with the guest ion

Table 6.1.: Overview over the different crown ethers and their photophysical and complexating properties. Sample medium: ethanol+water 8+2 (20 mM Tris pH 7.4)

Name	Substitution	Absorption peak	Emission peak	Absorption K_d	Emission K_d
Crown Ether 1	none	320 nm	346 nm	4.2 mM	6.3 mM
Crown Ether 3	<i>ortho</i> -methyl <i>ortho</i> -methoxy	275 nm		n.a.	n.a.
Crown Ether 4	<i>ortho</i> -chloro	250 nm	n.a.	0.21 mM	n.a.
Crown Ether 5	<i>ortho</i> -methoxy	253 nm	365 nm	0.65 mM	0.07 mM
Crown Ether 6	<i>ortho</i> -methyl	252 nm	366 nm	0.49 mM	1.0 mM
Crown Ether 7	<i>para</i> -methoxy	230 nm	370 nm	n.a.	1.6 mM
MECE	<i>ortho</i> -methoxyethoxy	255 nm	365 nm	0.09 mM	0.11 mM
Triazacryptand	cryptand specific	254 nm	370 nm	0.02 mM	0.06 mM

Bibliography

- (1) Valeur, B.; Berberan-Santos, M. N., *Molecular Fluorescence: Principles and Applications*, Second edition, OCLC: ocn775030634; Wiley-VCH ; Wiley-VCH Verlag GmbH & Co. KGaA: Weinheim, Germany : [Chichester, England], 2012; 569 pp. (cit. on p. 3).
- (2) Lakowicz, J. R.; Masters, B. R. Principles of Fluorescence Spectroscopy, Third Edition. *Journal of Biomedical Optics* **2008**, *13*, 029901 (cit. on pp. 3, 29).
- (3) *IUPAC Compendium of Chemical Terminology: Gold Book*, 2.1.0; Nič, M., Jiráť, J., Košata, B., Jenkins, A., McNaught, A., Eds.; IUPAC: Research Triangle Park, NC, 2009 (cit. on p. 6).
- (4) Born, M.; Oppenheimer, R. Zur Quantentheorie Der Molekeln. *Annalen der Physik* **1927**, *389*, 457–484 (cit. on p. 7).
- (5) Lehn, J.-M. Supramolecular Chemistry -Scope and Perspectives Molecules, Supermolecules, and Molecular Devices (Nobel Lecture). *Angewandte Chemie International Edition in English* **1988**, *27*, 89–112 (cit. on p. 15).
- (6) Ariga, K.; Kunitake, T., *Supramolecular Chemistry - Fundamentals and Applications: Advanced Textbook*; Springer-Verlag: Berlin Heidelberg, 2006 (cit. on p. 15).
- (7) Schneider, H.-J., *Applications of Supramolecular Chemistry*; CRC Press: 2012 (cit. on p. 15).
- (8) Yuan, C.; Chang, Y.; Mao, J.; Yu, S.; Luo, W.; Xu, Y.; Thayumanavan, S.; Dai, L. Supramolecular Assembly of Crosslinkable Monomers for Degradable and Fluorescent Polymer Nanoparticles. *Journal of Materials Chemistry B* **2015**, *3*, 2858–2866 (cit. on p. 15).

Bibliography

- (9) Zhang, Z.; Luo, Y.; Chen, J.; Dong, S.; Yu, Y.; Ma, Z.; Huang, F. Formation of Linear Supramolecular Polymers That Is Driven by CH Interactions in Solution and in the Solid State. *Angewandte Chemie International Edition* **2011**, *50*, 1397–1401 (cit. on p. 15).
- (10) Wang, F.; Zhang, J.; Ding, X.; Dong, S.; Liu, M.; Zheng, B.; Li, S.; Wu, L.; Yu, Y.; Gibson, H. W.; Huang, F. Metal Coordination Mediated Reversible Conversion between Linear and Cross-Linked Supramolecular Polymers. *Angewandte Chemie International Edition* **2010**, *49*, 1090–1094 (cit. on p. 15).
- (11) Szente, L.; Szemán, J. Cyclodextrins in Analytical Chemistry: Host–Guest Type Molecular Recognition. *Analytical Chemistry* **2013**, *85*, 8024–8030 (cit. on p. 15).
- (12) Slone, R. V.; Benkstein, K. D.; Bélanger, S.; Hupp, J. T.; Guzei, I. A.; Rheingold, A. L. Luminescent Transition-Metal-Containing Cyclophanes (“Molecular Squares”): Covalent Self-Assembly, Host-Guest Studies and Preliminary Nanoporous Materials Applications. *Coordination Chemistry Reviews* **1998**, *171*, 221–243 (cit. on p. 15).
- (13) Kim, H. J.; Lee, M. H.; Mutihac, L.; Vicens, J.; Kim, J. S. Host–Guest Sensing by Calixarenes on the Surfaces. *Chem. Soc. Rev.* **2012**, *41*, 1173–1190 (cit. on p. 15).
- (14) Gokel, G. W.; Leevy, W. M.; Weber, M. E. Crown Ethers: Sensors for Ions and Molecular Scaffolds for Materials and Biological Models. *Chemical Reviews* **2004**, *104*, 2723–2750 (cit. on pp. 15, 24).
- (15) Liu, K.; Kang, Y.; Wang, Z.; Zhang, X. 25th Anniversary Article: Reversible and Adaptive Functional Supramolecular Materials: “Noncovalent Interaction” Matters. *Advanced Materials* **2013**, *25*, 5530–5548 (cit. on p. 16).
- (16) Rodnikova, M. N. Mechanism of Solvophobic Interactions. *Russian Journal of Physical Chemistry* **2006**, *80*, 1605–1607 (cit. on p. 16).
- (17) Schneider, H.-J. Mechanisms of Molecular Recognition : Investigations of Organic Host–Guest Complexes. *Angewandte Chemie International Edition in English* **1991**, *30*, 1417–1436 (cit. on p. 16).

- (18) Buschmann, H.-J. A Comparison of Different Experimental Techniques for the Determination of the Stabilities of Polyether, Crown Ether and Cryptand Complexes in Solution. *Inorganica Chimica Acta* **1992**, *195*, 51–60 (cit. on pp. 16, 36).
- (19) Blair, S. M.; Kempen, E. C.; Brodbelt, J. S. Determination of Binding Selectivities in Host-Guest Complexation by Electrospray/Quadrupole Ion Trap Mass Spectrometry. *Journal of the American Society for Mass Spectrometry* **1998**, *9*, 1049–1059 (cit. on pp. 16, 36).
- (20) Hirose, K. A Practical Guide for the Determination of Binding Constants. *Journal of inclusion phenomena and macrocyclic chemistry* **2001**, *39*, 193–209 (cit. on p. 16).
- (21) Pedersen, C. J. Cyclic Polyethers and Their Complexes with Metal Salts. *Journal of the American Chemical Society* **1967**, *89*, 2495–2496 (cit. on p. 17).
- (22) Pedersen, C. J.; Frensdorff, H. K. Macrocyclic Polyethers and Their Complexes. *Angewandte Chemie International Edition in English* **1972**, *11*, 16–25 (cit. on p. 17).
- (23) Dietrich, B.; Lehn, J.; Sauvage, J. Diaza-polyoxa-macrocycles et macrobicycles. *Tetrahedron Letters* **1969**, *10*, 2885–2888 (cit. on p. 18).
- (24) Lehn, J.-M. In *Alkali Metal Complexes with Organic Ligands*, Springer Berlin Heidelberg: 1973, pp 1–69 (cit. on pp. 18, 21).
- (25) Hanson, I. R.; Parsons, D. G.; Truter, M. R. Complexes of Alkali Metal Salts with Bridged Macrocyclic Polyethers; X-Ray Crystal Structure of (1,4,7,14,17,20,28,35 - Octaoxa[23,29 · 218,34][7 · 7] - Orthocyclophane)Potassium Chloride Multihydrate. *Journal of the Chemical Society, Chemical Communications* **1979**, *0*, 486–488 (cit. on p. 18).
- (26) Dietrich, B.; Lehn, J. M.; Sauvage, J. P. Oxathia-Macrobicyclic Diamines and Their “Cryptates”. *Journal of the Chemical Society D: Chemical Communications* **1970**, *0*, 1055–1056 (cit. on p. 18).
- (27) Buhleier, E.; Wehner, W.; Vögtle, F. Ligandstruktur und Komplexierung, XIII: 2,2-Bipyridin als Baustein für neue Aza-Kronenether und Cryptanden. *Chemische Berichte* **1978**, *111*, 200–204 (cit. on p. 18).

Bibliography

- (28) Weber, V. E.; Vögtle, F. Kristalline 1:1-Alkalimetallkomplexe Nichtcyclischer Neutralliganden. *Tetrahedron Letters* **1975**, *16*, 2415–2418 (cit. on p. 18).
- (29) Vögtle, F.; Sieger, H. „Nichtcyclische Kronenether“: Das Endgruppen-Konzept. *Angewandte Chemie* **1977**, *89*, 410–412 (cit. on p. 19).
- (30) Vögtle, F.; Weber, E. Vielzählige nichtcyclische Neutralliganden und ihre Komplexbildung. *Angewandte Chemie* **1979**, *91*, 813–837 (cit. on p. 19).
- (31) Gokel, G. W.; Dishong, D. M.; Diamond, C. J. Lariat Ethers. Synthesis and Cation Binding of Macrocyclic Polyethers Possessing Axially Disposed Secondary Donor Groups. *Journal of the Chemical Society, Chemical Communications* **1980**, 1053 (cit. on pp. 19, 24, 86).
- (32) Beresford, G. D.; Stoddart, J. F. The syntheses and complexing properties of oxo-12-crown-3 and oxo-18-crown-5. *Tetrahedron Letters* **1980**, *21*, 867–870 (cit. on p. 20).
- (33) Cram, D. J.; Kaneda, T.; Helgeson, R. C.; Lein, G. M. Spherands - Ligands Whose Binding of Cations Relieves Enforced Electron-Electron Repulsions. *Journal of the American Chemical Society* **1979**, *101*, 6752–6754 (cit. on p. 20).
- (34) Izatt, R. M.; Eatough, D. J.; Christensen, J. J. In *Alkali Metal Complexes with Organic Ligands*; Springer-Verlag: Berlin/Heidelberg, 1973; Vol. 16, pp 161–189 (cit. on pp. 21, 22).
- (35) Christensen, J. J.; Eatough, D. J.; Izatt, R. M. The Synthesis and Ion Bindings of Synthetic Multidentate Macrocyclic Compounds. *Chemical Reviews* **1974**, *74*, 351–384 (cit. on p. 21).
- (36) Vögtle, F.; Weber, E. Neue Komplexligand-Systeme für Alkalimetall-Ionen. *Angewandte Chemie* **1974**, *86*, 126–127 (cit. on p. 22).
- (37) Tuemmler, B.; Maass, G.; Weber, E.; Wehner, W.; Voegtle, F. Noncyclic Crown-Type Polyethers, Pyridinophane Cryptands, and Their Alkali Metal Ion Complexes: Synthesis, Complex Stability, and Kinetics. *Journal of the American Chemical Society* **1977**, *99*, 4683–4690 (cit. on p. 22).
- (38) Simon, W.; Morf, W. E.; Meier, P. C. In *Alkali Metal Complexes with Organic Ligands*; Springer-Verlag: Berlin/Heidelberg, 1973; Vol. 16, pp 113–160 (cit. on p. 22).

- (39) Petránek, J.; Ryba, O. A New Type of Macrocyclic Polyether-Diamide Ligand - Binding Properties for Alkaline Earth Ions. *Tetrahedron Letters* **1977**, *18*, 4249–4250 (cit. on p. 22).
- (40) Frensdorff, H. K. Stability Constants of Cyclic Polyether Complexes with Univalent Cations. *Journal of the American Chemical Society* **1971**, *93*, 600–606 (cit. on p. 23).
- (41) Burgermeister, W.; Winkler-Oswatitsch, R. Complex Formation of Monovalent Cations with Biofunctional Ligands. *Topics in Current Chemistry* **1977**, *69*, 91–204 (cit. on p. 23).
- (42) Cox, B. G.; Schneider, H.; Stroka, J. Kinetics of Alkali Metal Complex Formation with Cryptands in Methanol. *Journal of the American Chemical Society* **1978**, *100*, 4746–4749 (cit. on p. 24).
- (43) De Jong, F.; Reinhoudt, D.; Huis, R. Kinetics of Complexation between Tert-Butylammonium Hexafluorophosphate and Crown Ethers. *Tetrahedron Letters* **1977**, *18*, 3985–3988 (cit. on p. 24).
- (44) Kado, S.; Kimura, K. Single Complexation Force of 18-Crown-6 with Ammonium Ion Evaluated by Atomic Force Microscopy. *Journal of the American Chemical Society* **2003**, *125*, 4560–4564 (cit. on p. 25).
- (45) De Silva, A. P.; Gunnlaugsson, T.; Rice, T. E. Recent Evolution of Luminescent Photoinduced Electron Transfer Sensors. A Review. *The Analyst* **1996**, *121*, 1759 (cit. on p. 26).
- (46) Grynkiewicz, G.; Poenie, M.; Tsien, R. Y. A New Generation of Ca²⁺ Indicators with Greatly Improved Fluorescence Properties. *Journal of Biological Chemistry* **1985**, *260*, 3440–3450 (cit. on p. 26).
- (47) *Topics in Fluorescence Spectroscopy: Volume 4: Probe Design and Chemical Sensing*; Lakowicz, J. R., Ed.; Topics in Fluorescence Spectroscopy; Springer US: 1994 (cit. on p. 26).
- (48) Wolfbeis, O. S. Fiber-Optic Chemical Sensors and Biosensors. *Analytical Chemistry* **2006**, *78*, 3859–3874 (cit. on p. 26).
- (49) De Silva, A. P.; Gunaratne, H. Q. N.; Gunnlaugsson, T.; Huxley, A. J. M.; McCoy, C. P.; Rademacher, J. T.; Rice, T. E. Signaling Recognition Events with Fluorescent Sensors and Switches. *Chemical Reviews* **1997**, *97*, 1515–1566 (cit. on p. 26).

Bibliography

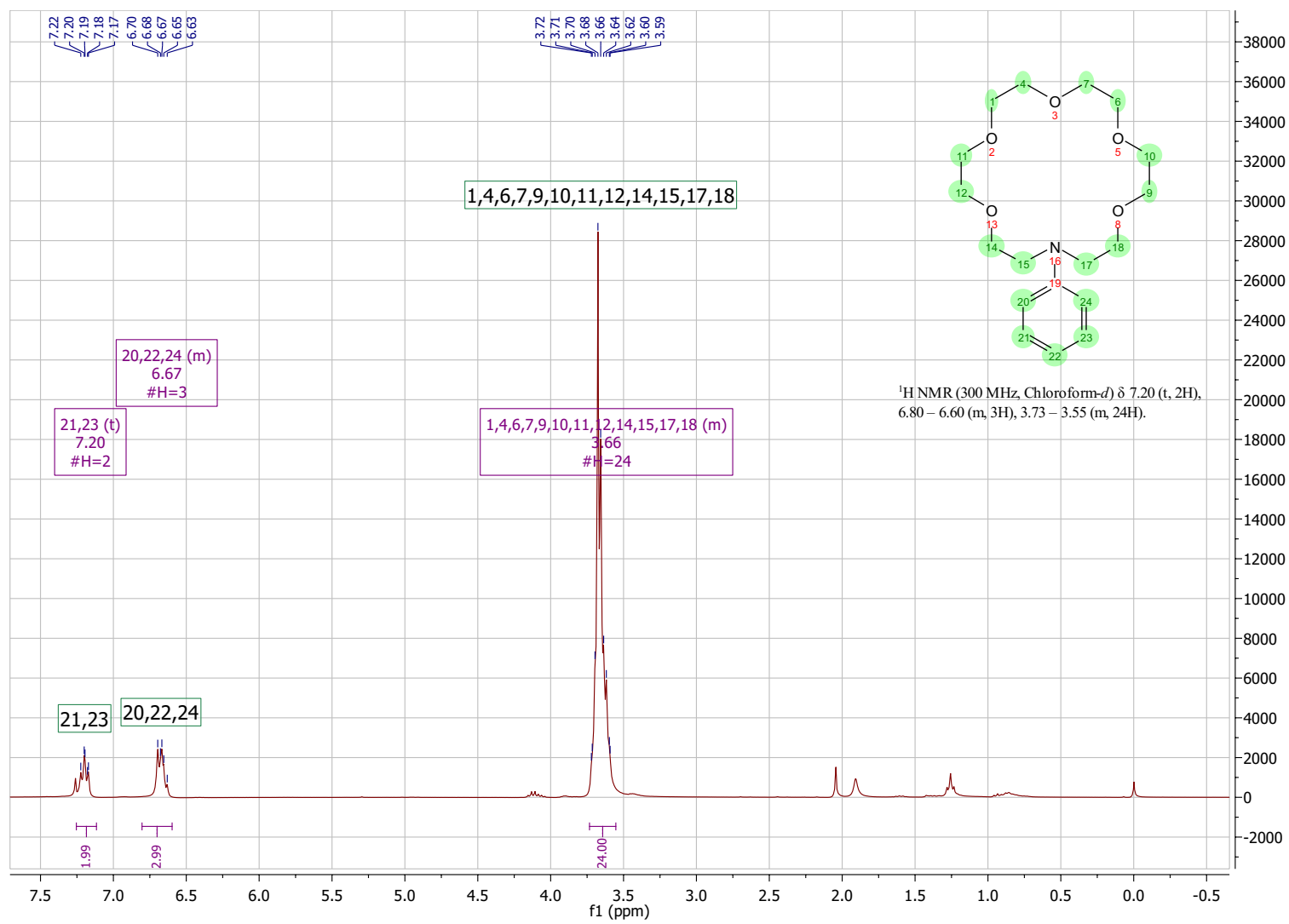
- (50) De Silva, A. P.; de Silva, S. A. Fluorescent Signalling Crown Ethers; ‘Switching on’ of Fluorescence by Alkali Metal Ion Recognition and Binding in Situ. *J. Chem. Soc., Chem. Commun.* **1986**, 1709–1710 (cit. on p. 27).
- (51) Müller, B. J.; Borisov, S. M.; Klimant, I. Red- to NIR-Emitting, BODIPY-Based, K⁺-Selective Fluoroionophores and Sensing Materials. *Advanced Functional Materials* **2016**, *26*, 7697–7707 (cit. on pp. 27, 67).
- (52) De Silva, A. P.; Gunaratne, H. Q. N.; Gunnlaugsson, T.; Nieuwenhuizen, M. Fluorescent Switches with High Selectivity towards Sodium Ions: Correlation of Ion-Induced Conformation Switching with Fluorescence Function. *Chemical Communications* **1996**, 1967 (cit. on p. 27).
- (53) *Molecular Luminescence Spectroscopy: Methods and Applications. 3: ...* Schulman, S. G., Ed.; Chemical Analysis 77,3, OCLC: 632797950; Wiley: New York, 1993, 467 pp. (cit. on p. 27).
- (54) Jin, T. A New Na⁺ Sensor Based on Intramolecular Fluorescence Energy Transfer Derived from Calix[4]Arene. *Chemical Communications* **1999**, 2491–2492 (cit. on p. 29).
- (55) Chen, G.; Song, F.; Xiong, X.; Peng, X. Fluorescent Nanosensors Based on Fluorescence Resonance Energy Transfer (FRET). *Industrial & Engineering Chemistry Research* **2013**, *52*, 11228–11245 (cit. on p. 29).
- (56) Dos Remedios, C. G.; Moens, P. D. J. Fluorescence Resonance Energy Transfer Spectroscopy Is a Reliable “Ruler” for Measuring Structural Changes in Proteins: Dispelling the Problem of the Unknown Orientation Factor. *Journal of Structural Biology* **1995**, *115*, 175–185 (cit. on p. 30).
- (57) Connors, K. A., *Binding Constants: The Measurement of Molecular Complex Stability*, OCLC: 816724411; J. Wiley: New York, 1987 (cit. on p. 33).
- (58) *Physical Methods in Supramolecular Chemistry*, 1. ed; Davies, J. E. D., Lehn, J.-M., Atwood, J. L., Eds.; Comprehensive Supramolecular Chemistry executive ed. Jerry L. Atwood ... Chairman of the ed. board Jean-Marie Lehn ; Vol. 8, OCLC: 258172029; Pergamon: Oxford, 1996, 660 pp. (cit. on p. 33).

- (59) *Cyclodextrins*, 1. ed; Szejtli, J., Lehn, J.-M., Atwood, J. L., Eds.; Comprehensive Supramolecular Chemistry executive ed. Jerry L. Atwood ... Chairman of the ed. board Jean-Marie Lehn ; Vol. 3, OCLC: 258171861; Pergamon: Oxford, 1996, 693 pp. (cit. on p. 33).
- (60) Motulsky, H. J.; Ransnas, L. A. Fitting Curves to Data Using Nonlinear Regression: A Practical and Nonmathematical Review. *The FASEB Journal* **1987**, *1*, 365–374 (cit. on p. 34).
- (61) Motulsky, H.; Christopoulos, A. Fitting Models to Biological Data Using Linear and Nonlinear Regression., 351 (cit. on p. 34).
- (62) Benesi, H. A.; Hildebrand, J. H. A Spectrophotometric Investigation of the Interaction of Iodine with Aromatic Hydrocarbons. *Journal of the American Chemical Society* **1949**, *71*, 2703–2707 (cit. on pp. 34, 67, 70).
- (63) Lineweaver, H.; Burk, D. The Determination of Enzyme Dissociation Constants. *Journal of the American Chemical Society* **1934**, *56*, 658–666 (cit. on p. 34).
- (64) Scott, R. L. Some Comments on the Benesi-Hildebrand Equation. *Recueil des Travaux Chimiques des Pays-Bas* **2010**, *75*, 787–789 (cit. on p. 34).
- (65) Haldane, J. B. S. Graphical Methods in Enzyme Chemistry. *Nature* **1957**, *179*, 832 (cit. on p. 34).
- (66) Scatchard, G. The Attractions of Proteins for Small Molecules and Ions. *Annals of the New York Academy of Sciences* **1949**, *51*, 660–672 (cit. on p. 34).
- (67) Thordarson, P. Determining Association Constants from Titration Experiments in Supramolecular Chemistry. *Chem. Soc. Rev.* **2011**, *40*, 1305–1323 (cit. on pp. 35, 36).

Appendix

Appendix A.

NMR Spectra

Figure A.1.: $^1\text{H-NMR}$ spectrum of crown ether **1**

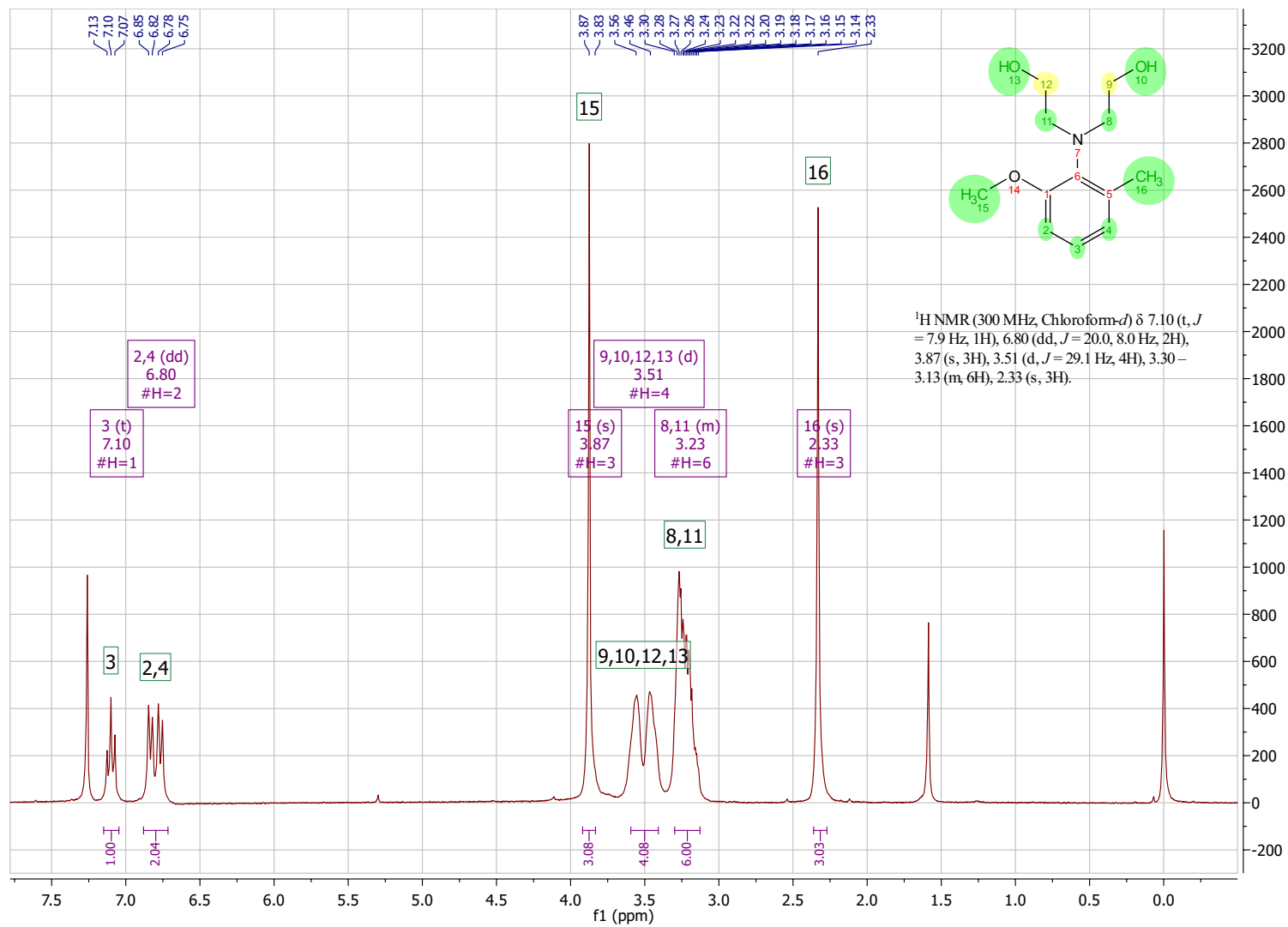
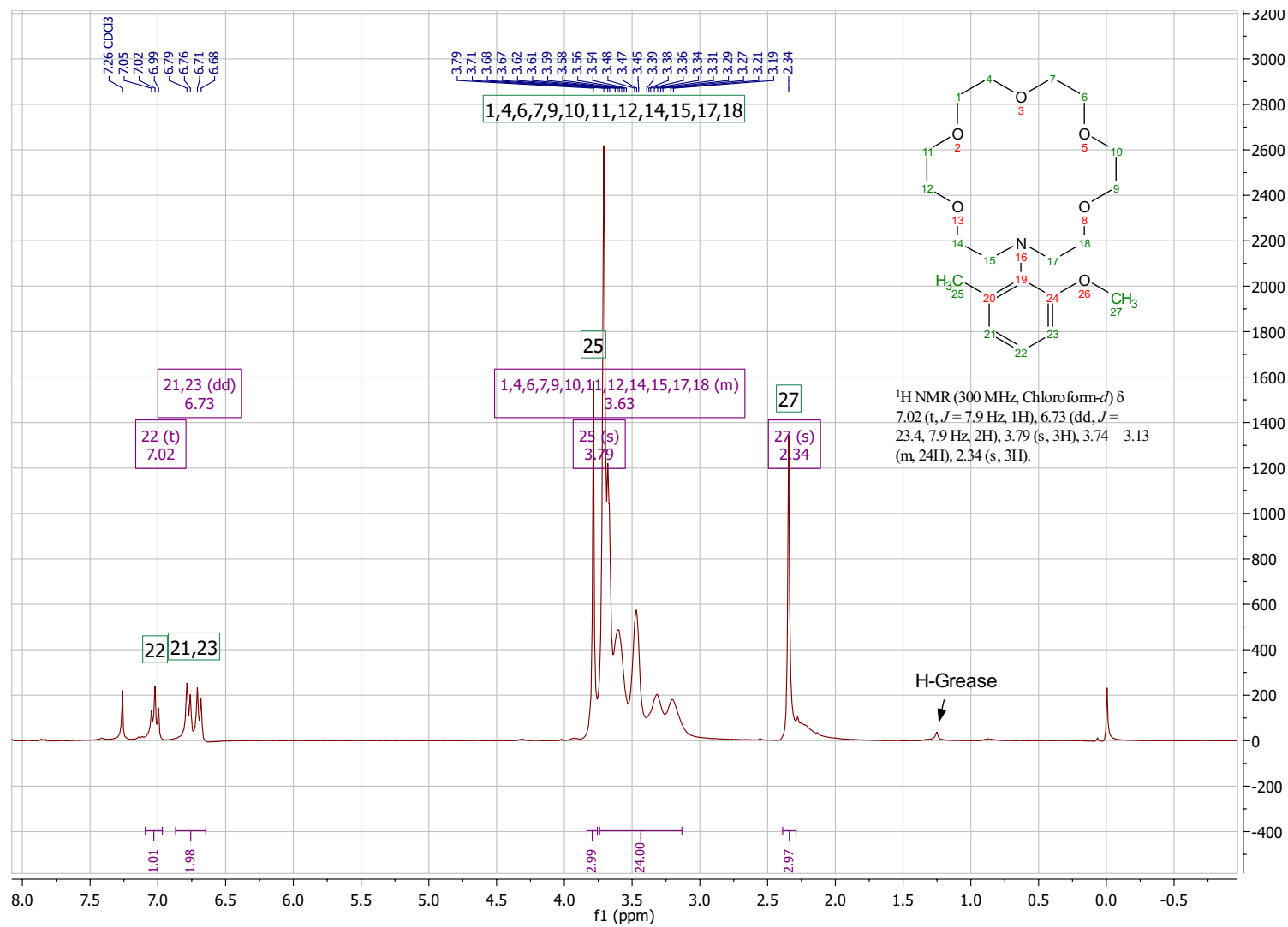


Figure A.2.: $^1\text{H-NMR}$ spectrum of precursor **3a**

Figure A.3.: ¹H-NMR spectrum of crown ether **3**

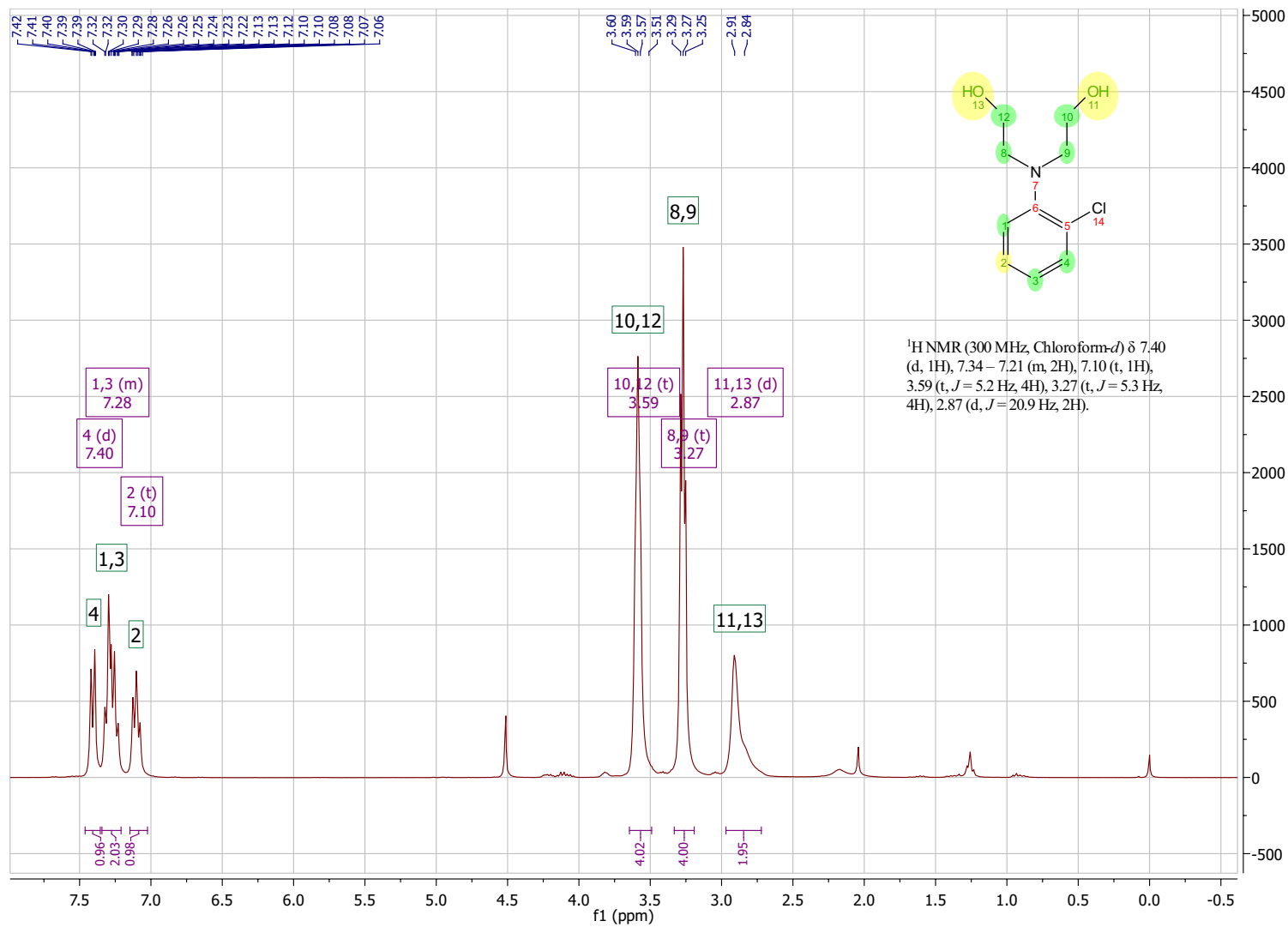
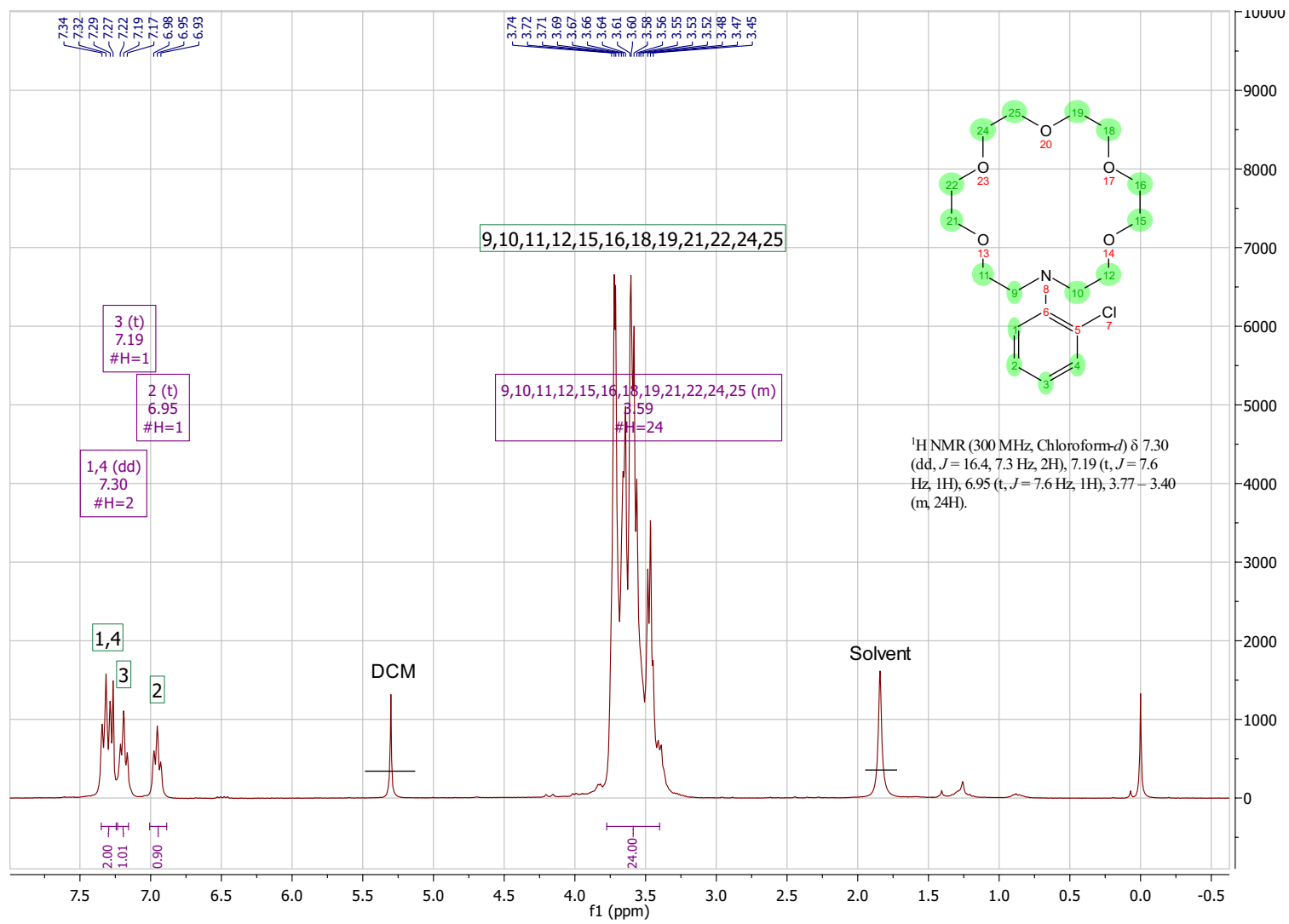


Figure A.4.: ¹H-NMR spectrum of precursor **4a**

Figure A.5.: ¹H-NMR spectrum of crown ether 4

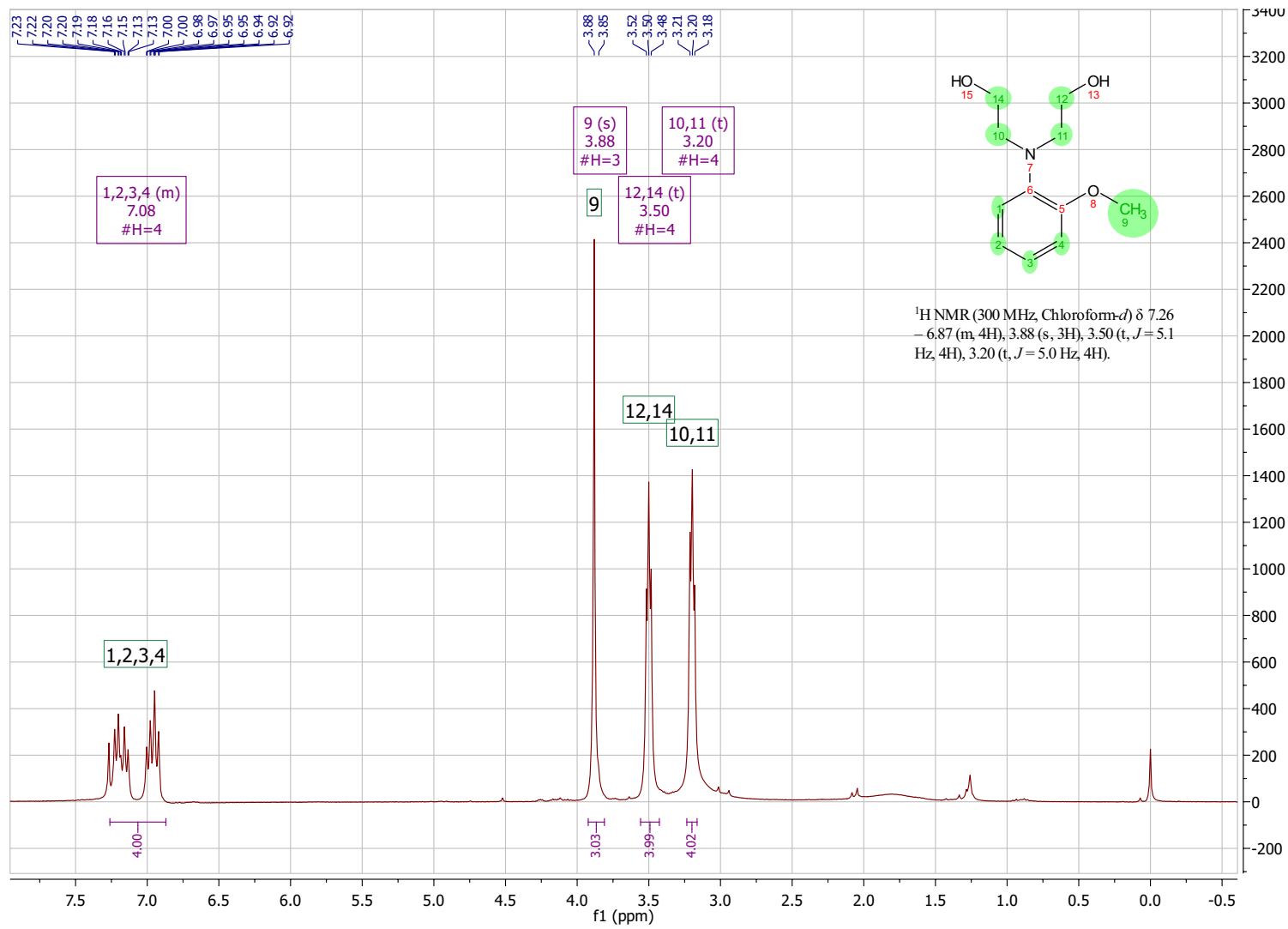
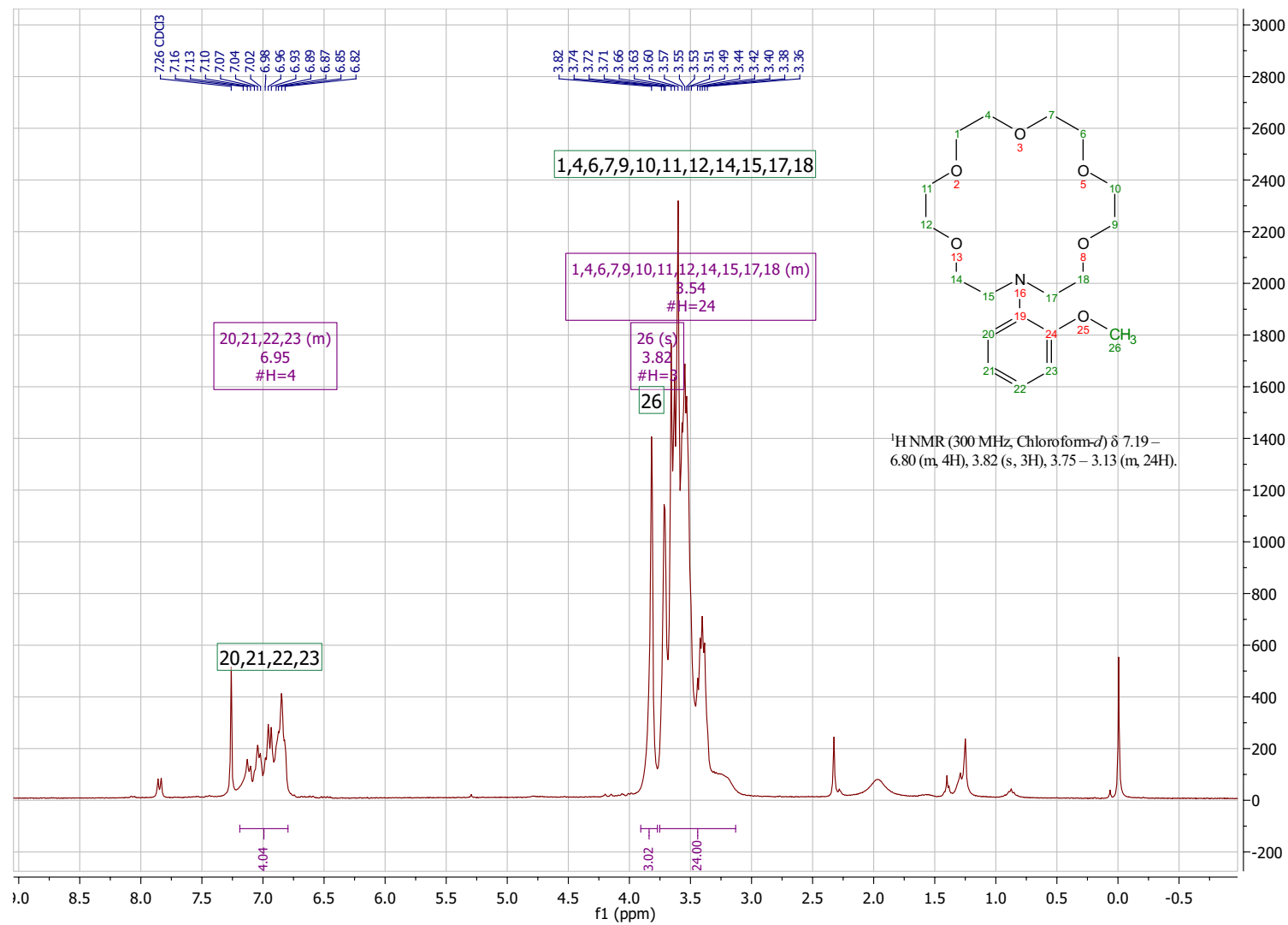


Figure A.6.: $^1\text{H-NMR}$ spectrum of precursor **5a**

Figure A.7.: $^1\text{H-NMR}$ spectrum of crown ether 5

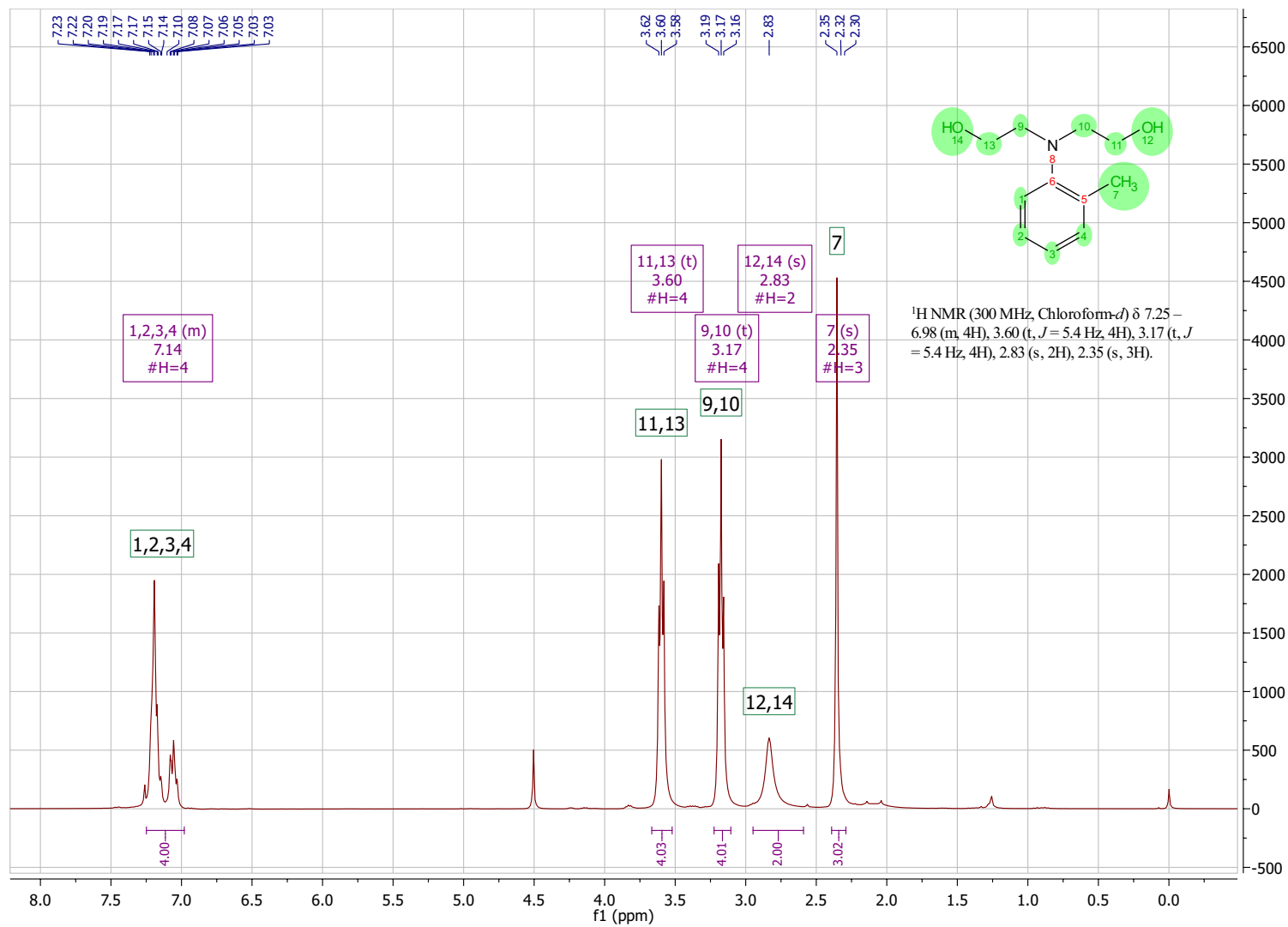
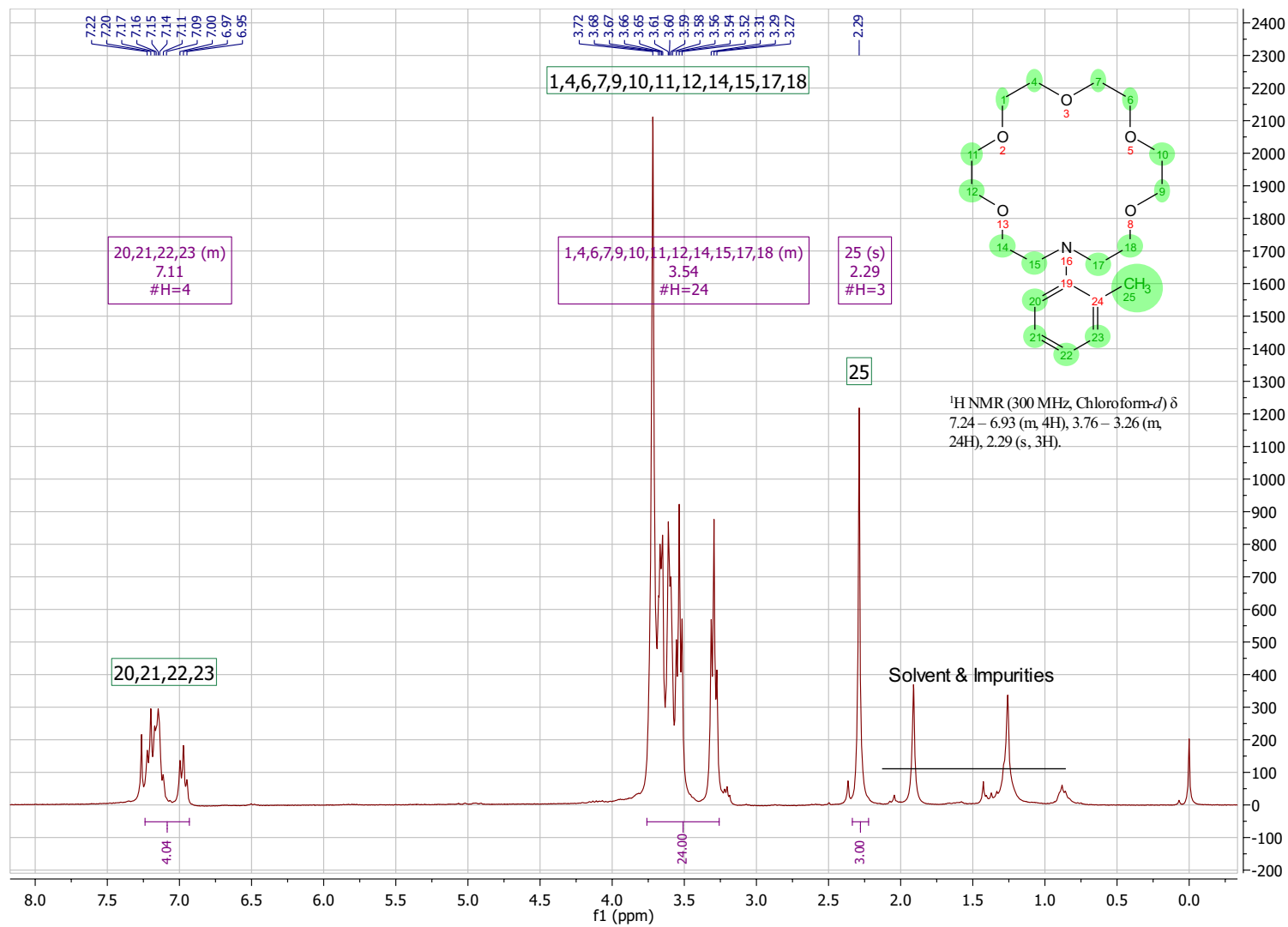


Figure A.8.: $^1\text{H-NMR}$ spectrum of precursor **6a**

Figure A.9.: ^1H -NMR spectrum of crown ether **6**

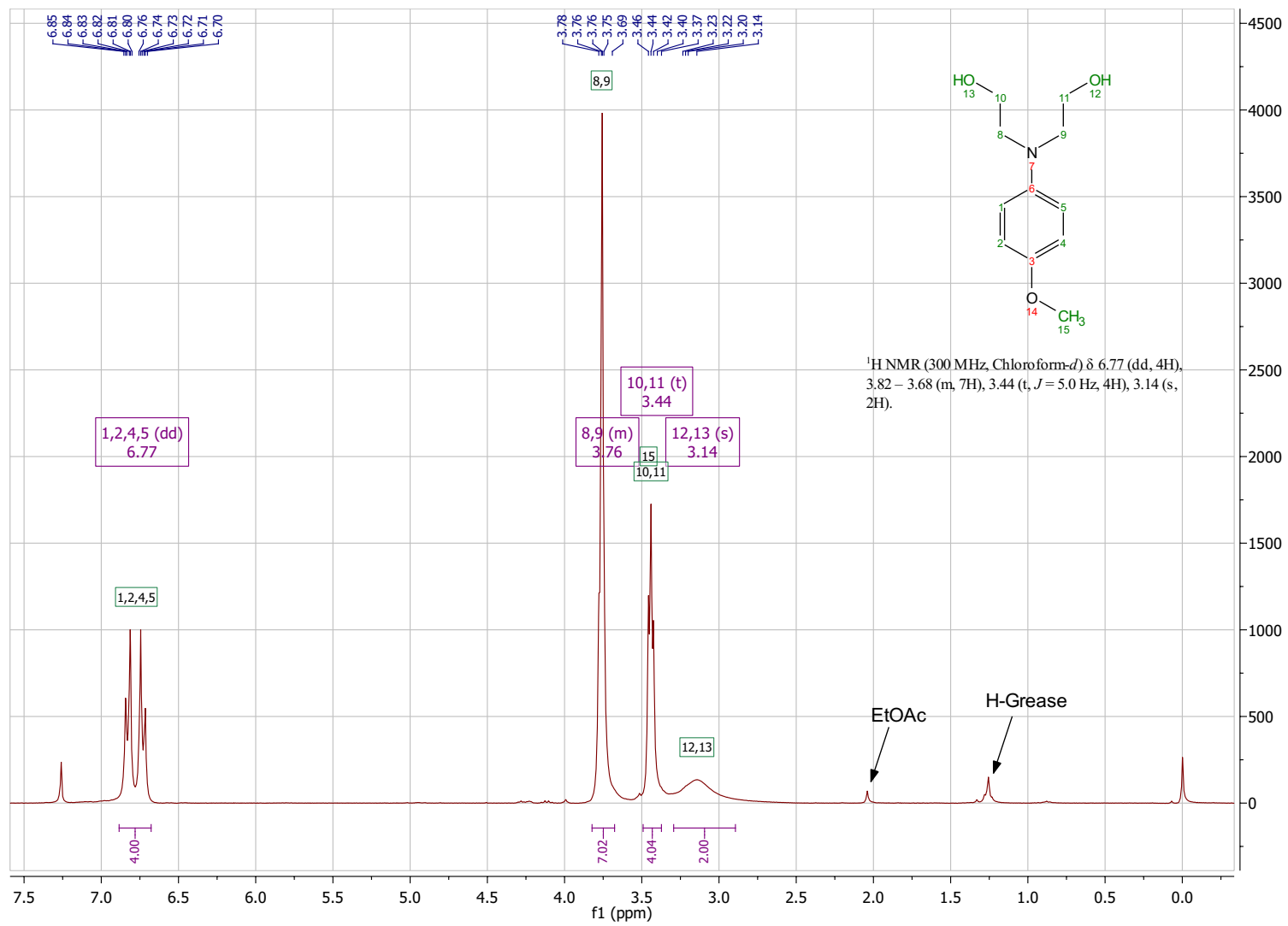
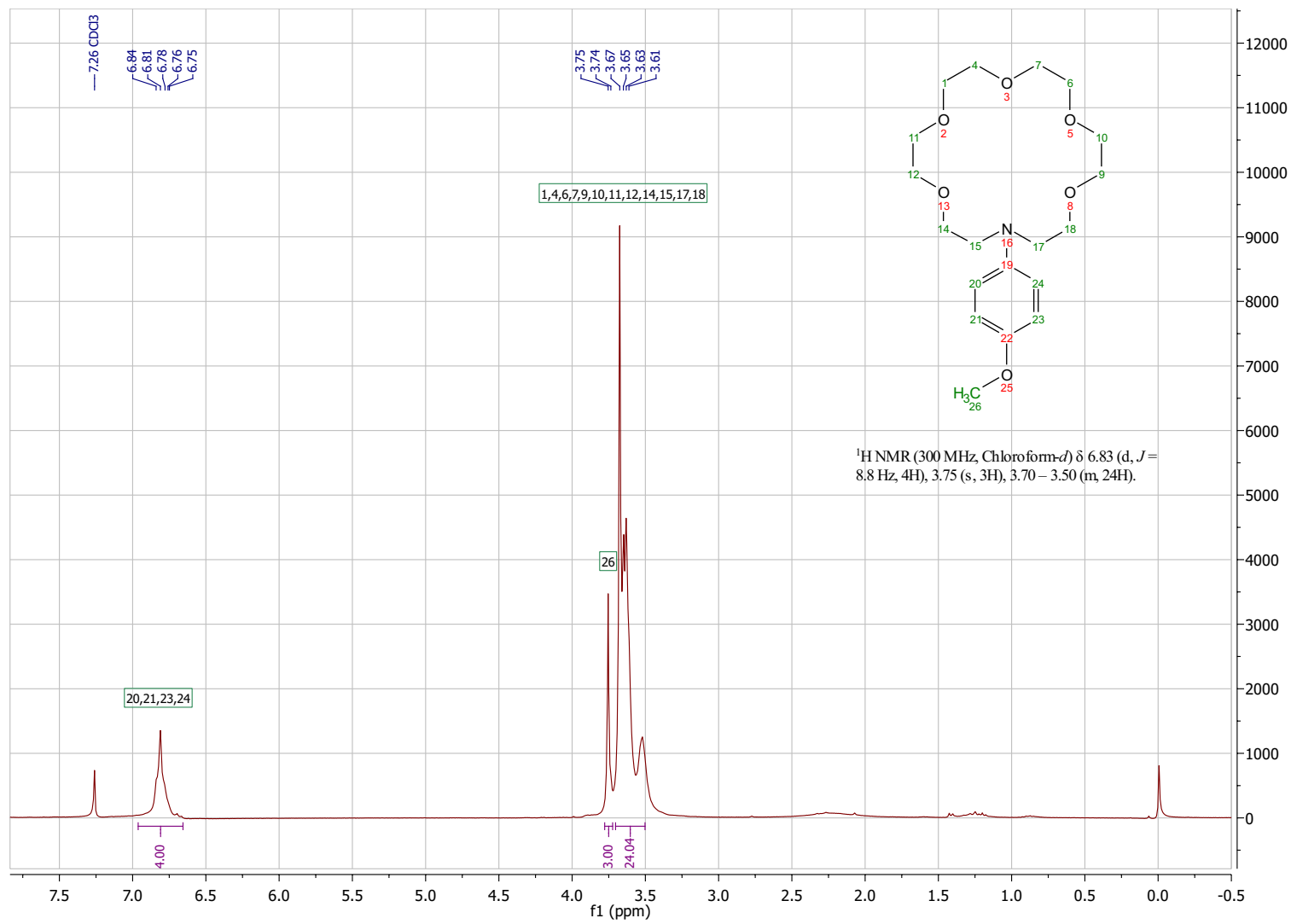


Figure A.10.: ¹H-NMR spectrum of precursor **7a**

Figure A.11.: $^1\text{H-NMR}$ spectrum of crown ether **7**

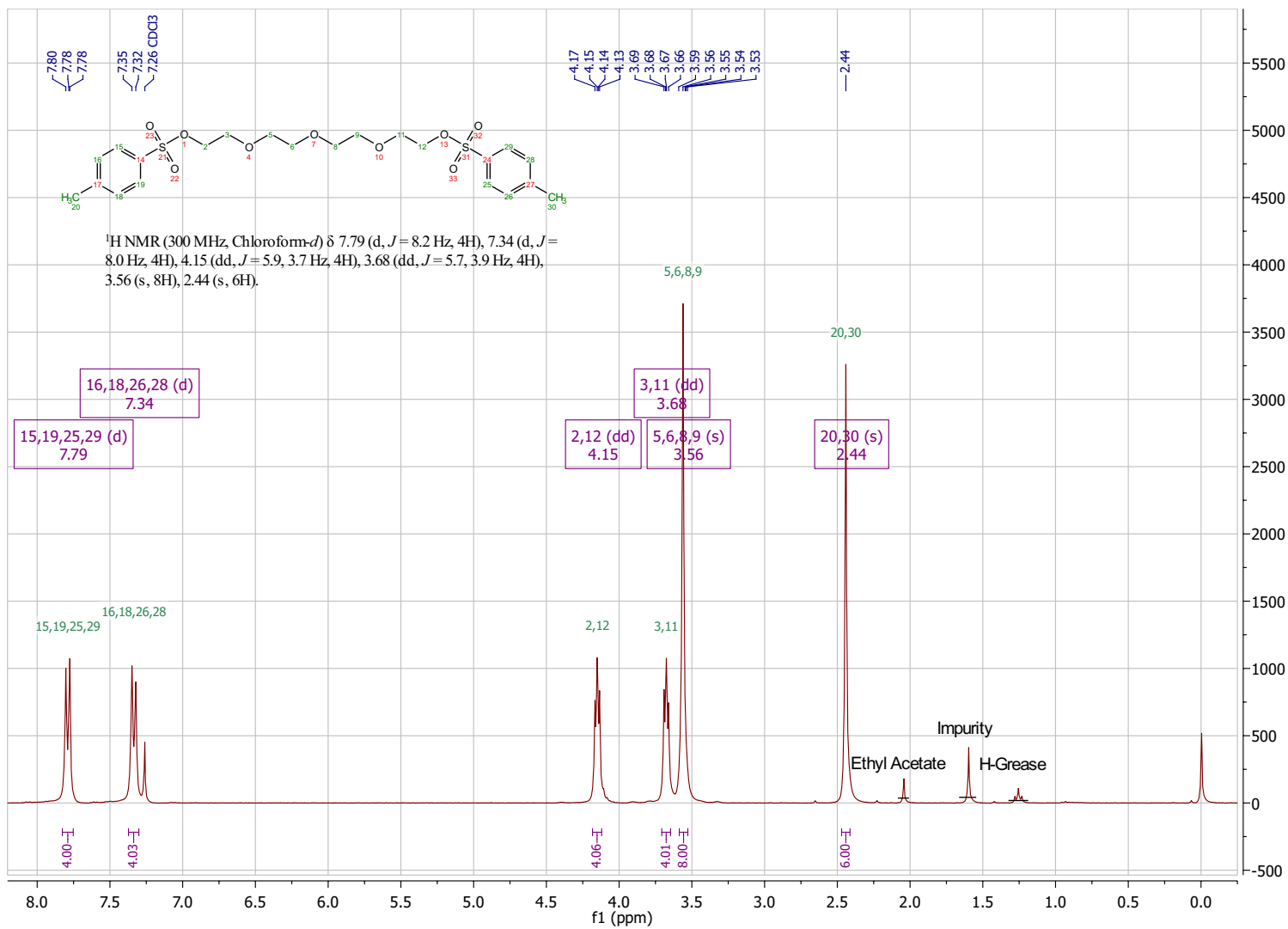
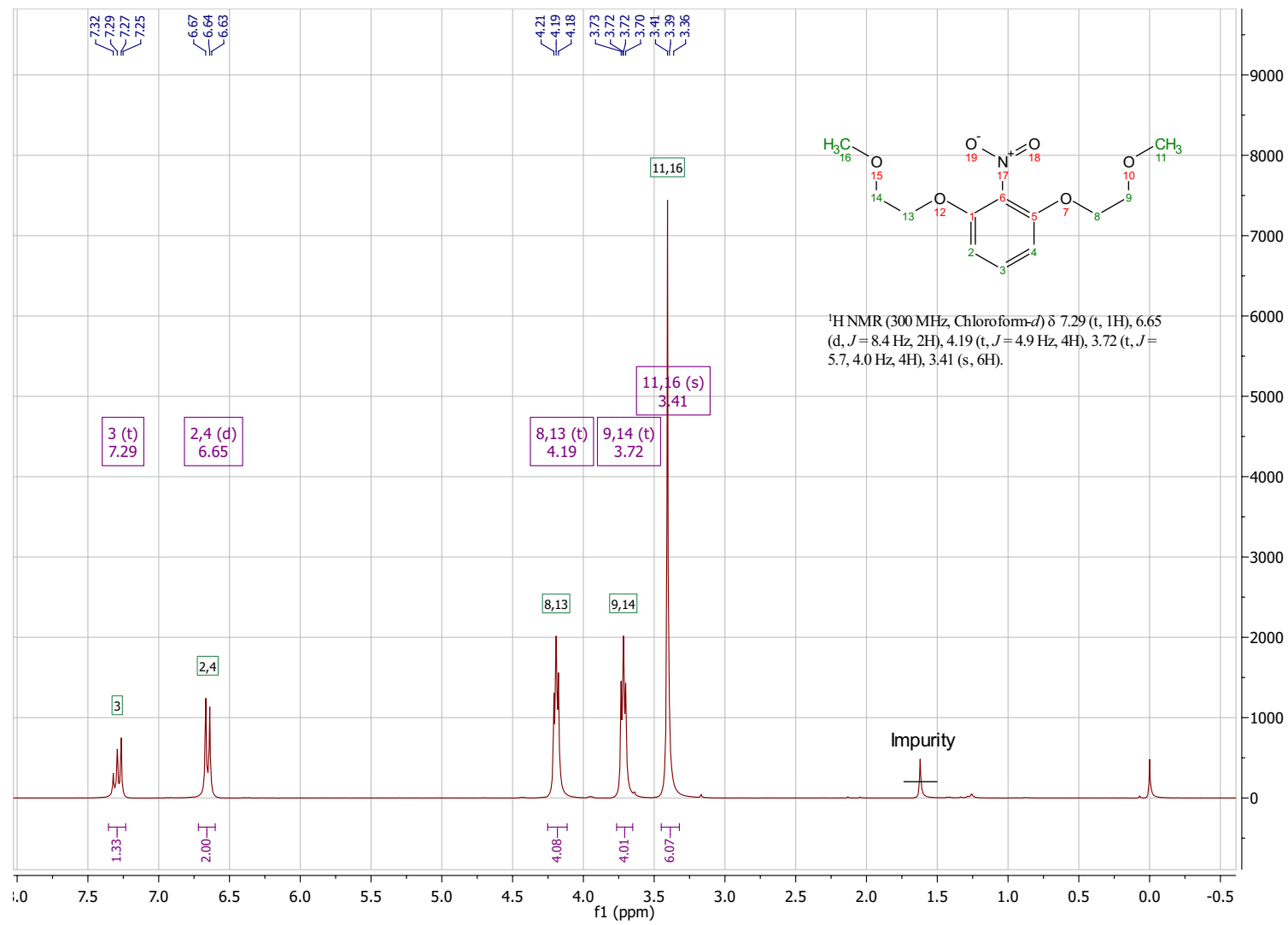


Figure A.12.: ¹H-NMR spectrum of Crown Forming Agent

Figure A.13.: ¹H-NMR spectrum of precursor **2a**

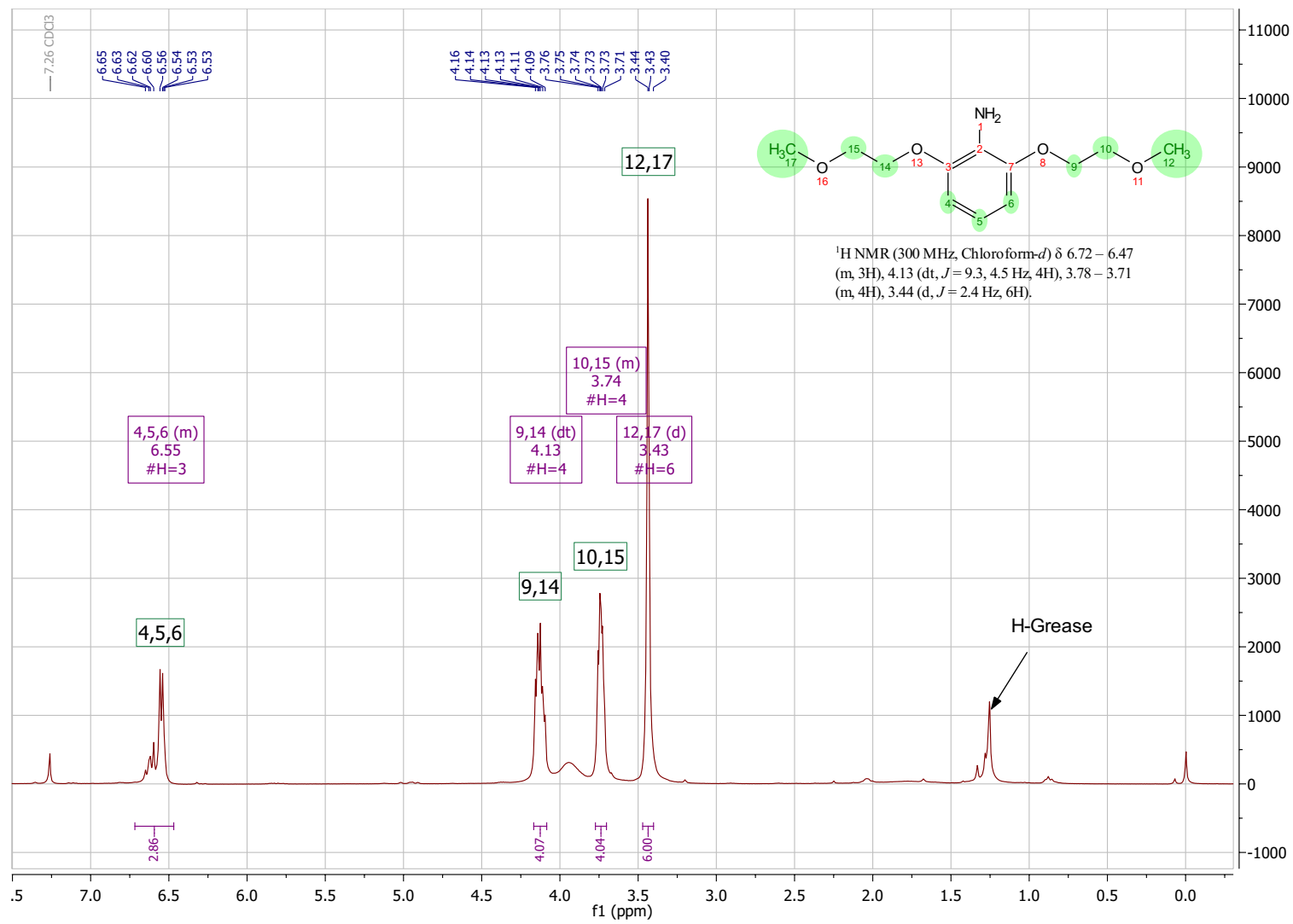
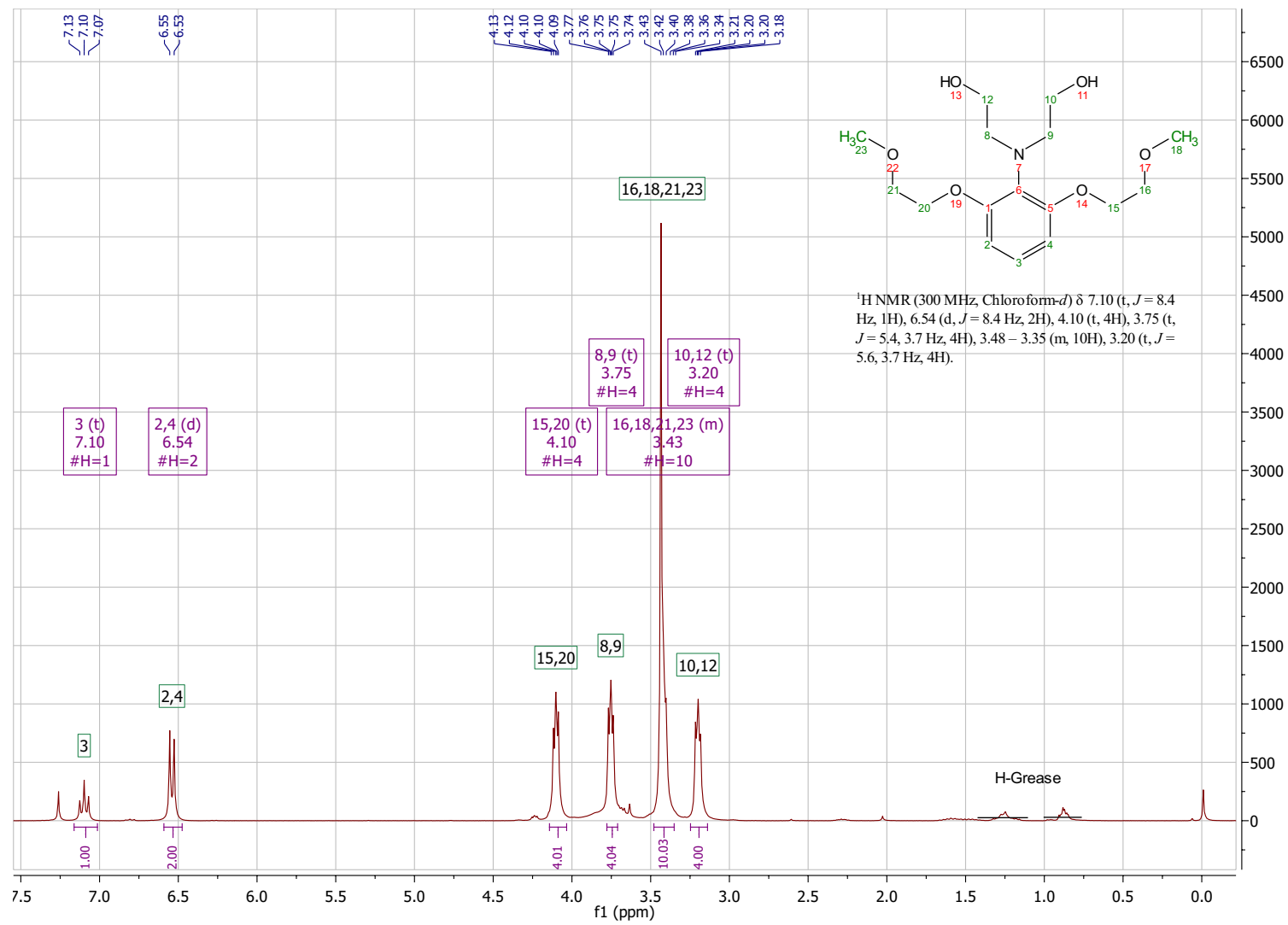


Figure A.14.: ¹H-NMR spectrum of precursor **2b**

Figure A.15.: ¹H-NMR spectrum of precursor **2c**

Appendix B.

UV-Vis Spectra

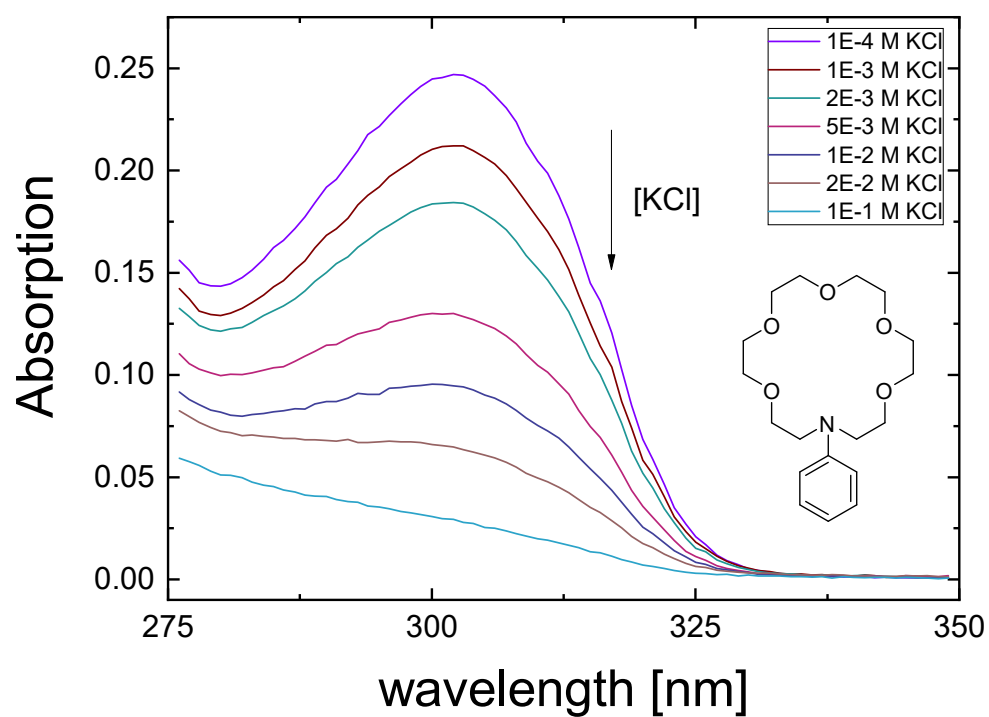


Figure B.1.: Crown Ether 1 - Zoomed response peak

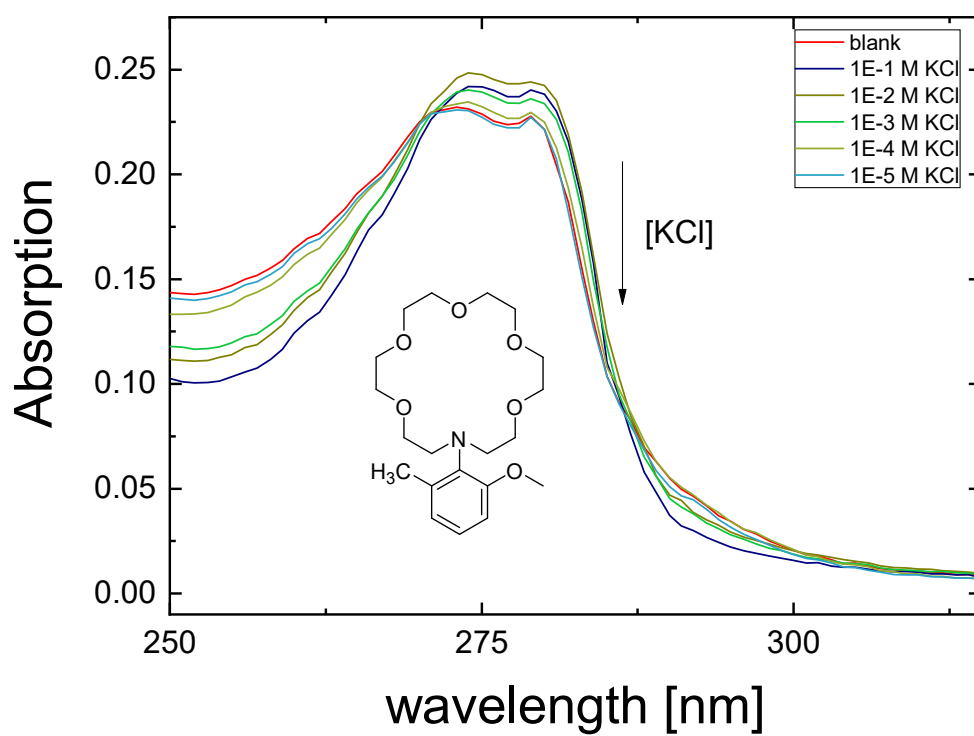


Figure B.2.: Crown Ether 3 - Zoomed response peak

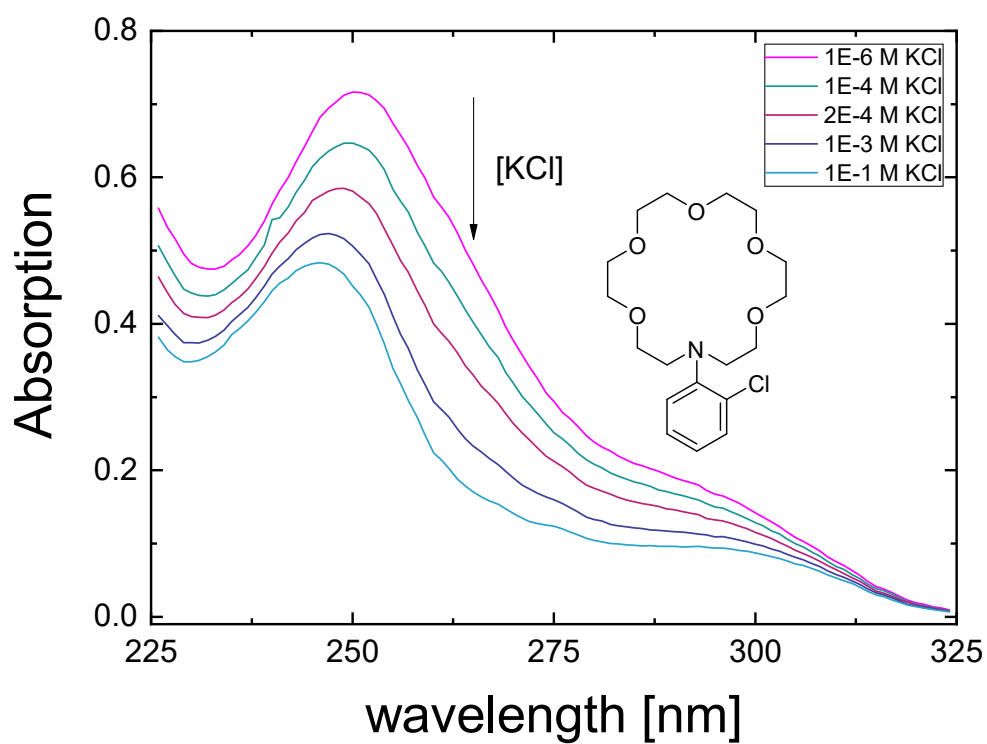


Figure B.3.: Crown Ether 4 - Zoomed response peak

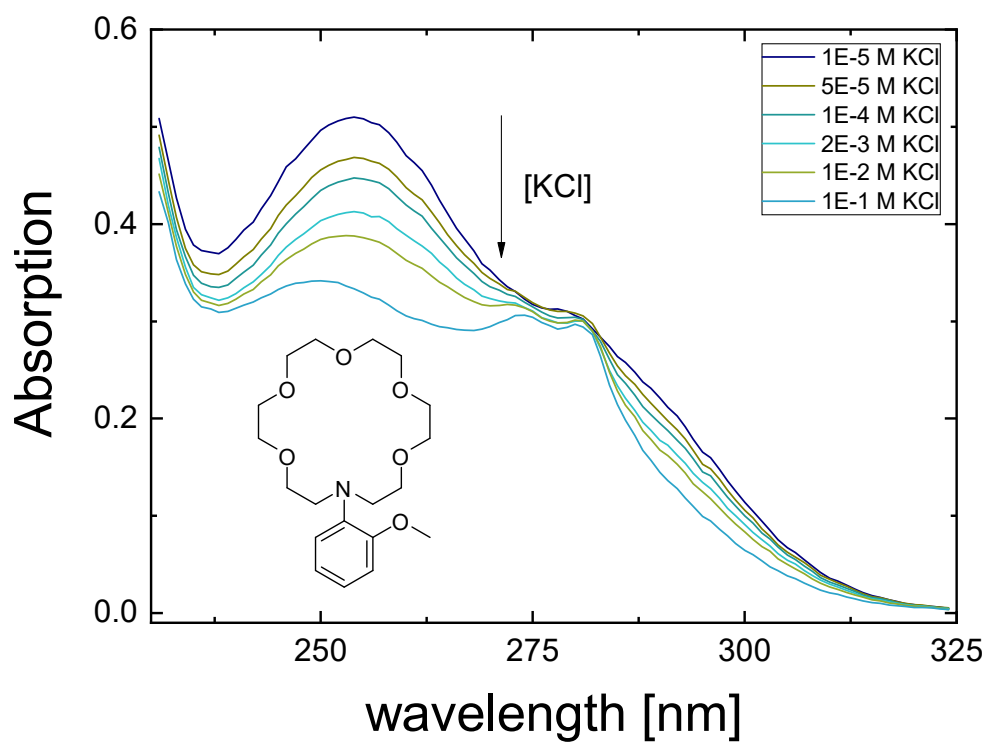


Figure B.4.: Crown Ether **5** - Zoomed response peak

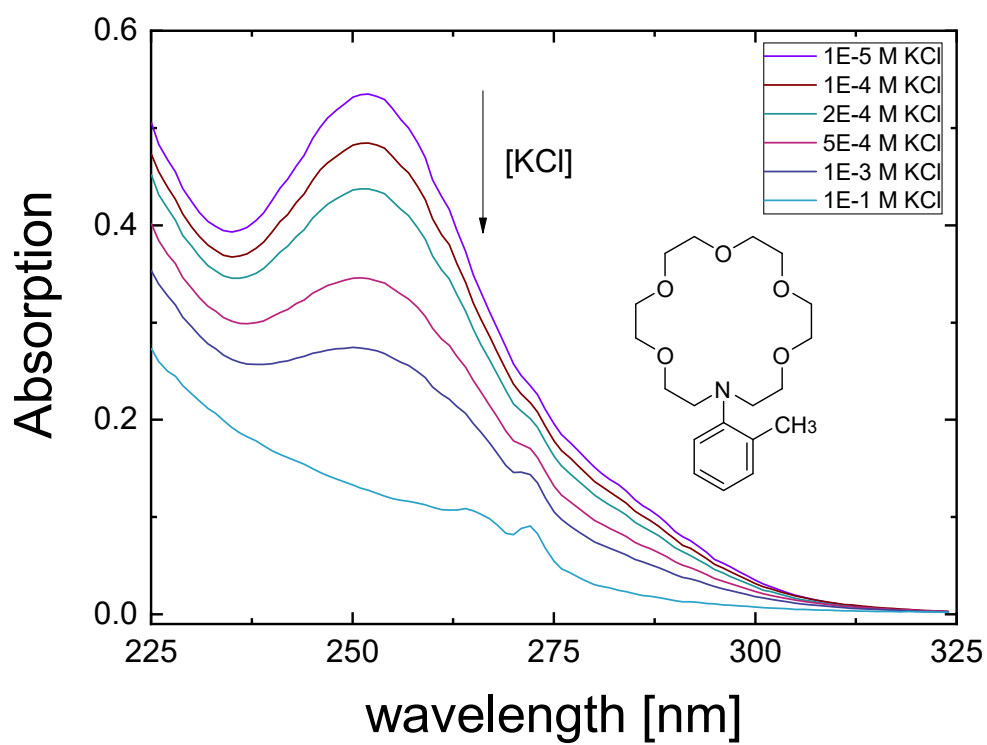


Figure B.5.: Crown Ether **6** - Zoomed response peak

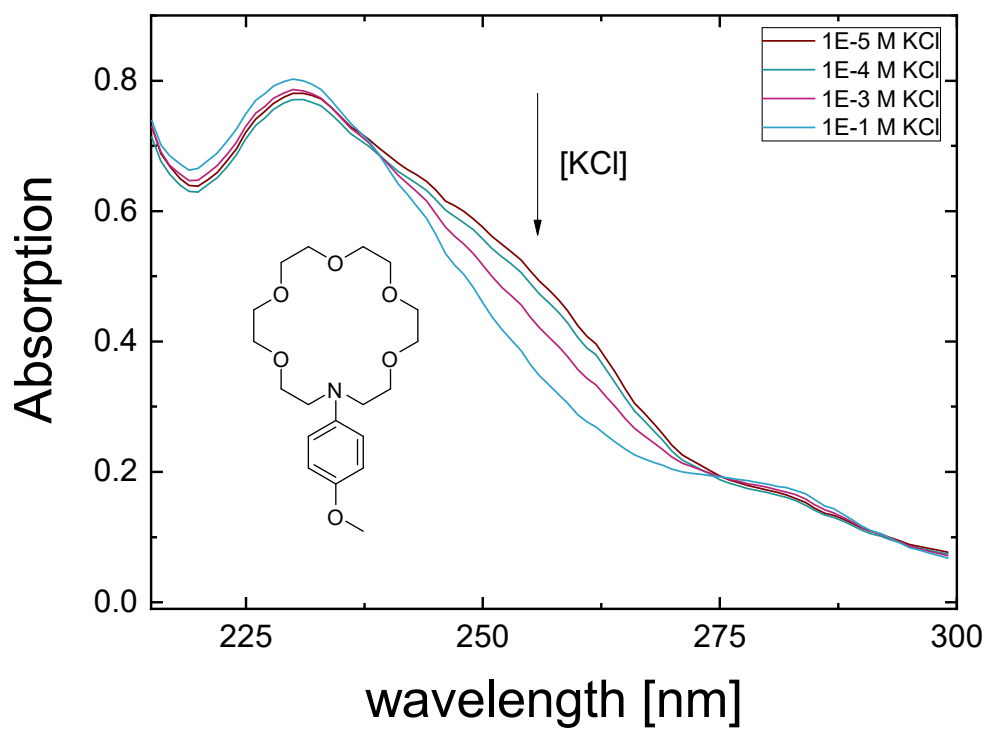


Figure B.6.: Crown Ether 7 - Zoomed response peak

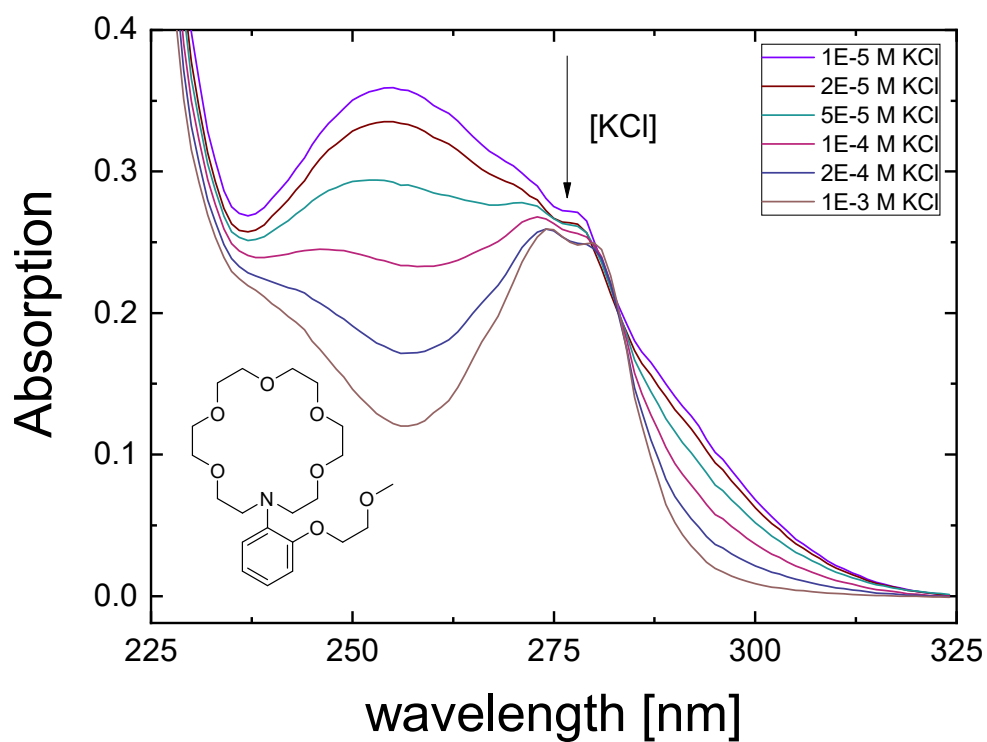


Figure B.7.: Methoxyethoxy Crown Ether - Zoomed response peak

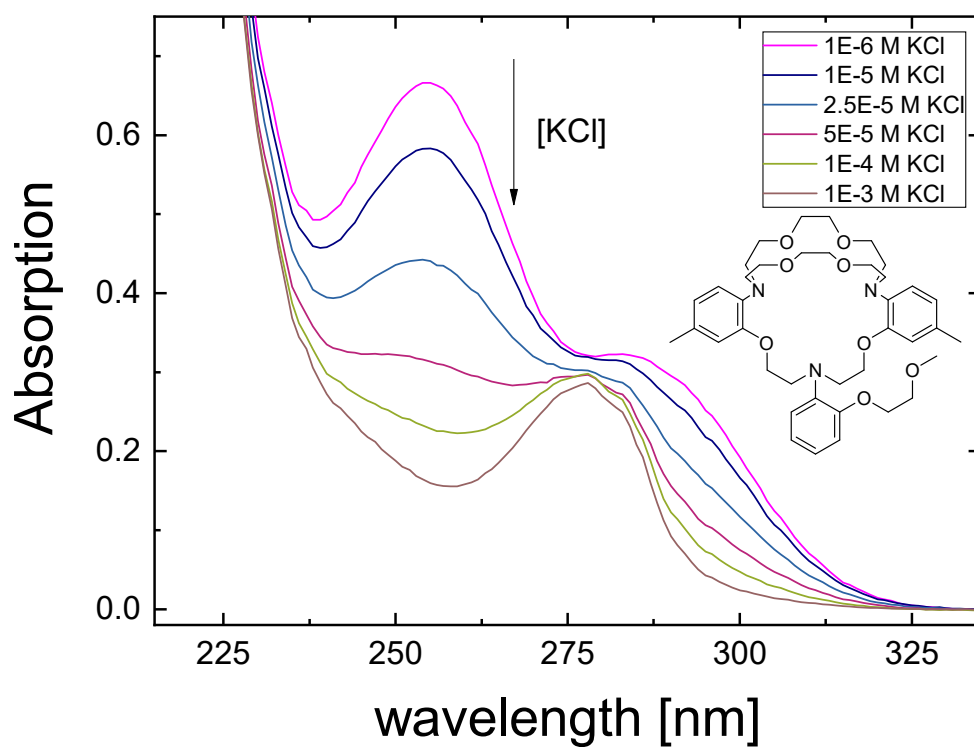


Figure B.8.: Triazacryptand - Zoomed response peak

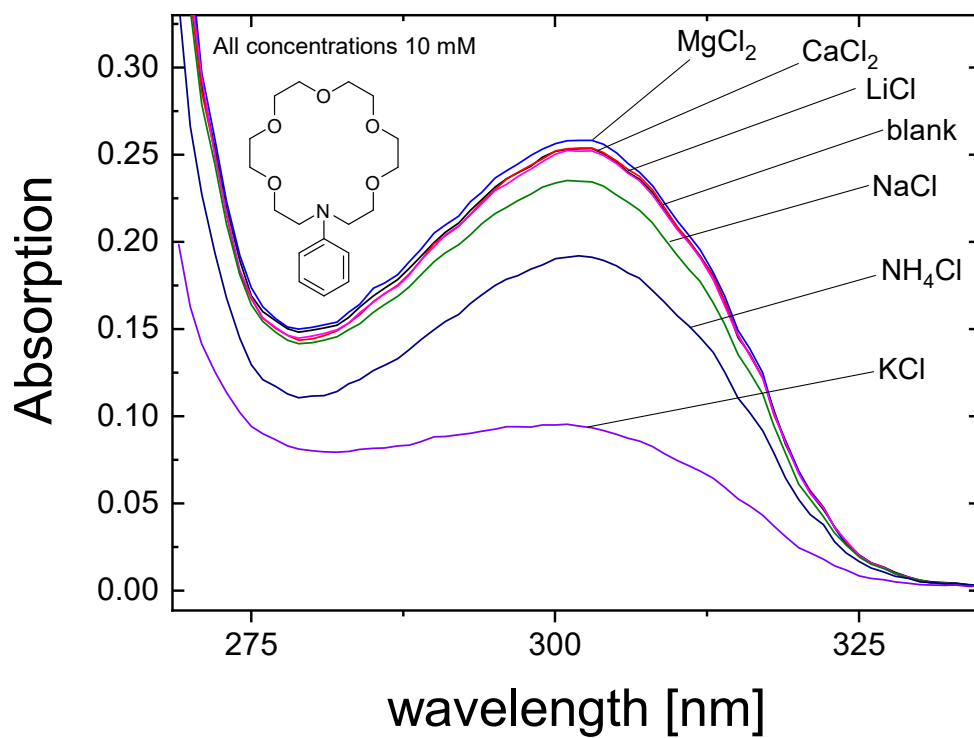


Figure B.9.: Crown Ether 1 - Cross Sensitivity

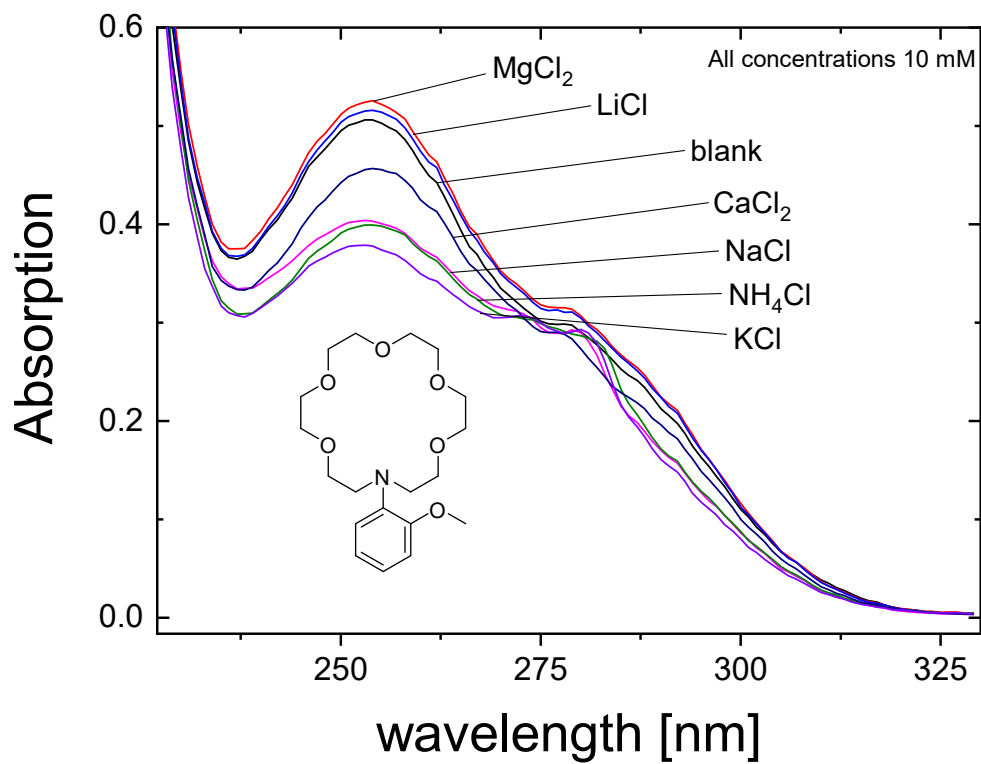


Figure B.10.: Crown Ether 5 - Cross Sensitivity

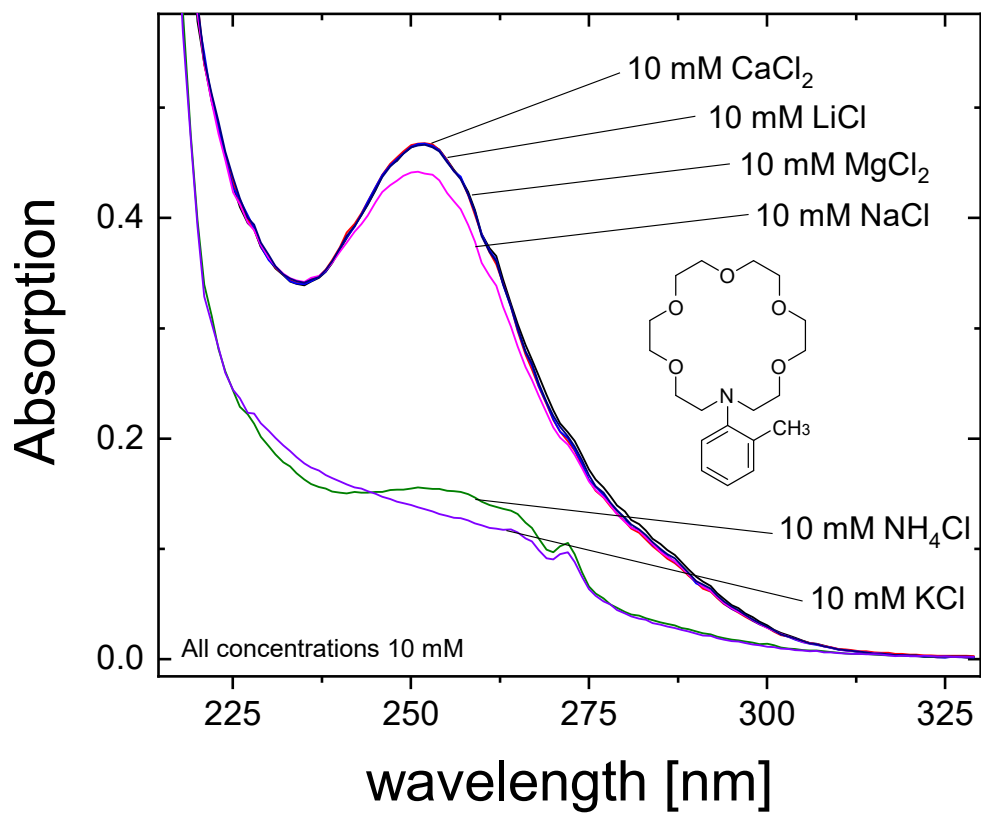


Figure B.11.: Crown Ether 6 - Cross Sensitivity

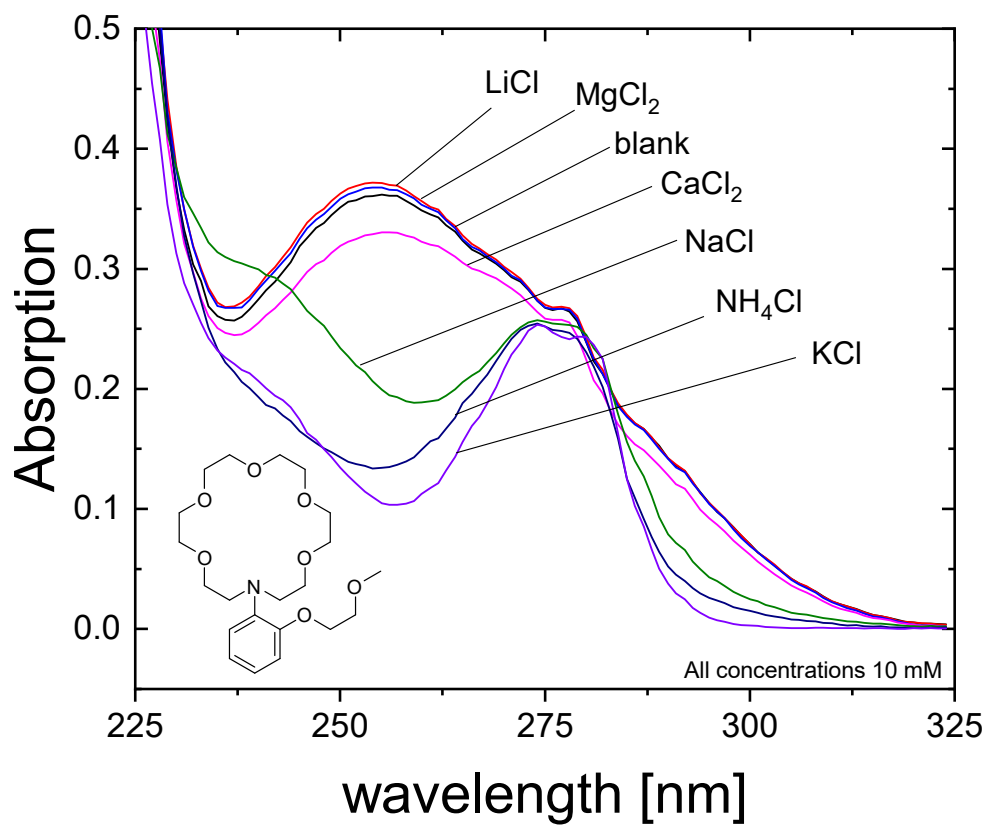


Figure B.12.: Methoxyethoxy Crown Ether - Cross Sensitivity

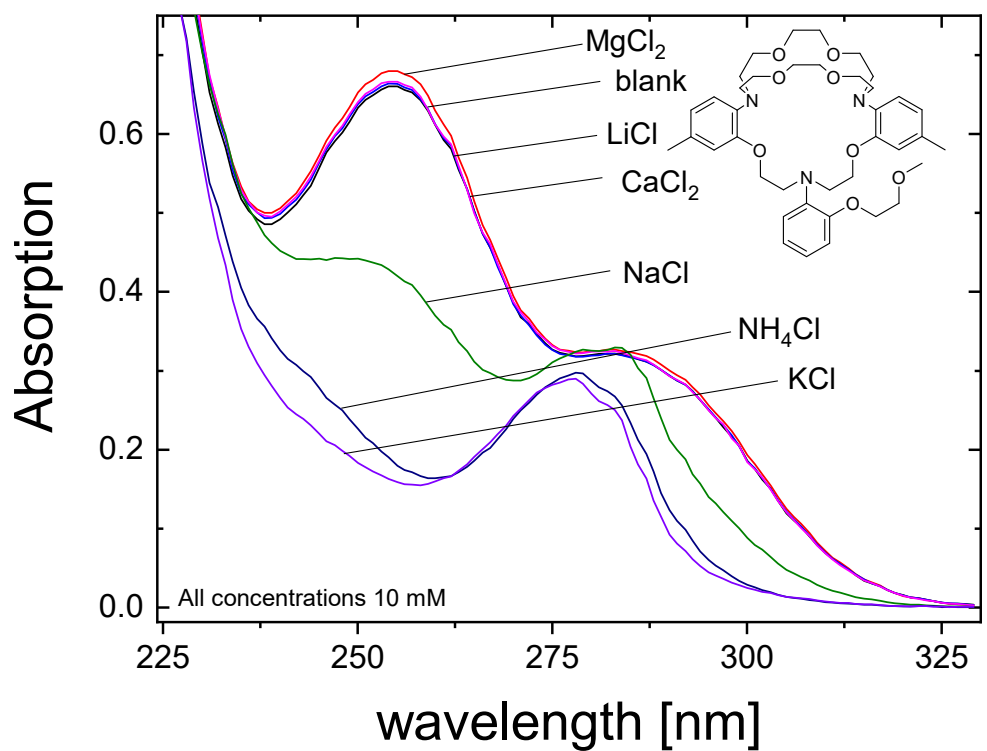


Figure B.13.: Triazacryptand - Cross Sensitivity

Appendix C.

Fluorescence Spectra

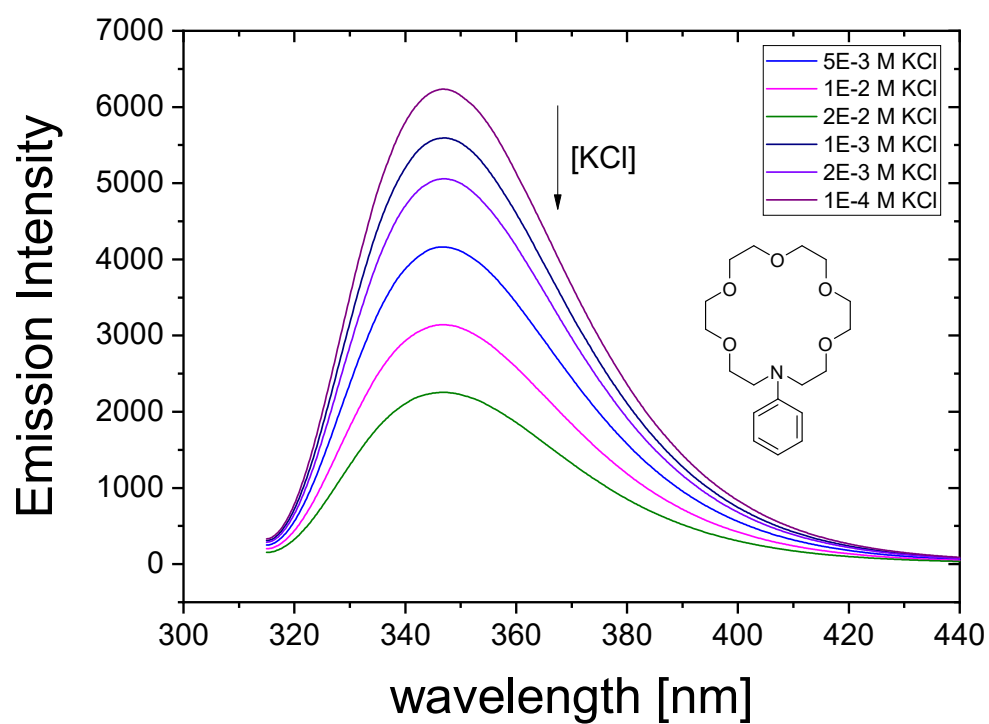


Figure C.1.: Crown Ether 1 - Fluorescence

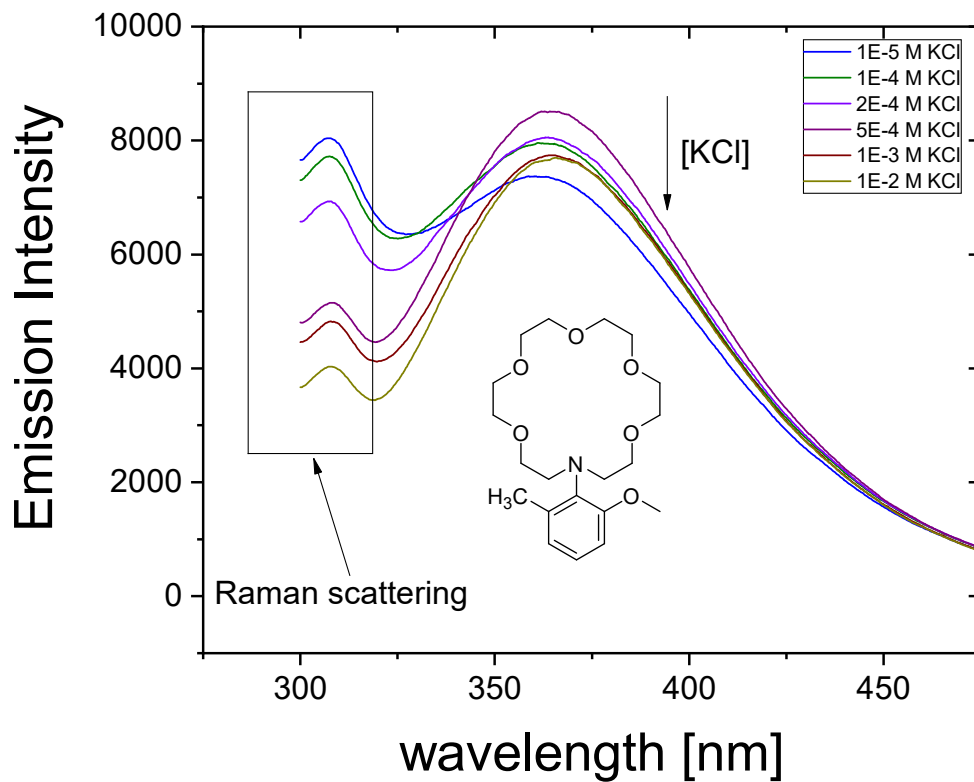


Figure C.2.: Crown Ether **3** - Fluorescence

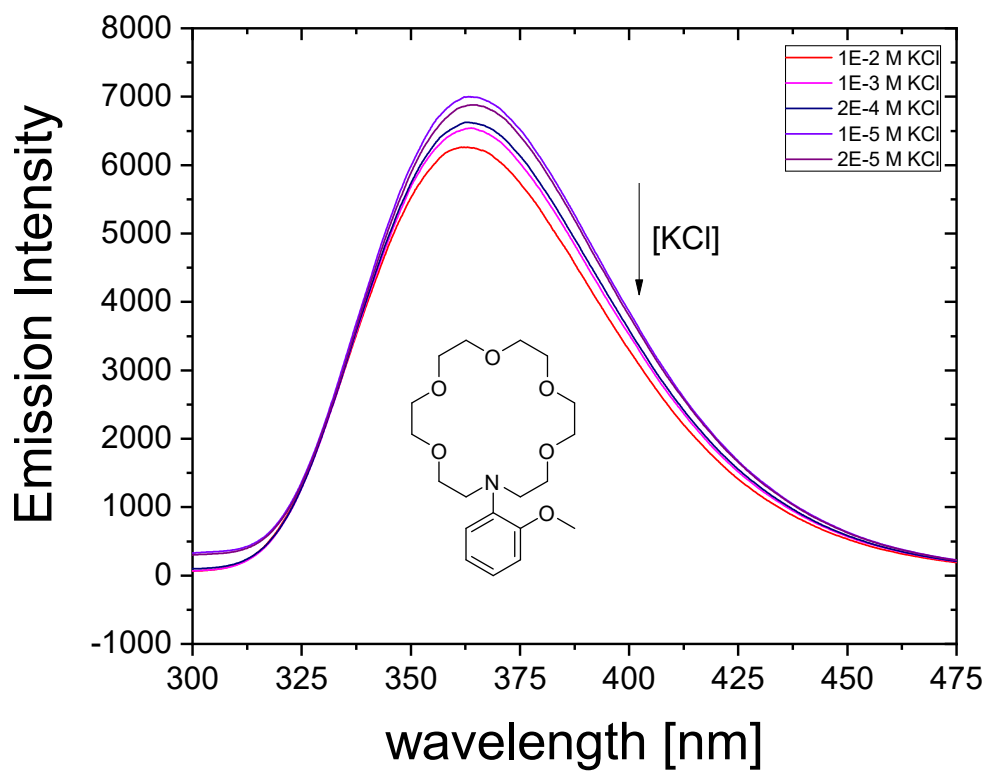


Figure C.3.: Crown Ether **5** - Fluorescence

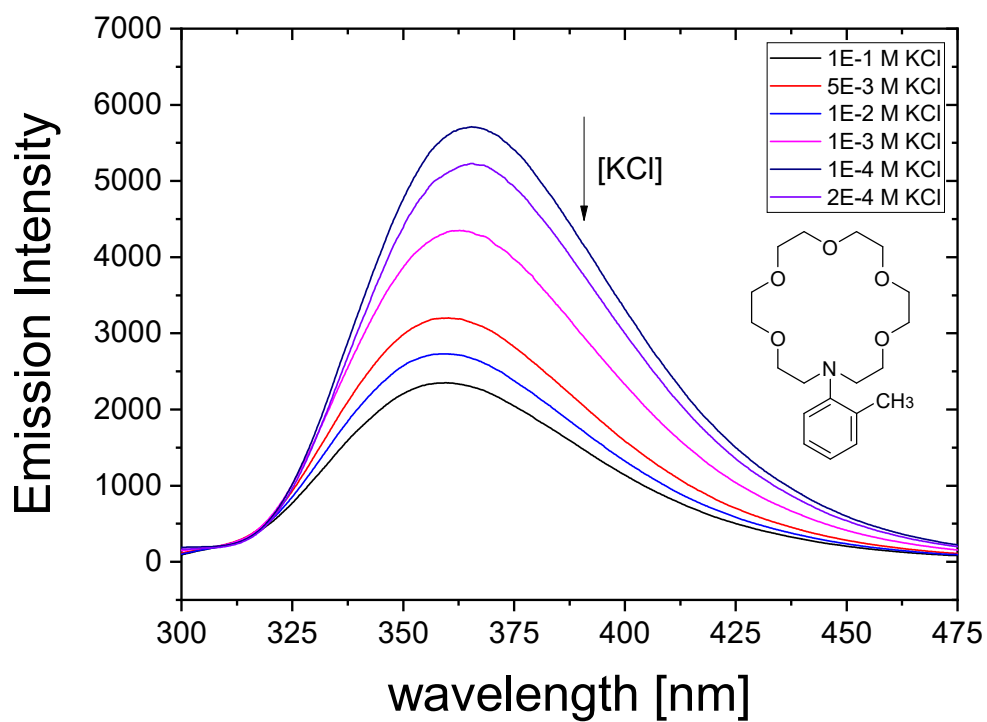


Figure C.4.: Crown Ether 6 - Fluorescence

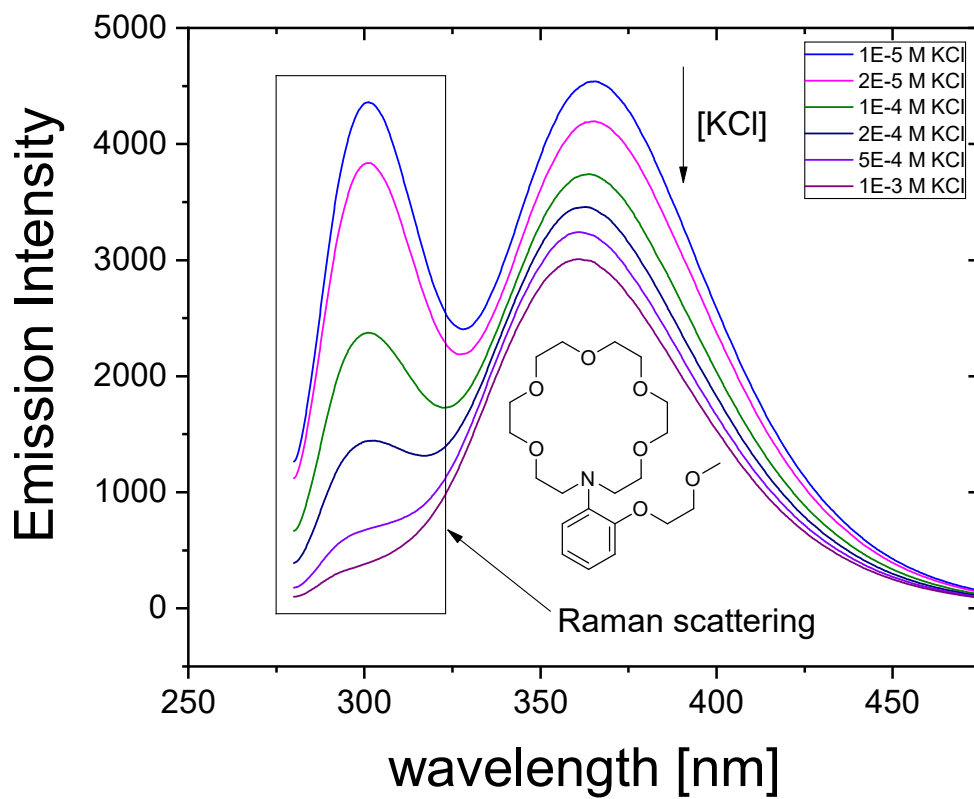


Figure C.5.: Methoxyethoxy Crown Ether - Fluorescence

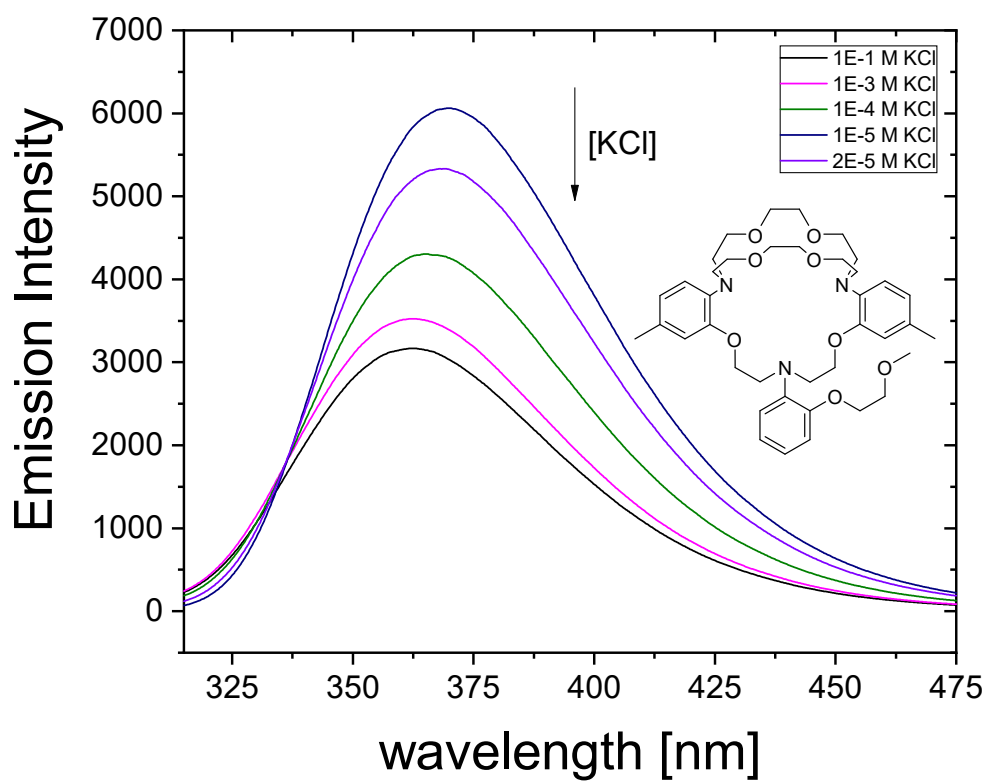


Figure C.6.: Triazacryptand - Fluorescence